ELECTRONIC INTERACTIONS IN TETRAPYRROLE PIGMENTS; STUDIES O PLANAR, NONPLANAR PORPHYRINS AND CROWNED PHTHALOCYANINE:

A Thesis Submitted
In Partial Fulfilment of the Requirements
for the Degree of
DOCTOR OF PHILOSOPHY

by
DAMODAR REDDY

to the
DEPARTMENT OF CHEMISTRY
INDIAN INSTITUTE OF TECHNOLOGY KANPUR
MARCH, 1992

CHM-1995-D-REC...F

*Dedicated
to
my
Parents*

STATEMENT

I hereby declare that the matter embodied in this thesis "Electronic Interactions in Tetrapyrrole Pigments; Studies on Planar, Nonplanar Porphyrins and Crowned Phthalocyanines", is the result of investigations carried out by me in the Department of Chemistry, Indian Institute of Technology, Kanpur, India, under the supervision of Dr. T.K. Chandrashekar.
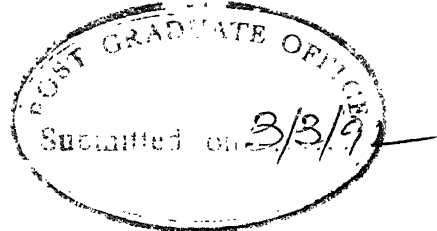
In keeping with the general practice of reporting scientific observations, due acknowledgement has been made wherever the work described is based on the findings of other investigators.

DAMODAR REDDY

Kanpur:

March 1992

CERTIFICATE

It is certified that the work contained in the thesis entitled "Electronic Interactions in Tetrapyrrole Pigments; Studies on Planar, Nonplanar Porphyrins and Crowned Phthalocyanines", by DAMODAR REDDY, has been carried out under my supervision and the same has not been submitted elsewhere for a degree.

(T.K. Chandrashekar)
Thesis Supervisor
Department of Chemistry
I.I.T. Kanpur - 208016
INDIA

Kanpur:

March 1992

CERTIFICATE OF COURSE WORK

This is to certify that Mr. DAMODAR REDDY has satisfactorily completed all the courses required for the Ph.D. degree. The courses include:

Chm 505	Principles of Organic Chemistry
Chm 511	Physical Organic Chemistry
Chm 524	Modern Physical Methods in Chemistry
Chm 525	Principles of Physical Chemistry
Chm 542	Advanced Inorganic Chemistry II
Chm 545	Principles of Inorganic Chemistry
Chm 646	Bio-Inorganic Chemistry
Chm 800	General Seminar
Chm 801	Special Seminar
Chm 900	Post-graduate Research

Mr. DAMODAR REDDY was admitted to the candidacy of the Ph.D. degree in September 1988 after he successfully completed the written and oral qualifying examinations.

(S.S. Katiyar)
HEAD
Department of Chemistry
I.I.T. Kanpur

(B.D. Gupta)
Convenor
Departmental Post-graduate
Committee, Dept. of Chemistry
I.I.T., Kanpur

ACKNOWLEDGEMENTS

TABLE OF CONTENTS

Results and Discussion

The thesis entitled, "Electronic Interactions in Tetrapyrrole Pigments; Studies on Planar, Nonplanar Porphyrins and Crowned phthalocyanines", consists of seven chapters.

The first chapter describes an overview of the literature on electron transfer and charge transfer interactions in biological systems involving chlorophylls and metalloporphyrins. In addition, the importance of nonplanar conformation of porphyrin systems in many biological systems are highlighted.

The second chapter describes the general experimental techniques and methods employed for evaluation of physical parameters. There are four sections. Section 1 gives the details of the chemicals and purification methods. Section 2 describes the synthesis of the precursor compounds for various porphyrins and phthalocyanines reported in this thesis. In section 3, a brief outline of the physico-chemical techniques employed and details of the Instruments used are given. In section 4, the methods of calculation of physical parameters are given.

The third chapter presents the interaction of various metalloporphyrins ($M = Co^{2+}$, Zn^{2+} and Cu^{2+}) and metallochlorin (Co^{2+}) with an electron acceptor, 4,6-dinitrobenzofuroxan (BFO). It was found that Zn^{2+} and Cu^{2+} porphyrins form simple charge-transfer complex as a result of $\pi-\pi$ interaction. In the case of cobalt(II) porphyrins the interaction of BFO leads to an electron transfer from Cobalt(II) to BFO resulting in the

formation of Cobalt(III) porphyrins and BFO⁻ radical. The rate of oxidation is found to be dependent on the porphyrin ring substituents as well as on the solvent mixture used. In the case of Cobalt(II) tetraphenylchlorin (CoTPC), first the oxidation of Co(II)TPC to Co(II)TPP occurs and this is followed by metal oxidation to give the Cobalt(III) porphyrins. The oxidation of the Co(II) porphyrins and formation of the anion radical of BFO has been monitered with ESR, optical, ^{1}H and ^{19}F NMR methods.

The fourth chapter describes the interaction of metalloderivatives (Cu^{2+}, Zn^{2+} and Co^{2+}) of tetrakis(4-N-methylpyridyl) porphyrin (MTMPyP) with electron donors. The donors used are Adenine, Guanine, Cytosine and Thymine. This interaction is described interms of 1:1 molecular complexes. The binding constants evaluated from optical studies vary as CuTMPyP > ZnTMPyP with a given base and this variation is accounted interms of structure of the macrocycle. The bindig constants for adenine complexes are larger than for cytosine complexes with a given metalloderivative. The Co^{II}TMPyP undergoes oxidation to Co^{III}TMPyP in the presence of molecular oxygen and adenine. ESR studies of the complexes reveal that the π - complexation results in changes in the electronic structure of the central metal ion.

The fifth chapter presents the synthesis, characterization, cation and solvent induced dimerization of metallophthalocyanines (MtCRPc; M = Ag^{2+}, VO^{2+}) appended with four crown ether voids at 3,4-positions. The optical and ESR studies indicated an electronic coupling between a pair of metallophthalocyanine moieties in a cofacial geometry. The blue shifts in the optical

xi

absorption spectrum on dimerization is explained on the basis of exciton theory. The ESR studies allowed an estimation of metal-metal distance.

Chapter six describes the spectroscopic studies on nonplanar porphyrins both in the ground and excited states. The nonplanarity in the porphyrin skeleton is due to the introduction of short bridging groups across the porphyrin periphery. Specifically short chains containing para or meta xylyldioxy groups covalently linked at the ortho position of phenyl groups of 5,10,15,20 tetraphenylporphyrin (H_2TPP) results in the formation of basket handle porphyrins with different structures. Isomer I (cross-trans-linked) of para derivative (PSI) and isomer II (Adjacent-trans-linked) and isomer III (Adjacent-cis-linked) [MSII and MSIII] of meta derivative has been characterized by various spectroscopic methods. Electronic and ^{1}H NMR spectral studies indicate significant distortion of the porphyrin skeleton in these derivatives. Protonation of free base derivatives resulted in a small blue shift of Q-bands inmarked contrast to unstrapped derivative and this has been attributed to the lack of conjugation between phenyl group and porphyrin plane because of restricted rotation of phenyl porphyrin bond. The bridging xylyl group does not interfere with the axial ligation of metal derivatives (Co^{2+} and Zn^{2+}) of MSII and MSIII. Electrochemical studies indicate easier oxidations and harder reductions for free base derivatives relative to the corresponding unstrapped derivative. The easier oxidations are attributed to the loss of coplanarity due to distortion and the harder reductions are

attributed to destabilization of anions and dianions due to the lack of solvation.

The excited state properties of these basket handle porphyrins and their Zn^{2+} derivatives were determined by fluorescence and photoexcited triplet ESR methods. Fluorescence spectral studies indicate that these porphyrins are less fluorescent than the parent H_2TPP. This difference is ascribed to the enhanced rate of intersystem crossing from $S_1 \rightsquigarrow T_1$ and increased natural radiative life times. The rate of radiative fluorescent decay roughly follows the molar extinction coefficient of the lowest energy Q-band. The estimated excited state potentials suggests that the cross-trans-linked isomer (PSI) is a better electron donor in the first excited singlet state. Zero field splitting parameters D and E of the three isomers calculated from photoexcited triplet ESR spectra show small but significant differences and this has been attributed to the distortion of the porphyrin plane caused by introduction of short bridging group. The electron spin polarization (ESP) pattern remain same as in H_2TPP indicating the usual spin orbit coupling mechanism for Intersystem crossing. All these spectral data indicates that considerable distortion is present in the porphyrin skeleton upon introduction of short bridging groups.

The seventh chapter gives the summary of the investigations carried out in this thesis.

CHAPTER 1

GENERAL INTRODUCTION

The electronic interactions in biological systems are known. Electronic interactions involved in biological systems are broadly classified into two major types; (i) interaction between Chromophore (usually chlorophylls, Pheophytin, porphyrins and metalloporphyrins) and planar organic π-system containing electron withdrawing groups (electron acceptors) or electron releasing groups (electron donors) which results in the formation of charge-transfer complex (molecular complex). The major stabilization for these complexes arises from the π-π interaction between the donor and the acceptor. This is possible when electron donor and acceptor are positioned face to face which are separated by Van der Waals distance. A weak π-π interaction between porphyrin donor (D) and organic acceptor (A) results in the formation of charge transfer complex.

$$D + A \rightleftharpoons [DA] \qquad\qquad 1.1$$

On the other hand a strong π-π interaction between donor and acceptor results in the transfer of electron from donor to acceptor resulting in the formation of charge separated species.

$$D + A \rightleftharpoons D^+ + A^- \qquad\qquad 1.2$$
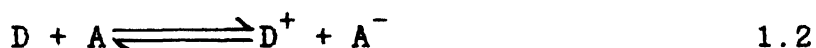
(ii) Interaction between two identical chromophores (porphyrins, chlorophylls or phthalocyanines) oriented in a face to face geometry separated by Van der Waals interaction level. This results in the coupling between two π- systems disturbing the π- electron distribution.

In this thesis, the electronic interactions described above has been studied using porphyrins, metalloporphyrins and crowned phthalocyanines and conventional electron acceptors and donors. This thesis is divided into three parts as follows; Part I describes the interaction between planar metalloporphyrins and electron acceptor/donors. Formation of both charge-transfer complexes and the charge-separated species as a result of complete electron transfer has been observed. Part II describes the electronic interactions between the two chromophores (metallo crowned phthalocyanines) which are oriented in a face to face geometry separated by distance of about 4.5 to 5A$^{\circ}$. The face to face orientation in this species are induced by addition of alkali cations and some specific solvent compositions. The spectroscopic changes observed upon dimer formation in these systems has been explained on the basis of exciton formalism. Part III of the thesis describes the effect of nonplanarity in the porphyrin skeleton on the ground and excited state properties. The nonplanarity in porphyrin skeleton is due to the introduction of a short bridging group across the porphyrin periphery. It has been shown that the electron donating capability of a porphyrin skeleton increases both in the ground and excited state in a nonplanar conformation relative to its planar structure.

Before a detailed discussion of the results of this thesis, a brief survey of the various aspects of (a) Charge-transfer complexes, (b) electron-transfer reactions and (c) importance of nonplanar conformation of a tetrapyrrole pigments in biological systems are given in the following sections.

1.1 CHARGE-TRANSFER COMPLEXES:

A wide variety of association products of two or more molecules come under the general term "charge-transfer Complex". The reversible association of two neutral molecules with interactions greater than Van der Waals forces, possessing definite stoichiometry, but not causing too much change in the properties of the components would be an appropriate operational definition for a charge-transfer complex.

The first most obvious property is the transfer of charge from one molecule to another. Electron and charge- transfer are vitally important in biology. The biochemistry of these systems is still unclear but charge-transfer complexing is a possible method by which molecules in such processes could receive and pass on charge. There is no invivo evidence for such complexes although many molecules or their analogues, thought to be active in these systems, can form charge- transfer complex invitro. The charge-transfer complex forces are relatively long range as compared to chemical forces. Thus, typical distances between molecules in these complexes are 3.2 to 3.4 A^{o} whereas chemical bond lengths are less than about 1.5 A^{o}. Charge-transfer would therefore facilitate interaction between mobile molecules over so comparatively long separation. Charge-transfer forces usually hold the components in the complex together in specific orientation. This could perhaps act to bring large biomolecules together with their prosthetic groups correctly aligned for interaction.

The nature of the intermolecular forces between the components in a charge-transfer complex is still unclear. There

are several theoretical approaches in literature to explain the spectral features of the charge-transfer complexes. The most widely accepted theory was put forward by Mulliken[1] and it is based on the intermolecular charge-transfer concept.

According to Mulliken, the formation of molecular complexes take place between two molecules, one an electron acceptor and the other an electron donor relative to each other. The complex exists in two states, a ground state and an excited state. In the ground state, the two molecules experience the normal physical forces (Van der Waals type) in addition to a small amount of charge-transferred from donor to the acceptor which contributes some additional binding energy to the complex. The excited state is promoted when the ground state complex absorbs light of suitable energy. In the excited state, the electron which was only slightly shifted towards the acceptor is almost wholly transferred. It is the transfer of the electron on absorption of light gives the characteristic colours of these complexes. According to Mulliken's valence bond model, the ground state wavefunction Ψ_N of 1:1 donor- acceptor complex is given by.

$$\Psi_N = a\ \Psi_0(A,\ D) + b\ \Psi_1(D^+ - A^-) \qquad 1.3$$

The first term in the equation is the 'no bond' wave function of donor and acceptor molecules in close proximity with no charge-transfer between them. However, it can include contributions from classical electrostatic forces, Van der Waals forces, various dispersion forces and dipole interactions. The second term is the 'dative' wave function of the two molecules bound together by an electron being totally transferred from a

donor to an acceptor. The other contributions to the ground state wave function such as the locally excited states and higher energy states are usually neglected. The coefficients $\underline{a}$ and $\underline{b}$ decide the type of complex formed. That is, for a loosely bound charge-transfer complex $a^2 \gg b^2$.

Another approach to the energetics of the inter molecular charge - transfer transitions has been made by Dewar and Coworkers[2,3] using simple molecular orbital description. The problem has been treated using the perturbation theory for weak interactions. The interaction energies in the ground state are small compared with the transition energies to the excited states of the complex such that the transition may be considered as arising from the transfer of an electron from a highest filled molecular orbital in the donor to the lowest unoccupied molecular orbital in the acceptor. Various MO calculations have been made to predict the ground state stabilisation energies of the complexes. Murrel[4,5] demonstrated a relationship between the stability of a charge-transfer complex and the intensity of the charge- transfer band. Other MO treatments to explain the energetics of molecular charge-transfer transitions include (a) a semiempirical linear combination of MO's by Flurry et al.[6] and (b) the delocalization method of Fukai et al.[7]

The existence of charge- transfer complexes and its implication in biochemical reactions have been the subject of study by many workers. A brief report of the various investigations that have been carried out on the charge-transfer complexes of tetrapyrrole pigments is given here.

Among the biologically important compounds, tetrapyrrole pigments occupy a significant position: porphyrins, pheophytins,

phthalocyanines and corrins represent a few members of this class of compounds. The porphyrins differ from one another in the number and nature of substituents on the peripheral positions of the tetrapyrrole ring. The available structural studies on a few heme proteins indicate a strong evidence for the ubiquitous nature of molecular interaction between porphyrin π- system and certain aromatic residues. The molecular complexes formed between tetrapyrrole pigments and the aromatic compounds are of importance because of their involvement in redox catalysis[8-11], their utility as model for the study of aromatic residue – porphyrin interaction in heme proteins[12,13], light induced electron transfers in photosynthesis[14-17], and herbicidal activity[18].

Heathcote and Slifkin[19,20] in their study on the molecular complexes of vitamin B_{12} and vitamin B_{12b} (corrin ring system) with various organic acceptors and donors, have shown that vitamin B_{12} behaved as a charge donor towards acceptors like glutamic acid, iodine, chloranil etc. While vitamin B_{12b} functioned as a charge acceptor in presence of amino acids, aliphatic amines, purines and pyrimidine. These results are in contrast to the theoretical predictions of Veillard and Pullman[21] who have suggested that vitamine B_{12} should function as an electron acceptor.

The plant pigments, chlorophylls are responsible for photosynthetic activity. There has been numerous reports concerning the molecular association of chlorophylls and pheophytins with other biologically important molecules like quinones, riboflavin, components of chloroplast pigments and bovine serum albumin[22]. The formation of π- complexes between

6

chlorophyll and quinones has been postulated in the primary stages of the photosynthetic processes. The plant pigments exhibit endogamous interactions and the source of stabilization in such complexes has been traced to π-π interaction[23]. It has been shown by Livingstone[24] that a variety of electron acceptors quench the fluorescence of chlorophyll with the possible formation of exciplexes. A more detailed study on the mode of molecular interaction has been presented by Larry and Winkle[25]. In their study on the molecular complexes of chlorophyll and pheophytin with TNB, they have shown that the existence of 1:1 π-complexes. The ^{1}H NMR spectra of these complexes revealed the conformational mobility of phytyl chains of pigments on molecular complexation.

1.2 ELECTRON-TRANSFER REACTIONS:

Electron transfer reactions in biological systems can be broadly classified into three categories: (i) electron- transfer involving only the metal center (ex: cytochromes), (ii) electron-transfer involving only porphyrin π-system (ex: chlorophylls and pheophytin), and (iii) electron - transfer involving both metal center and porphyrin π-system (ex: cytochrome P$_{450}$, catalases and peroxidases).

Some examples in which the electron-transfer occurs from the metal center are given here. Cytochromes are electron- transfer agents in many biological processes and electron addition or removal involves only Iron center. Cytochromes are heme containing proteins which are involved in electron- transfer chains in the mitochondria and chloroplast, in which electron-transfer is associated with the presence of the Fe(III)/Fe(II)

redox couple[26]. Cytochromes are also involved in aspects of the nitrogen cycle and in enzymic reactions associated with photosynthesis.

In model systems, the porphyrins containing Fe, Mn, Co undergo metal centered electron-transfer reactions. Kadish and coworkers[27] have demonstrated by electrochemical experiments on tetraphenyl porphyrin (TPP) Fe(III) chloride [Fe(TPP)Cl], and Fe(TPP)ClO$_4$ in pyridine and dichloromethane under a CO atmosphere undergo metal centered electron-transfer reactions. Also, it has been shown by electrochemical experiments that Mn(III)TPPCl[28] in various co-ordinating solvents undergoes metal centered electron-transfer. There are many reports in literature on the electron-transfer reactions of Cobalt(II) porphyrins under a variety of conditions[29-34] and in all the cases, the end product is [Co(III) porphyrin]$^+$ cation.

Chlorophylls and pheophytins on photo excitation are known to undergo electron-transfer reactions where electron is coming out from the π-system of the macrocycle. The first step in the photosynthesis is the absorption of light by chlorophyll. The resulting electronic excitation passes from one chlorophyll to another in a light harvesting complex until the excitation is trapped by a chlorophyll with special properties at reaction center (RC). At RC, the energy of the excited electron is converted into a separation of charge between donor chlorophyll and acceptor pheophytin. The importance of this reaction lies in the fact it proceeds without any radical pair recombination[35]. In view of the close structural resemblance between chlorophylls and porphyrins many investigations are concerned with porphyrin donors. In addition to their utility as models for the study of

photochemical electron-transfers, these systems have also been used for the study of model reactions of cytochrome activity, heme oxygenation and others[36].

Among the model systems, the porphyrins containing metals Zn^{2+}, Mg^{2+} and Cd^{2+} are known to undergo electron- transfer reactions. In these metalloporphyrins the first electron addition or removal involves porphyrin π- system. Fajer and Davis[36a] have described π- cation radicals and π- anion radicals of Zn^{2+} and Mg^{2+} porphyrins in a recent review. These radical anions and cations were generated either by photo excitation or by chemical method. ESR studies confirmed that the electron addition or removal involves only porphyrin π-system.

Cytochrome P_{450}, catalases and peroxidases are the examples in which the electron-transfer reaction involve both metal center and porphyrin π-system. Peroxidase, chloroperoxidase and catalase are one of the class of heme enzymes[37], catalyses the overall two electron oxidation of organic substrates with H_2O_2 as the oxidant or electron acceptor. These hemes are having fifth axial ligand either oxygen donors or nitrogen donors.

$$AH_2 + H_2O_2 \longrightarrow A + 2H_2O \qquad\qquad 1.4$$

The catalytic cycle of these enzymes are shown in fig. 1.1. The oxidation of the high spin, penta co-ordinate ferric native enzyme (1) by hydrogen peroxide to form a semi stable [Fe(IV) heme]$^+$ intermediate (2). Compound (2) is a highvalent oxo-iron complex that is two oxidation equivalents above ferric enzymes. Compound (2) is generally thought to be an Fe^{IV} porphyrin π- cation radical[38]. The next step of these enzymatic pathway involves the one electron reduction of [Fe^{IV} porphyrin]$^{+\cdot}$ by the
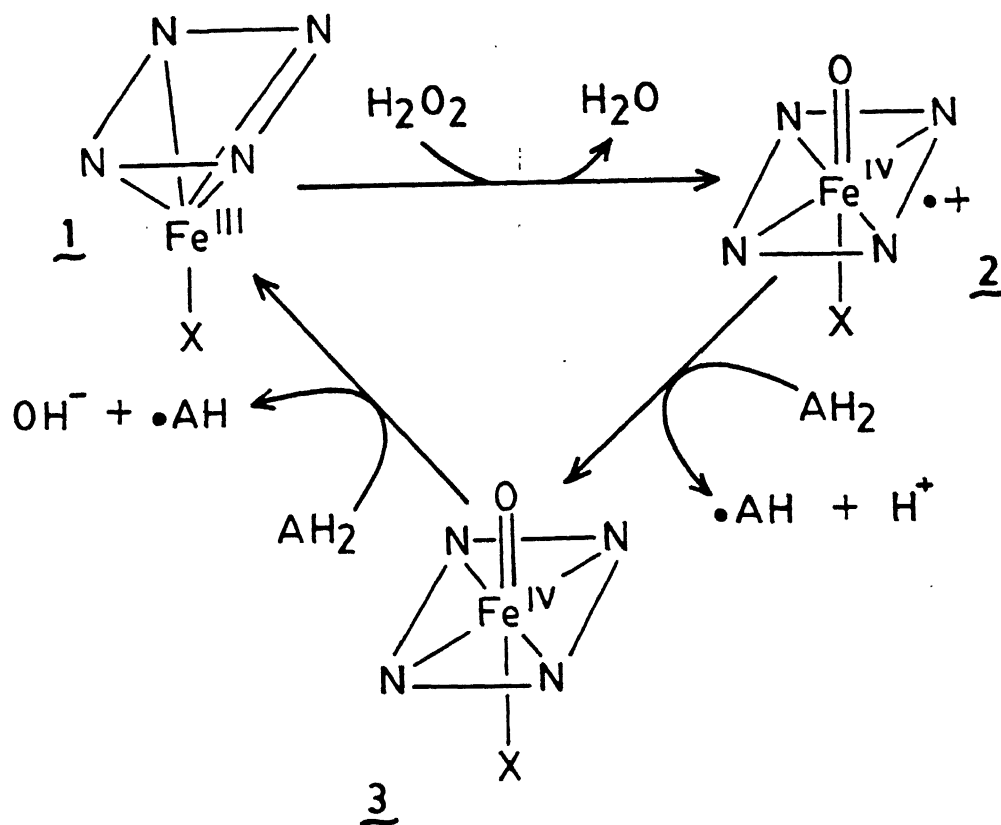
X = -S Cystine (Cytochrome P_{450})
-N Histidine (Peroxidase)
-O Tyrosine (Catalase)

Fig. 1.1 Catalytic cycle proposed for catalases and peroxidases.

organic substrate. This produces a second intermediate that is [Fe^{IV} porphyrin] **3**. Finally, [Fe^{IV} porphyrin] reduced back to the native ferric state with concomitant one electron substrate oxidation. Two one electron oxidized substrate molecules non-enzymatically disproportionate to give one two electron oxidized product and an unoxidized substrate molecule. The model complexes for the highvalent states of these enzymes have been reported by Groves[39], Balch[40], and others[41]. Recent work by Ortiz de Montellano and co-workers strongly suggests that the substrate oxidation reactions catalyzed by these enzymes take place at the heme edge and not at the oxo-ferryl group[42].

1.3 THERMODYNAMIC AND KINETIC ASPECTS OF ELECTRON-TRANSFER REACTIONS:

Consequences of light absorption by molecules is that it leads to an increase in the electron affinity and decrease in the ionization potential of the molecular systems. Hence an electronically excited state of a molecule is expected to be better oxidant and a better reductant relative to the ground state. It is known that those electronically excited states which, in fluid solution, live long enough to encounter a molecule of another solute, can often be involved in electron-transfer reaction[43]. The energetics of light induced charge separation is schematically represented in fig. 1.2 . The energetics of the radical – pair $D^+ \sim A^-$ (where D represents a porphyrin donor and A represents an acceptor) formation is dictated by both the oxidation potential of D and the reduction potential of 'A'. The free energy change accompanying the excited state electron-transfer (ΔG_{et}) can be expressed as[44]
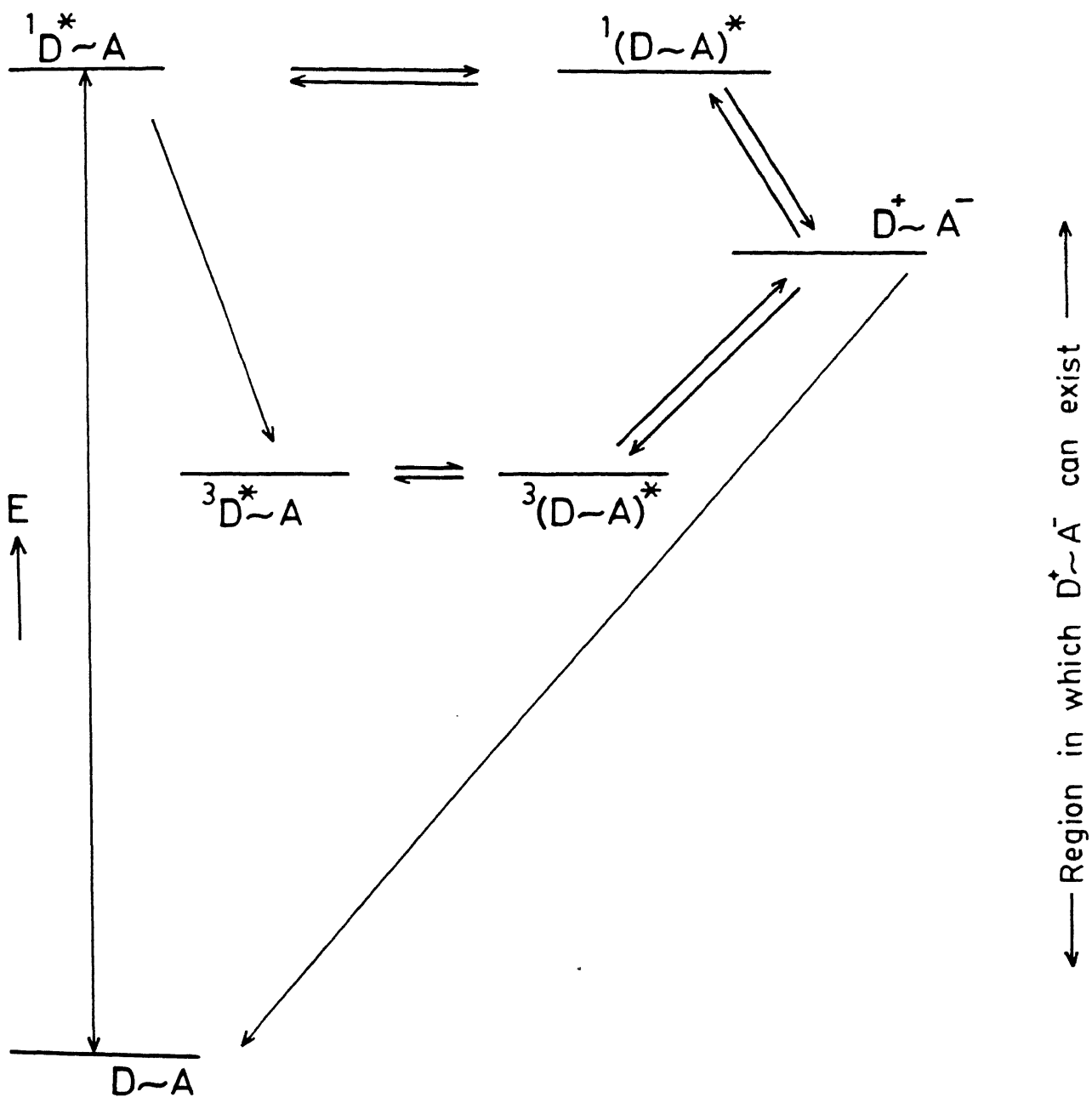
Fig. 1.2 Schematic representation of the possible events of photoexcited porphyrin in the presence of acceptor.

$$\Delta G_{et} = E(D^+/D) - E(A/A^-) - E_{o-o} \qquad 1.5$$

where $E(D^+/D)$ and $E(A/A^-)$ refer to one electron reduction potentials of the oxidized donor and the reduced acceptor, respectively and E_{o-o} refers to the first excited singlet/triplet state energy of the donor. This expression neglects coloumb interactions, solvation effects and entropy considerations. The thermodynamic criterion for a photoinduced electron transfer can then be formulated as that the singlet excitation energy should be more than that of the energy of the redox state.

Apart from the above thermodynamic considerations, the kinetic requirements also play an important role in electron-transfer processes. It is known that there exists always a competetion among the various intra and inter molecular deactivation pathways for an excited state. Thus, even if the electron-transfer is thermodynamically allowed it can take place only if it is fast enough to win the competetion with other intra and intermolecular deactivation processes. The kinetic theories developed for thermal electron-transfer processes can be applied to the excited state electron-transfer as well[45]. For an excited state electron-transfer, the kinetic scheme is as follows.

$$D^* + A \underset{K_{-d}}{\overset{K_d}{\rightleftharpoons}} (D^*A) \underset{K_{-et}}{\overset{K_{et}}{\rightleftharpoons}} [D^+A^-] \xrightarrow{K_s} \text{products} \qquad 1.6$$
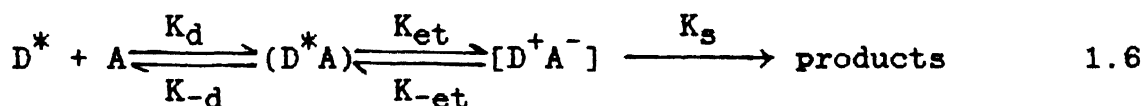
where K_d is the diffusion rate constant, K_{-d} is the dissociation rate of the precursor complex (D^*A). K_{et} and K_{-et} are the unimolecular rate constants for the electron transfer steps, and K_s includes all the steps (except K_{-et}) which cause the

disappearance of the successor complex (D^+A^-). Using a simple steady state treatment for this outer sphere electron-transfer, it can be shown that if $K_{-et} \ll K_s$ and $K_{et} \ll K_{-d}$

$$K_q = \left(K_d/K_{-d}\right) K_{et} \qquad 1.7$$

where K_q is the experimental rate constant for the reaction $D^* + A \longleftrightarrow D^+ + A^-$. The rate constant for the electron transfer step is given by

$$K_{et} = K_{et}^o \ \exp \left(- \Delta G^{\#} /RT\right)$$

$$= KK_BT/h \ \exp \left(- \Delta G^{\#} /RT\right) \qquad 1.8$$

where K_{et}^o is the frequency factor, $\Delta G^{\#}$ is the standard free-energy of activation, K is the transmission coefficient and $K_BT/h = 6 \times 10^{12} s^{-1}$ at 25^oC. It is assumed in the formulation of the above equation that the electron-transfer step must obey Frank-condon principle. Hence, the $\Delta G^{\#}$ in equation (1.8) can be expressed as

$$\Delta G^{\#} = \Delta G^{\#}(0)[1 + \Delta G/4 \Delta G^{\#}(0)]^2 \qquad 1.9$$

where $\Delta G^{\#}(0)$ is the so called intrinsic reorganization parameter, which is related to the changes in the nuclear coordinates that must occur prior to electron-transfer (both inner sphere and solvent induced) as required by the Frank-Condon principle. ΔG is the same as ΔG_{et} equation (1.5). The term K in equation (1.8) contains useful information regarding the electronic interaction between the donor and the acceptor which is governed by the extent and strength of orbital overlap between the donor and the acceptor.

The important parameters that govern the excited state electron transfer processes are:

(1)   The nature of the donor and its oxidation potential.

(2)   The nature of the acceptor and its reduction potential.

(3)   The distance between the donor-acceptor pair.

(4)   The orientation of the acceptor relative to the donor.

(5)   The nature of intervening medium.

Intermolecular interactions between porphyrins and several aromatic acceptor molecules result in quenching of the excited state of the porphyrin in fluid solutions[46]. This is often attributed to excited state electron-transfer leading to the redox ion intermediates. This can arise from either the excited singlet state or the triplet state and often the efficiency of these processes are known to be very low. Inpart, the low efficiency is due to the short life times of the porphyrin singlet excited state (typically nanosecond region) which require very high concentration of the quencher for bimolecular diffusion to compete with the nonradiative deactivation of the excited state. The triplet excited state, with its long lifetime (typically millisecond region) has no such problems and quenching can lead to high yields of redox ion intermediates. However, in several cases it has been established that the porphyrin triplet states cannot involve themselves in the electron-transfer reactions owing to the restrictive thermodynamic considerations[47].

1.4 IMPORTANCE OF NONPLANAR CONFORMATION OF A PORPHYRIN SKELETON IN BIOLOGICAL SYSTEMS:

The existence of porphyrin macrocycle in a variety of non-planar conformations is believed to be an important criterion for its involvement in several biomolecules of different functions. A brief survey on importance of nonplanar conformation in biological systems and the relevent model systems are highlighted in this section.

A recent review by Scheidt and Lee[48] has emphasised the relationship between stereochemistry of a variety of metallotetrapyrroles and their function. Work done on π-cation radical complexes, O_2 bound species, tetrapyrroles with N-substituents, the stereochemistry of ring reduced tetrapyrroles and other novel porphyrin systems are highlighted in this review. Furthermore, the importance of porphyrin-porphyrin (π-π) interaction in the solid state has been described. Fajer et al.[49] have studied the interaction of iron porphyrins and its radical cation. In this system there is a strong antiferromagnetic coupling between the metal center and radical center and this has been attributed to the distorted conformation of the porphyrin macrocycle.

Kratky and Coworkers[50] reported X-ray structures of several low spin Ni(II) hexahydro and tetrahydroporphinoids (Fig. 1.3). The co-ordination hole contraction is characterized by a deformation of the ligand system towards a saddle shaped, ruffled conformation of approximate S_4 symmetry. The central metal ion is coplanar with the four co-ordinating nitrogen centers whereas the four meso carbon atoms are situated alternatively above and below this co-ordination plane. Increasing steepness of the
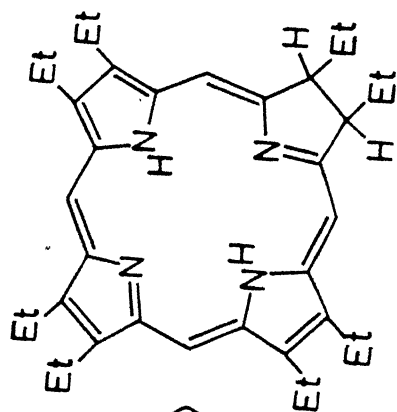
PHLORIN

OCTAETHYL CHLORIN

OCTAETHYL ISOBACTERIOCHLORIN

TETRAPHENYL CHLORIN

OCTAETHYL BACTERIOCHLORIN

Fig. 1.3 Structures of various reduced porphyrins.

saddle is associated with decreasing metal nitrogen distances. In the saddle conformation of hydroporphinoid Ni(II) complexes, the hydropyrrole rings assume half chair conformations whereby the individual half chairs are conformationally constrained in such a way that the inclination of their peripheral single bond parallels the inclination of the ligand saddle. The co-ordination hole contraction of hydroporphinoid ligands is observed experimentally to exert control on the stereochemistry and reactivity of the ligand periphery as well as on the axial electrophilicity of the central metal ion.

Stolzenberg and Coworkers[51-56] in a recent series of papers have related the distorted conformation of Nickel hydroporphyrins with stability of the macrocycle. X-ray structural studies show that the macrocycle in nickel hydroporphyrin complexes invariably experiences a marked S_4 ruffling and is saddle shaped. Ruffling is a consequence of the flexibility of hydroporphyrins. The chemical and electrochemical oxidations of Ni porphyrin, chlorin, and isobacteriochlorin complexes in the octaethyl and methyl-substituted octaethyl chlorin series were investigated in nonaqueous media, EPR and absorption spectroscopy were used to characterize the one and two electron oxidized complexes. The first oxidation of all complexes yielded nickel (II) cation radicals. Unlike Ni(TPP)$^{+\cdot}$, the cation radical complexes did not undergo internal electron transfer to afford nickel(III) complexes at low temperatures. Nickel(II) dication complexes were the product of the second oxidation of nickel porphyrins and chlorins in acetonitrile. The second oxidation of nickel isobacteriochlorins afforded nickel(III) cation radical complexes. These results suggest that the greatly enhanced

stability of oxidized cis- Ni(OEC) species is not a consequence of redox activity of the coordinated nickel but rather of the ruffled conformation of the macrocycle. Also, the chemical and electrochemical reductions of Nickel porphyrin and hydroporphyrin complexes in the octaethyl, tetraphenyl, and methylated octaethyl chlorin series were investigated in nonaqueous media. UV-vis, EPR, and ^{1}H NMR spectroscopy were used to characterize the reduced species obtained by electrochemical and chemical means. The site of reduction depends upon the method of reduction (and the time scale of the method), the saturation level of the macrocycle, and the identity of these substituents on the macrocycle. Ni(OEP) is reduced to the anion radical Ni(OEP)$^{\cdot-}$, which undergoes further reduction to afford the stable, diamagnetic phlorin anion complex Ni(OEPH)$^-$. Ni(OEC) and Ni(DMOEiBC) are reduced to transient Ni(I) complexes. Ni^I(OEC)$^-$ reacts further to give the chlorin-phlorin anion complex Ni(OECH)$^-$, Ni(OEiBC) is reduced to Ni^I(OEiBC)$^-$. Aside from reduced F$_{430}$, Ni^I(OEiBC)$^-$ is the first stable Ni(I) tetrapyrrole and is the only known nickel(I) complex that has a π-system extending over the entire macrocycle. Chemical reductions of Ni(TPP), NiTPC and Ni(TPiBC) produce mixtures of anion radical, phlorin anion, and phlorin dianion species. The macrocycle that appear best able to accomodate the large, approximately 2.1 A$^\circ$ Ni-N distance required by Ni(I) are those that were shown to ruffle in neutral, low-spin nickel(II) complexes. One consequence of ruffling is a reduction in the macrocycle core size to give smaller Ni-N distances (1.92 A$^\circ$) than typically observed in a porphyrin environment. Apparently, the hole size/ligand field strength of hydroporphyrins can be varied over

a wide difference between porphyrins, hydroporphyrins, corrins, oxoporphyrins and other tetrapyrrole macrocycles is their optimal hole size and the range of hole sizes that are readily accessible in their complexes. The effects of the stereochemistry of the macrocycle substituents are discussed, and an explanation is developed for the widely varying affinities of Nickel tetrapyrroles for axial ligands.

The X-ray structure of heme proteins by Perutz et al.[57] and Deathearage et al.[58] conforms the presence of porphyrin macrocycle in a domed conformation. The conformation of the heme groups and their interactions with the globin are altered. Short contacts with globin side chains effect cyanide binding to the hemes, and change in the globin ligand contact upon substitution of cyanide for H_2O inturn directly effects the globin structure. Although the ligand peaks lie off the heme axes, the atoms Fe-C-N may still lie on a straightline, with this line not normal to the mean heme plane. This linear binding conformation is consistent with the observed motion and deformation of the porphyrin.

Recent X-ray structure on the reaction center (RC) of Rhodopseudomonas viridis by Deisenhofer and Coworkers[59] have demonstrated the existence of nonplanar macrocycles in the bacterial photosynthetic reaction center (RC). In these chlorophyll molecules, twisting of the pyrrole rings by as much as 17° is observed for several of the tetrapyrroles including the bacteriochlorophylls of the special pair (RC). On excitation of the RC leads to charge separation and electron transfered through a series of acceptors from the bacteriochlorophyll b dimer to Quinones.

Pfaltz et al.[60] and Furenlid et al.[61] have reported the presence of nonplanar macrocycles in enzyme methyl reductase which is isolated from <u>Methanobacterium thermoautotrophicum</u>. It consists of cofactor F_{430} (Fig. 1.4). F_{430} is a nickel (II)-corphin derivative, which has all four pyrrole rings and two of the four bridging meso carbon atoms reduced. Related Ni Corphinates exhibit some of the most nonplanar tetrapyrrole structures known. This enzyme catalyses the final stages of reduction of CO_2 to methane in methanoic bacteria. Detection of EPR signals attributable to Ni(I) in the catalytic cycle of <u>Mb. Thermoautotrophicum</u> has led to intensive investigations of the reductive chemistry of F_{430} and of Ni porphyrins and hydroporphyrins. Reduction of Ni(II) F_{430} and isobacterio chlorins unabiguously results in Ni(I) species where as porphyrins, chlorins and hexahydro and octahydro porphyrins yield anions variously ascribed to Ni(I) or N(II) radicals with some metal character.

In model systems distortion in the porphyrin skeleton can be induced by attaching a short bridge across the porphyrin periphery. To the best of our knowledge there are only two reports in literature where considerable distortion of the porphyrin skeleton upon introduction of short bridging group has been achieved. Thus, Dolphin and Coworkers[62] have characterized pyrrole strapped porphyrins and preliminary X-ray data confirms the expected distortion. On the other hand Walker and coworkers[63] used very short alkyl chains (butyl, pentyl, hexyl) as a bridging group. Spectroscopic and X-ray data of one of the isomers confirms the presence of distortion in the porphyrin skeleton.
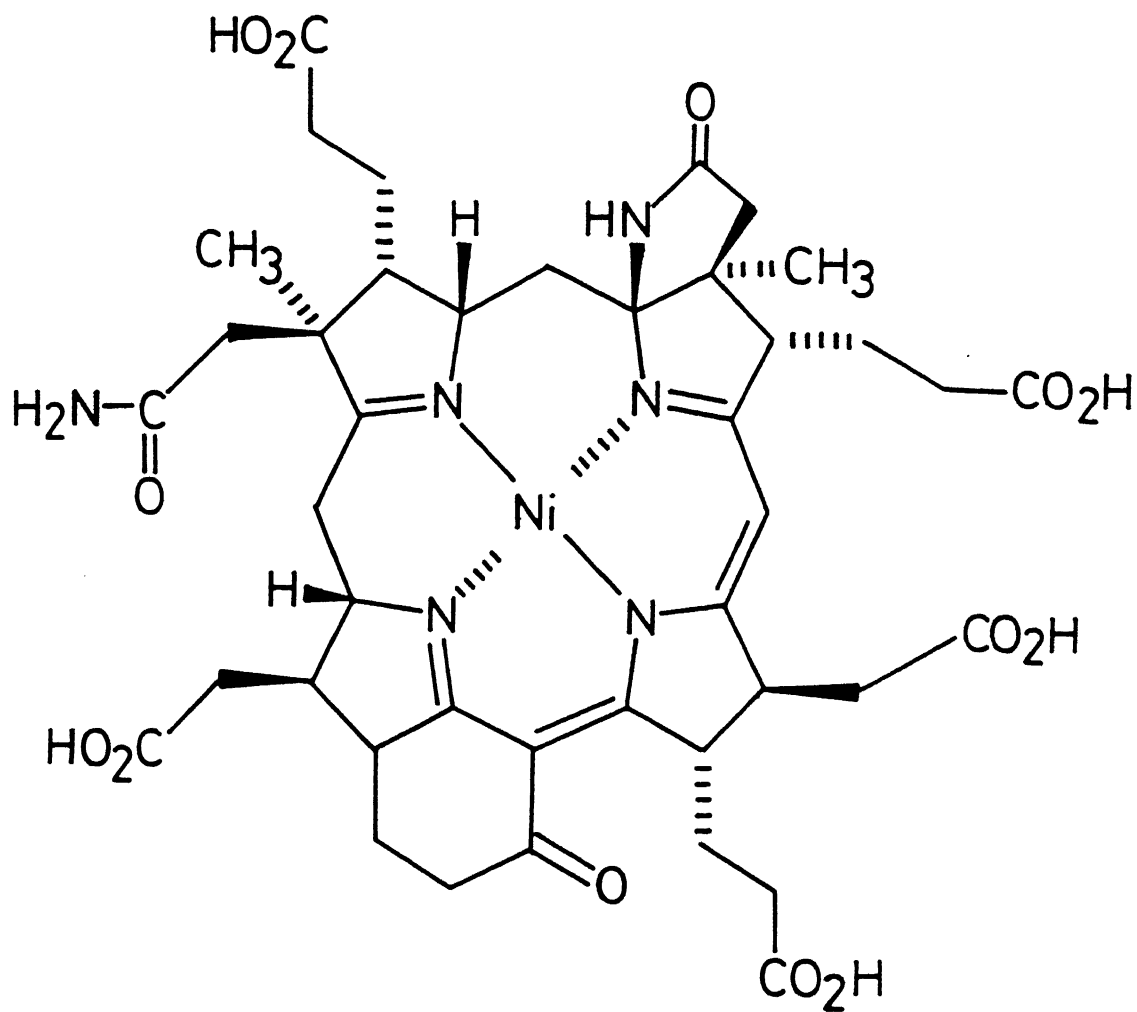
Fig. 1.4 Structure of co-factor F_{430}

Thus, in 'this thesis an attempt has been made using the porphyrins, metalloporphyrins and crowned phthalocyanines as model systems to study the various electronic interactions between the π-systems. The details of the work has been described in the following chapters.

CHAPTER 2

GENERAL EXPERIMENTAL METHODS AND TECHNIQUES

In this chapter, the materials employed at the various stages of investigation, a description of the methods used to synthesize the precursor compounds for various porphyrins and phthalocyanines, and the purification procedure of the chemicals and solvents are given. Also, brief outline of the physico-chemical techniques employed and details of the instruments used are given.

2.1 MATERIALS EMPLOYED:

The common solvents used for synthesis were purified according to the reported procedures.[64]

Pyrrole, salicylaldehyde and Benzo-15-crown-5 were procured from "Aldrich chemical company, USA" and pyrrole was distilled before use (b.P-129-131°C).

Solvents for NMR measurements, $CDCl_3$, $DMSOd_6$, C_6D_6, D_2O, CD_3OD, TFAd and Pyridine d_5 were also obtained from "Aldrich chemical Company, USA" and were used as received.

p-Anisaldehyde, 2-(dimethylamino)ethanol, p-xylene, m-xylene, ortho nitroaniline and Tetrabutylammonium bromide were procured from "Merck chemical company, W. Germany" and were used as received.

Buffer tablets (PH7) and anhydrous potassium carbonate (K_2CO_3) were obtained from "Qualigens fine chemicals, Bombay, India" and were used as received.

Adenine, Guanine, Cytosine and Thymine were procured from "Sisco Research Laboratories, India" and were used without further purification.

Aluminium oxide (basic and neutral) and Silicagel (60-120 mesh) were purchased from "Acme Laboratory chemicals, Bombay, India" and were used as received.

Dimethyl formamide (DMF) A.R. grade and Iron powder were procured from "Sarabhai chemicals, India" and were used as received.

Sodium acetate, KCl, CsCl (AR grade) were purchased from "B.D.H., India" and were used as received.

Benzaldehyde (A.R. grade), N-bromosuccinamide (NBS), potassium cyanide, sodium metabisulfite, KOH, NaOH, Bromine, Glycerol, propionic acid (L.R. grade), pyridine, chloroform, dichloromethane, Methanol, petroleum ether (60-80°C), Toluene, diethylether, acetic acid, 1,2 dichloroethane, Dimethyl-sulfoxide, Conc. H_2SO_4, Conc.HCl and Conc.HNO_3 were procured from "S.d.fine chemicals, India".

2.2 METAL SALTS EMPLOYED:

Cobalt(II)acetate tetrahydrate, copper(II) acetate monohydrate, Nickel(II) acetate tetrahydrate, Zinc(II) acetate dihydrate, vanadylsulphate pentahydrate were of A.R. grade obtained from "S.d. fine chemicals, Bombay, India" and were used as received.

Copper(II) sulfate and Silver nitrate were obtained from "Nice chemical company, India" and were used as received.

2.3 SOLVENTS EMPLOYED FOR SPECTROSCOPIC MEASUREMENTS:

The following solvents were used for spectroscopic measurements:

(a) Chloroform (A.R. grade) from S.d.fine (India) was distilled over P_2O_5 [64].

(b) Dichloromethane (L.R. grade) from S.d.fine (India) was washed twice with 10% aqueous Na_2CO_3 solution, twice with water, dried over anhydrous $CaCl_2$ and distilled over P_2O_5 [64].

(c) Methanol (L.R. grade) from S.d.fine (India) was refluxed over calcium oxide for 2 hours and then distilled over Magnesium methoxide cake[64].

(d) Benzene (L.R. grade) from S.d.fine (India) was stirred with Conc.H_2SO_4 for 3-4 hours. It was then washed with sodium bicarbonate solution followed by distilled water. It was dried over anhydrous $CaCl_2$ overnight, distilled and stored over sodium wire.

(e) Dimethylformamide (DMF) from "Sarabhai Chemicals" (India) A.R. grade, was used as received.

(f) Toluene (spectroscopic grade) from S.d. fine (India) was used as received.

2.4 SYNTHESIS OF 4,6-DINITROBENZOFUROXAN (BFO):

The synthesis of BFO involved two steps.

(a) Preparation of Nitrosobenzene[65]:

10g. of ortho-nitroaniline was dissolved in 150 ml of saturated alcoholic potassium hydroxide. A solution of sodium hypochlorite, prepared by passing Cl_2 gas through a solution of sodium hydroxide in water till the solution turns yellow, was added to a cooled solution of ortho-Nitro aniline in alcoholic KOH with constant shaking until the crimson colour had entirely disappeared. Then the mixture was poured into an open dish and

left to crystallise. 9.5 g of the product, nitrosobenzene, separated out in a pure state. It was crystallised from ethanol to get yellowish white needles (m.p. 72°C).

(b) **Preparation of 4,6-dinitrobenzofuroxan from nitrosobenzene[66]:**

10 g of nitrosobenzene dissolved in about 150 ml of Conc.H_2SO_4 was nitrated by the addition of a mixture of 15 ml of Conc.HNO_3 and 40 ml of Conc.H_2SO_4. The mixture was cooled at first and then warmed to 40°C and poured into water. The product, crystallised from acetic acid, gave yellow needles m.P. 172°C.

λ_{max} (nm) in CH_2Cl_2

233, 261, 276, 333, 422 (observed).
234, 260, 277, 330, 420 (lit.[67]).

2.5 PREPARATION OF COPPER(I) CYANIDE[64]:

50 g (0.2 mol) of powdered Copper(II) sulphate pentahydrate was dissolved in 160 ml of warm water (40-50°C) in a 500 ml beaker equipped with stirrer. Prepared solutions of 14 g (0.074 mol) of sodium metabisulphite in 40 ml of water (A) and of 14 g (0.215 mol) of potassium cyanide in 40 ml of water (B), and filtered the solutions A and B to remove insoluble matter. The solutions A and B was heated separately at 60°C. Copper(II) sulphate solution was made faintly acid to congo red with dilute H_2SO_4 and solution A added to it with mechanical stirring during 1 or 2 minutes, followed immediately by solution B. A slight frothing was observed. Filtered the hot solution after about 10

minutes and washed product thoroughly with boiling water and finally with rectified spirit. Dried at 100-110°C to a fine soft powder. Yield: 16.7 g (93%).

2.6 PREPARATION OF α, α'-DIBROMO m-XYLENE[68]:

A 500 ml three necked round bottomed flask was fitted with a dropping funnel with the tip extended to reach almost bottom of the flask and an efficient condenser leading to a gas absorption trap. m-xylene (53 g, 0.5 mole) was placed into the three necked flask which was heated with an oil bath and was illuminated with table lamps (3x200 watt lamps) placed 1-5 cm from the upper portion of the flask. When the temperature of m-xylene reached 125°C, dropwise addition of 176 g (1.1 mole) of bromine was commenced with stirring over a period of 1.5 hours. The mixture was stirred at 125°C under illumination for an additional 30 minutes. It was then allowed to cool to 60°C and poured into 100 ml of boiling (60-68°C) petroleum ether contained in a beaker, the transfer being assisted with small amounts of warm solvent. As the homogeneous solution cooled slowly to room temperature it was stirred frequently to prevent caking of the brown crystalline product that separated. After the mixture was cooled and the bulk of the dibromide had crystallised, the beaker was placed in a refrigerator for 12 hours. The product was filtered and washed twice with petroleum ether (60-80°C) (2x25 ml). The crude product which was recrystallized from chloroform- ethanol (3:1) gave pure product. m.P: 75-77°C, yield: 48%. ^{1}H NMR (CDCl$_3$): 4.43 ppm (4H, s,-CH$_2$-); 7.23 ppm (m, 4H, phenyl).

2.6 PREPARATION OF α, α'-DIBROMO p-XYLENE[68]:

Followed same procedure as mentioned for preparation of α, α' dibromo-m-xylene. m.P: 145-147°C; yield: 60%.
^{1}H NMR (CDCl$_3$): 4.4 ppm (4H, s, -CH$_2$); 7.3 ppm (4H, s, phenyl).

2.7 PREPARATION OF TETRABUTYLAMMONIUM PERCHLORATE (TBAP):

50 gr (0.16 mole) of tetrabutylammonium bromide was dissolved in 500 ml of distilled water and a white precipitate was obtained on addition of 31.16 gr (0.31 mole) of perchloric acid (99.9%). The precipitate was filtered and the crude product was washed with large excess of water to remove excess perchloric acid. The crude product was recrystallized from ethanol; it gave pure white crystalline tetrabutylammonium perchlorate (TBAP).

2.8 PHYSICO-CHEMICAL TECHNIQUES:

The details of the instruments used for characterization and evaluation of spectroscopic data are given below:

The optical absorption spectra were recorded on a SHIMADZU UV-160 Spectrophotometer with temperature facility. ^{1}H and ^{19}F NMR spectra of cobalt porphyrins were recorded on a Jeol Fx 90 Q multinuclear NMR spectrometer. ^{1}H NMR of other compounds were recorded on a Bruker 400 MHZ, Bruker 270 MHZ and Varian (Model JEMNI) 200 MHZ NMR spectrometers. ESR measurements were made on a Varian E- 109 x-band spectrometer at liquid nitrogen temperature. IR spectra were recorded on a perkin-Elmer model 580 Infrared spectrophotometer. FAB Mass spectra were taken on JMS 01SG2 (Jeol) Mass spectrometer.

Cyclic voltammetric studies were made with a BAS Model CV-27 polarographic analyzer utilizing the three electrode configuration of a Glossy Carbon (working electrode), Pt wire (counter electrode) and a Ag/AgCl electrode as the reference electrode. An omnigraphic Model 100 x-y recorder was used to record the current voltage output. Half wave potentials were measured as the average of cathodic and anodic peak potentials.

Fluorescence spectra were recorded either on a Spex Romalog System with Spex photon counting and Spectra physics model 165 Ar-ion laser (λ_{exc} = 528 nm) as the excitation source, or on Jobin Yvon Spectrofluoremeter model JY-3CS.

The triplet ESR measurements were made on VARIAN E-9 X-band spectrometer. The spectra were recorded with and without field modulation at -150°C. The pulsed laser (wavelength 560 nm) source was used for photoexcitation. In method (A) the field modulation used was 100 KHZ and light intensity modulation of 80 HZ with detection employing a pair of lock-in-amplifier tuned to the modulation frequencies. The field modulation amplitude employed was 40 G and the microwave power about 5 mW. The ESR signals were measured 0.5μs after laser excitation. The spectra were recorded in the derivative form and by using light modulation a doublet radical signal in the center of the spectrum is removed. Also, this detection method takes advantage of the signal enhancement provided by spin polarization. In the method B, no field modulation was used and the signal was detected after 1μs of the laser excitation; with this technique the signal to noise ratio is improved because of the large spin polarization in the triplets shortly after their formation. The spectra were

obtained in this method using absorption mode (not derivative mode).

2.9 METHODS:

The fluorescence quantum yield, ϕ_f was estimated from the emission and the absorption spectra following the equation[69];

$$\phi_f = \{[F(sample)]\ [A(H_2TPP)]/[F(H_2TPP)][A(sample)]\}\ \phi_f(H_2TPP)$$

where the [F(sample)] and [F(H_2TPP)] are the integrated fluorescence intensities of the sample and 5,10,15,20-tetraphenyl porphyrin (H_2TPP). [A(sample)] and [A(H_2TPP)] are the absorbance of sample and H_2TPP at excitation wavelength and $\phi_f(H_2TPP)$ is the quantum yield of H_2TPP which is taken as 0.11.[70] The natural radiative life times (τ^o) were calculated from the absorption and the emission spectra using Birks-Dyson[71] modification of Strickler-Berg[72] equation which is based on mirror symmetry between the absorption and emission spectra, following the equations;

$$1/\tau^o = 2.880 \times 10^{-9}\ \eta^2\ <\ \bar{\nu}_f^{-3}>_{av}^{-1}\int \varepsilon(\bar{\nu})\ \bar{\nu}^{-1}d \qquad\qquad 2.1$$

where η is the Index of refraction of the solvent used $<\ \bar{\nu}_f^{-3}>_{av}^{-1}$ is the reciprocal of the mean value of $\bar{\nu}^{-3}$ in the fluorescence spectrum, and this is defined by following relation;

$$<\ \bar{\nu}_f^{-3}>_{av}^{-1} = \int F(\bar{\nu})d\bar{\nu}\ \Big/ \int F(\bar{\nu})\ \bar{\nu}^{-3}\ d\bar{\nu} \qquad\qquad 2.2$$

where $\int F(\bar{\nu})\ d\bar{\nu}$ is the Integrated fluorescence intensity and was evaluated directly from fluorescence spectrum by calculating the area under the curve of $F(\bar{\nu})$ versus $\bar{\nu}$.

$\int F(\bar{\nu}) \bar{\nu}^{-3} d\bar{\nu}$ was evaluated from modified fluorescence spectrum by calculating the area under the curve of $F(\bar{\nu}) \bar{\nu}^{-3}$ versus $\bar{\nu}$.

$\int \mathcal{E}(\bar{\nu}) \bar{\nu}^{-1} d\bar{\nu}$ was calculated by evaluating area under the absorption [$Q_x(0,0)$ and $Q_y(0,0)$] curve of $\mathcal{E}(\bar{\nu}) \bar{\nu}^{-1}$ vs $\bar{\nu}$. where $\mathcal{E}(\bar{\nu})$ is the molar extinction coefficient as a function of wave number ($\bar{\nu}$) and $F(\bar{\nu})$ is the fluorescence intensity as a function of wave number ($\bar{\nu}$).

The rate of fluorescent radiative decay (K_f) and rate of intersystem crossing (K_{isc}) were calculated using the relation:

$$K_f = 1/\tau^0 \qquad\qquad 2.3$$

$$K_{isc} = \{K_f[(1 - \phi_f)/ \phi_f]\} \qquad 2.4$$

The excited state redox potentials were estimated from the emission spectra and the ground state redox potentials following the relation.[73]

$$^*E^0(P^+/^*P) = E^0(P^+/P) - E_{o-o}(P-^*P) \qquad 2.5$$

$$^*E^0(^*P/P^-) = E^0(P/P^-) + E_{o-o}(P-^*P) \qquad 2.6$$

where the $E_{o-o}(P-^*P)$ is the energy of the $Q_{(0,0)}$ transition of the emitting excited state of the porphyrin, $^*E^0(^*P/P^-)$ and $^*E^0(P^+/^*P)$ are excited state reduction and oxidation potentials respectively and $E^0(P^+/P)$ and $E^0(P/P^-)$ refer to the ground state oxidation and reduction potentials respectively.

2.10 SUMMARY:

A brief account of various solvents, chemicals and methods of preparation of the starting materials used in the synthesis is given here. This chapter also describes the different spectrometers and other physical methods used in the present study.

CHAPTER 3

INTERACTION OF METALLOPORPHYRINS WITH AN ELECTRON ACCEPTOR, 4, 6 DINITROBENZOFUROXAN (BFO)

3.1 INTRODUCTION

Electron- transfer reactions of porphyrins and metallo-porphyrins have been studied in great detail during the past decade because of their involvement as electron-transfer agents in many biological reactions involving heme proteins,[74,75] photosynthetic reaction centers[59b,76-77] and artificial photocatalytic systems.[78-80] The addition or removal of an electron from metalloporphyrins could involve both the porphyrin Π-system and the central metal ion in the porphyrin core.[81,82] It is generally observed that for porphyrins containing metals like Zn, Cu, Cd, the first electron addition or removal involves the porphyrin Π-system. Their redox chemistry is a subject of numerous studies and the redox products have been characterised by spectroscopic,[83,84] electrochemical[85,86] and chemical methods.[87,88] On the other hand, porphyrins containing metals like Co, Fe and Mn fall into the second category where the metal ion participates in the redox chemistry.[27,28,89] In this regard cobalt (II) porphyrins have been widely studied and it has been shown that Co(II) porphyrins undergo facile oxidation to their cobalt(III) derivatives under a variety of conditions.[29-33,90,91] One such condition demands the presence of molecular oxygen and a donor axial ligand where the donor ligand co-ordinates to the metal center promoting electron transfer from cobalt to molecular oxygen.

Nitroaromatics have been employed as acceptors in the study of varioous electron donor-acceptor interactions. Among these, benzofuroxan and its nitro derivatives are shown to function as strong π-acceptors. An examination of the structure of 4,6-dinitrobenzofuroxan (BFO) shows two resonance structures, with following cannonical forms indicating a planar hybrid structure.
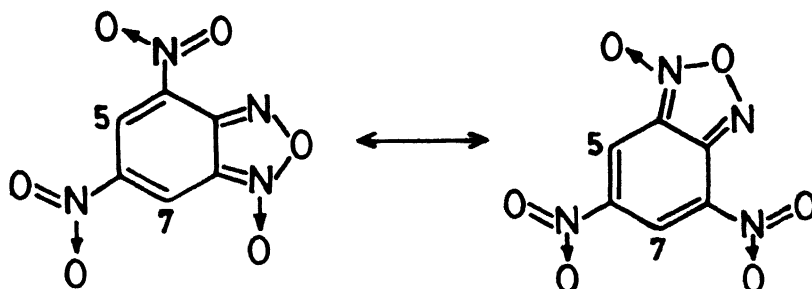
A survey of the work done on the molecular complexes of Benzofuroxan with various donors are given below.

Drost[92] was first to report the charge-transfer complexation of 4,6-dinitrobenzofuroxan with napthalene donor. Though a crystalline solid was reported to have isolated in the study, no X-ray crystal structural studies are available. Later, the acceptor abilities of a series of nitrobenzofuroxans with aromatic donors, napthalene, 2-phenylnapthalene, 1-phenyl napthalene, 1-n-hexyl napthalene and tetrahydronapthalene have been evaluated using spectral studies.[93] These investigations reveal that the relative order of acceptor strengths vary as Benzotrifuroxan > Nitrobenzo difuroxan > 4,6-dinitrobenzofuroxan > 5,6-dinitrobenzofuroxan. Nitrobenzofuroxans form coloured compounds on complexation with substituted benzenes exhibiting charge-transfer band at 478 nm in chloroform.[94] The formation of electron donor-acceptor complexes of nitrobenzofuroxans with indole, xylene, octahydroanthracene etc. have also been reported.[94]

A report on the molecular complexation of benzofuroxans with two porphyrins, Co(II) meso-porphyrin IX dimethylester and Co(II) etioporphyrin have been described by Hill et al.[95] These studies are restricted to the evaluation of binding constants and the associated thermodynamic parameters for the charge-transfer complexes formed. In this chapter, the studies on the interaction of metalloporphyrins (M = Co^{2+}, Zn^{2+} and Cu^{2+}) and Cobalt tetraphenyl chlorin (CoTPC) with 4,6-dinitrobenzofuroxan (BFO) (Fig. 3.1) monitered by spectroscopic methods have been described. Initially all the metalloporphyrins form molecular complexes with the electron acceptor BFO. However with time only cobalt (II) porphyrins and Co(II)TPC undergo oxidation to the corresponding Co(III) derivatives resulting in the formation of cobalt(III) porphyrins and the anion radical of BFO. The electron-transfer is facilitated in the presence of molecular oxygen. The rate of oxidation is found to be dependent on the porphyrin ring substituents as well as on the solvent mixture used. In the case of CoTPC, first the oxidation of cobalt(II) TPC to cobalt(II)TPP occurs and this is followed by metal oxidation to give the cobalt(III) porphyrin. The oxidation of the cobalt(II) porphyrins and formation of the anion radical of BFO has been monitored with the aid of ESR. The g-value and the line width of the BFO⁻ radical compare well with that of the anion formed by chemical reduction. ^{1}H and ^{19}F NMR data confirm the occurrence of the electron-transfer reaction.

3.2 EXPERIMENTAL

Purification of solvents for spectral studies and the synthesis of 4,6-dinitrobenzofuroxan have been described in chapter 2.

2

R = C6H5 ; CoTPC

3

BFO
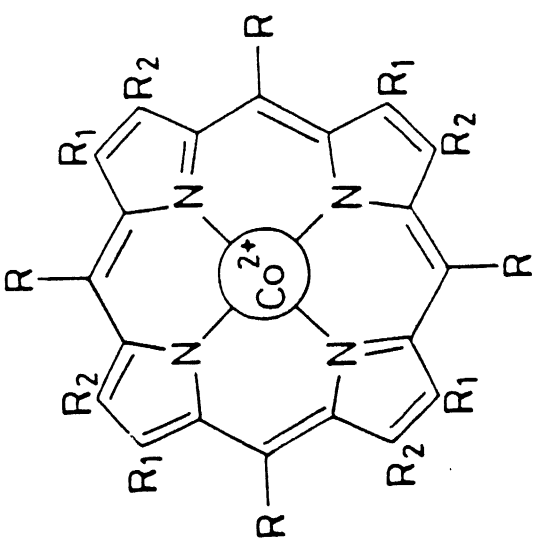
1

1a) R = C_6H_5 , $R_1 = R_2 = H$; CoTPP

1b) R = C_6D_5 , $R_1 = R_2 = H$; CoTPP(d_{20})

1c) R = —⟨benzene⟩—OCH_3 ; $R_1 = R_2 = H$; CoTPP(OCH_3)$_4$

1d) R = C_6F_5 , $R_1 = R_2 = H$; CoTPP(F_{20})

1e) R = C_6H_5 , $R_1 = Br$; $R_2 = H$; CoTPP(Br_4)

1f) R = H , $R_1 = R_2 = C_2H_5$; CoOEP
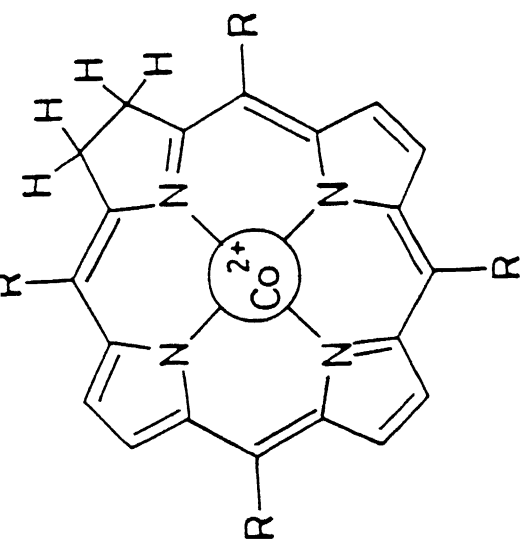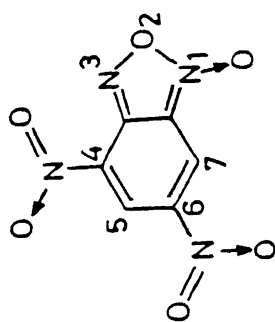
Fig. 3.1 Molecular structures of various cobalt(II) tetrapyrroles

and 4,6-dinitro benzofuroxan (BFO).

H_2TPP[96], H_2TPPd_{20}[97], $H_2TPP(OCH_3)_4$,[98] H_2TPPBr_4[99] were prepared following the literature procedures. H_2TPPF_{20} and H_2OEP were procured from Aldrich chemicals, USA. Tetraphenyl chlorin (H_2TPC) was prepared from H_2TPP by Whitlock's procedure.[100] The purity was checked by visible absorption and NMR spectra.

λ_{max}(nm)(ϵ)$CHCl_3$: 651 (41×10^3); 597 (6.0×10^3); 546 (11.5×10^3); 519.5 (16×10^3); 419 (18×10^4).

^1H NMR ($CDCl_3$): -1.44 PPm (2H, s, NH); 4.16 PPm (4H, s, β-CH_2), 7.6-8.2 PPm (20 H, m, Phenyl); 8.4-8.6 PPm (6H, m, pyrrole).

3.2.1 General method of preparation of Cobalt(II) porphyrins[101]

Cobalt(II)porphyrins [Co(II)P] were prepared by refluxing H_2P(P = porphyrin) and cobalt acetate in freshly distilled DMF containing a drop of acetic acid for 6 hours. The solvent was removed under reduced pressure and the resulting solid was washed with water to remove excess cobalt acetate. The crude product was purified by column chromatography over basic alumina using $CHCl_3$ as the eluent. Initially, the unreacted free base porphyrin moved as a purple band followed by the cobalt porphyrin which came as a reddish band. The pure cobalt porphyrin was obtained after recrystallization from $CHCl_3$:MeOH (1:1). The purity of these cobalt porphyrins was checked by visible absorption spectroscopy. The absorption data (Table 3.2) are in good agreement with literature values.[102]

CuTPP and ZnTPP were prepared using a similar method. Cu(II)acetate and Zn(II)acetate were employed as metal carriers. The visible absorption spectral data of CuTPP and ZnTPP are as follows.

CuTPP in benzene.

λ_{max}(nm)(log ϵ) :

580 sh (3.34), 541(4.32), 417(5.64) (observed)

580 sh (3.34), 540(4.30), 417(5.65) lit.[102]

ZnTPP in Benzene:

λ_{max}(nm)(log ϵ):

588(3.62), 512(3.5), 548(4.38) and 422(5.75) (observed).

589(3.62), 512(3.51), 548(4.38) and 422(5.75) lit.[102]

3.2.2 Preparation of Co(II) tetraphenyl chlorin (CoTPC):

Cobalt(II) TPC was prepared by refluxing H_2TPC (20 mg) and cobalt acetate (16 mg) in a mixture of freshly distilled DMF (10 ml) and acetic acid (10 ml) for 6 hours under argon. The solvent was removed under reduced pressure and the crude product obtained was washed with water to remove excess cobalt acetate and the resulting solid was dried. Recrystallization from $CHCl_3$-petroleum ether (1:1) afforded pure crystalline solid (14 mg, yield - 64%). Purity was checked by visible absorption spectrum in chloroform.

$$\lambda_{max} (nm) (\epsilon): 615 (14.07 \times 10^3); 570 \text{ sh}; 528(6.34 \times 10^3)$$
$$\text{and } 411 (11.33 \times 10^4)$$

3.2.3 Preparation of Co(III) TPP (OCH$_3$)$_4$Cl

Co(II) TPP(OCH$_3$)$_4$ (0.15 g) was suspended in methanol (150 ml) containing concentrated hydrochloric acid (1.5 ml). The suspension was stirred at room temperature in an open flask for several hours, till the solution gradually changed to reddish purple. The solution was filtered and concentrated under

reduced pressure. The separated crystalline solid was collected, washed with water, and then with a small amount of a methanol-water mixture (2:1), dried at room temperature, and was recrystallized from methanol and then from chloroform - ether (yield, 0.1 g). The purity was checked by visible absorption spectrum in chloroform, λ_{max} (nm) : 546, 581, 429; compares well with literature report.[103]

The CoTPP(d_{20})Cl was prepared using a similar method. H$_2$TPP(d_{20}) used as the starting material. The purity was checked by visible absorption spectrum in chloroform.

λ_{max} (nm) : 549.5, 586, 433.5.

3.3 RESULTS AND DISCUSSION:

3.3.1 Studies on Zn^{2+} and Cu^{2+} porphyrin derivatives:

The metal derivatives of H$_2$TPP and H$_2$TPP(OCH$_3$)$_4$ (M = Cu^{2+} and Zn^{2+}) exhibited intense absorption bands (Q-bands) in the visible region (500-600 nm) in chloroform. The electron acceptor, BFO has no absorption in this region and shows intense absorption only in UV region (see chapter 2 for details). Addition of increasing amounts of BFO to CHCl$_3$ solutions of metalloporphyrins (M = Zn^{2+} and Cu^{2+}) progressively decreased the intensity of the Q-bands of the donors with the appearance of isosbestic points with broadening of the Q-bands indicating the possible formation of molecular complexes between metalloporphyrin and BFO. The association constants for the interaction were evaluated by NMR method monitoring the proton chemical shifts observed for the BFO protons upon increasing addition of ZnTPP. A typical procedure is given below.

A stock solution of ZnTPP was prepared by weighing definite amount of ZnTPP (30 mg) into a 10 ml volumetric flask. This was dissolved in $CDCl_3$ containing 1% TMS and made up to the mark. In a similar manner the acceptor, BFO (25 mg) was weighed out into a 10 ml volumetric flask and was dissolved in $CDCl_3$ containing 1% TMS. 0.5 ml of the acceptor solution was added to each of the six NMR tubes. The resonance positions of the acceptor protons were recorded. Now, varying amounts of (0.1 ml - 0.5 ml) ZnTPP stock solution was added to each NMR tube containing 0.5 ml of BFO. The ^1H NMR spectra were recorded immediately after mixing. The concentrations of BFO and ZnTPP employed are given in Table 3.1.

The ^1H NMR spectrum of BFO in $CDCl_3$ consists of resonances centered at 9.15 ppm and 8.85 ppm corresponding to H^7 and H^5 protons respectively. It was found that the proton resonances of BFO shifts to higher field on increasing addition of ZnTPP. The multiplet structure of H^5 and H^7 proton resonances of BFO remained unaffected. The ^1H NMR shifts of BFO protons on addition of ZnTPP in $CDCl_3$ are given in table 3.1. The shifts experienced by BFO protons are analysed as follows. The formation of a 1:1 molecular complex can be described by the following equation,

$$D + A \rightleftharpoons DA \qquad\qquad 3.1$$

where D is the donor Zn porphyrin and A is the acceptor, BFO. It has been shown earlier[104] that the observed proton resonance shifts of the acceptor on addition of increasing amounts of donor are proportional to the association constant through the expression,

Table 3.1: Concentrations of ZnTPP and the observed shifts (δ) of BFO protons.[a]

Concentration of ZnTPP x 10^{-3} moles/dm^3	H^7	Shift	H^5	Shift
0	9.151	–	8.848	–
1.12	9.065	0.086	8.755	0.093
2.24	8.986	0.165	8.669	0.179
4.48	8.838	0.313	8.510	0.338
6.72	8.708	0.443	8.369	0.479
8.40	8.635	0.516	8.289	0.559

(a) Concentration of BFO employed is 1.09×10^{-2} M.

$$[1+K_1A(1-\Delta/\Delta_1)] = [K_1D(\Delta_1/\Delta - DK_1)] \qquad 3.2$$

Rearranging this,

$$1/\Delta = [(1/D\Delta_1)A(1-\Delta/\Delta_1) + 1/\Delta_1 + 1/K_1D\Delta_1] \qquad 3.3$$

where D is the concentration of the porphyrin, A is the total concentration of the acceptor, Δ is the observed shift of the proton resonance of the acceptor relative to that of the free acceptor, Δ_1 is the shift in the fully formed complex and K_1 is the association constant.

A simplified version of (3.3) can be obtained neglecting the term $A(1-\Delta/\Delta_1)$. Thus,

$$1/\Delta = 1/DK_1\Delta_1 + 1/\Delta_1 \qquad 3.4$$

A linear plot is obtained when $1/\Delta$ is plotted against $1/D$ yielding an intercept of $1/\Delta_1$ and a gradient of $1/\Delta_1K_1$. The values were computed using a least square fit. The calculated value of Δ_1 for H^5 proton is 2.514 ppm and for H^7 proton 2.733 ppm. These values were fitted into equation (3.3) to get the best fit for the plot of $1/\Delta$ vesus $A(1-\Delta/\Delta_1)$. A regression program was employed to arrive at the best value for K_1 and Δ_1. Thus the K_1 values obtained are, for H^5 proton, $58.3\times10^3 \pm 10$ dm^{-3} $mole^{-1}$ and for H^7 proton $56\times10^3 \pm 10$ $dm^{-3}mole^{-1}$.

The complexation of Cu^{2+} porphyrins was monitored by ESR studies. It is well known that the CuTPP gives well resolved spectra with hyperfine and super hyperfine lines [$g_\perp = 2.185$, $g_\parallel = 2.047$, $A_\perp^{Cu} = 208.1\times10^{-4}cm^{-1}$; $A_\parallel^{N} = 15.7\times10^{-4}cm^{-1}$, $A_\perp^{N} = 14.7\times 10^{-4}cm^{-1}$]. The addition of BFO to CuTPP shifts the signals to higher fields thereby decreasing the values of $g_\parallel$ and $g_\perp$. The ESR data are listed in table 3.3. Inspection of table

shows the following changes: a small decrease in $A_{||}^{Cu}$ values while $A_{\perp}^{Cu}$ values increase relative to that of free CuTPP. Also, there is simultaneous increase in both $A_{\perp}^{N}$ and $A_{||}^{N}$ values ($A_{||}^{N}$ = 15.72x10^{-4}cm^{-1} and $A_{\perp}^{N}$ = 16.81x10^{-4}cm^{-1}). These changes are in accordance with the formation of molecular complexes between CuTPP and BFO.

3.3.2 Studies on Cobalt(II) Porphyrins:

(a) Visible absorption methods:

The absorption spectra of various cobalt(II) porphyrins in organic solvents are well characterised.[83] Addition of increasing amounts of BFO to a CHCl$_3$ solution of various cobalt(II) porphyrins decreased the intensity of the Q-bands with the appearance of well defined isosbestic points indicating the formation of a molecular complex in solution. The stoichiometry of the complexes determined as described earlier[105] was found to be 1:1. However, with time, a red shift of the absorption bands (Q-bands ~ 14 nm and Soret ~ 20 nm) was observed in all the cobalt(II) porphyrins studied. The absorption changes of a solution containing cobalt(II) TPP (3.42 x 10^{-5}M) and BFO (1 x 10^{-3}M) with time in the presence of molecular oxygen is shown in Fig. 3.2. Co(II)TPP in CHCl$_3$ shows a strong Q_{0-1} band at 528 nm which completely obscured the very weak Q_{0-0} component and an intense Soret band at 411 nm. In the presence of BFO, with time, the following changes were observed: (i) The disappearance of Q_{0-1} band at 528 nm, (ii) the appearance of a new Q_{0-1} band at 544 nm and Q_{0-0} band at 584 nm and (iii) disappearance of the Soret band at 411 nm and appearance of a new Soret band at 430nm. These observed changes are consistent[82] with the oxidation of
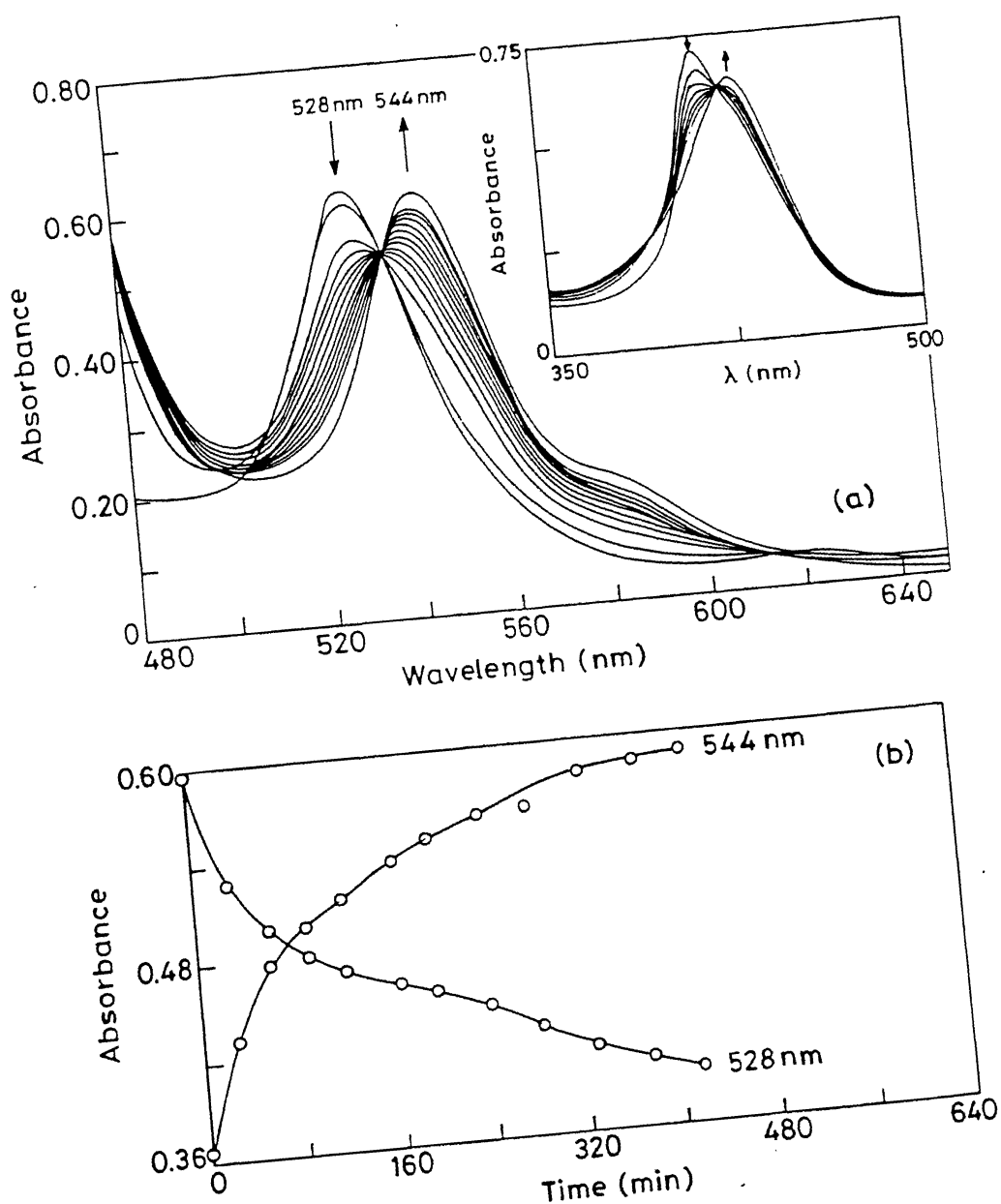
Fig. 3.2 (a) Absorption changes of CoTPP (3.42×10^{-5} M) in the presence of BFO (1×10^{-3} M) in $CHCl_3$ with time (0-415 min at ~ 30 min intervals). The insert shows the absorption changes with time of $CoTPP(OCH_3)_4$ (5×10^{-6} M) with BFO (1×10^{-4} M) in CH_2Cl_2 in the absence of molecular oxygen. (b) plot of absorption changes with time.

cobalt(II) TPP to [Co(III)TPP]$^+$ in the presence of BFO. The band positions match well with the absorption spectrum of cobalt(III)-TPPCl.[103] All the Cobalt(II) porphyrins listed in Fig. 3.1 show a similar behaviour upon interaction with BFO, but the time required for complete oxidation was different depending on the substituents present. The absorption data for all these cobalt(II) porphyrins before and after the interaction with BFO are listed in Table 3.2.

It is well known that the cobalt(II) protoporphyrin IX-dimethylester [Co(II)P] undergoes oxidation to its cobalt(III) derivative in presence of amine ligands and molecular oxygen.[29,31] It was argued that the coordinated amine ligand or coordinating solvent acts as electron donor promoting an electron transfer from [Co(II)P] to molecular oxygen to yield the final product [L$_2$Co(III)P]$^+$. In the present study, in order to understand the role of molecular oxygen, oxidation was also followed in the absence of oxygen. Samples were prepared on a high vacuum line. After several freeze/thaw cycles the solutions of BFO and cobalt(II) porphyrins were mixed and the optical cell was vacuum sealed. The spectrum recorded as a function of time [Insert Fig. 3.2] shows the existence of both cobalt(II) and cobalt(III) species in solution. However, the oxidation was not complete even after 24 hours. The presence of one isosbestic point at 424 nm suggests that only two species are present in solution. When the solution is exposed to air, a complete conversion to the cobalt(III) species is achieved within an hour. It is known that the coordination of a ligand in the axial position of cobalt(II) is very unfavourable,[34,106] whereas molecular oxygen can coordinate with a tendency of accepting

Table 3.2: **Optical absorption data of various Co(II) tetrapyrroles in the presence and absence of BFO.**

Porphyrin	Q-band(s) λ(nm)	Soret band λ(nm)	Time taken for complete oxidation (min)
Co(II)TPP	528.0	411	-
Co(II)TPP + BFO	544.0, 584	430	330
Co(II)TPP(OCH$_3$)$_4$	530.0	414	-
Co(II)TPP(OCH$_3$)$_4$+BFO	543.0, 583	433	270
CoTPP(Br$_4$)	545	424	-
CoTPP(Br$_4$) + BFO	556, 586	453	600
CoTPP(F$_{20}$)	527	406	-
CoTPP(F$_{20}$) + BFO	539, 579	430	450
CoOEP	552.5, 521	392	-
CoOEP + BFO	558.0, 527	412	25
CoTPP(d$_{20}$)	528	411	-
CoTPP(d$_{20}$) + BFO	544, 583	430	300
CoTPC	615, 528	410	-
CoTPC + BFO	543.5, 584	437	200
CoTPP(OCH$_3$)$_4$Cl	546, 581	429	-
CoTPP(d$_{20}$)Cl	549.5, 586	433.5	-
[a]CoTPP(OCH$_3$)$_4$	529	414	-
[a]CoTPP(OCH$_3$)$_4$ +2 pyridine	553, 593	440	b
[a]CoTPP(OCH$_3$)$_4$+ BFO	543, 580	433	b
[a]CoTPP(OCH$_3$)$_4$ +2 CH$_3$ONa	545, 583.0	432	b

a) in methanol:CHCl$_3$ (90:10).

b) in these cases the oxidation was instantanious.

electrons which leads to partial oxidation of cobalt giving the oxygen superoxide character.[107] The amount of electron transfer to O_2 depends on the nature of the ligands co-ordinated to cobalt, solvent acidity and solvent polarity.[108] In the present study, when the solvent was changed from $CHCl_3$ to $CHCl_3:CH_3OH$ (1:9 v/v), and methoxide as axial ligand, the oxidation was instantaneous. The rate of formation of the cobalt(III) derivative depends on the concentration of methanol and methoxide and increases when the concentrations of these reagents are increased. The ease of oxidation in these cases are found to be directly proportional to the base strength of the bound axial ligand. In fact, it has been recently shown that the alkoxides strongly bind along the Z-axis of cobalt(II) porphyrins by decreasing the tetragonal distortion of d^7 cobalt(II) to form an octahedral complex strongly promoting the oxidation.[32]

It is clear from the above discussion that oxidation is occurring both in the presence and absence of oxygen and the end product is the formation of anion radical of BFO. However, the presence of oxygen ensures complete conversion and enhances the rate of oxidation. One of the possible ways in which oxygen assists the electron transfer from porphyrin to BFO is via an intermediate of the type $[L^{\delta +}Co(II)(O_2)^{\delta -}]$ as suggested previously.[29,31-32] The short lived nature of this intermediate renders the detection of the superoxide formed, if any, difficult. On the contrary in the absence of oxygen any charge transfer has to be necessarily via the formation of the charge transfer complex with $\pi - \pi$ type interaction.

The interaction of BFO could also be of the coordinative type where it binds to cobalt axially. The presence of this type

of interaction is ruled out for the following reasons: (a) IR studies show that the strong NO_2 vibrations remain virtually unaffected by the formation of the complex. (b) The absence of absorption band shifts induced by interaction of BFO with Zn(II) and Cu(II) porphyrins even after 24 hours. (c) Kadish et al. have recently observed that binding of CO to cobalt porphyrins causes a negative shift of the first oxidation potential and a positive shift of the second oxidation potential.[89a] By contrast all three oxidation potentials remain unaltered in the presence of BFO indicating the absence of any site specific interaction. Thus it is reasonable to conclude that the interaction between the cobalt porphyrins and BFO is of $\pi-\pi$ type.

It is seen from table 3.2 that the rate of oxidation of cobalt(II) porphyrin to its cobalt(III) derivative depends on the porphyrin ring substituents. The presence of electron with-drawing substituents (Br, F) reduces the basicity of the macrocycle, while the presence of electron donating (C_2H_5, OCH_3) groups increases the basicity of the macrocycle.[109] It has been shown that the metal-ligand bond strength as well as the spin state of the metal ion is critically dependent on the basicity of the macrocycle. Hence the reduced basicity of the macrocycle reduces the rate of oxidation in $CoTPP(F_{20})$ and $CoTPP(Br_4)$ while the increased basicity of $CoTPP(OCH_3)_4$ and CoOEP account for the observed increase in rate of oxidation.

(b) Cobalt(II) Chlorins:

The effect of the interaction with BFO on the optical absorption spectrum of cobalt(II) chlorin is shown in Fig. 3.3. The absorption spectrum of cobalt(II) chlorin in $CHCl_3$ is
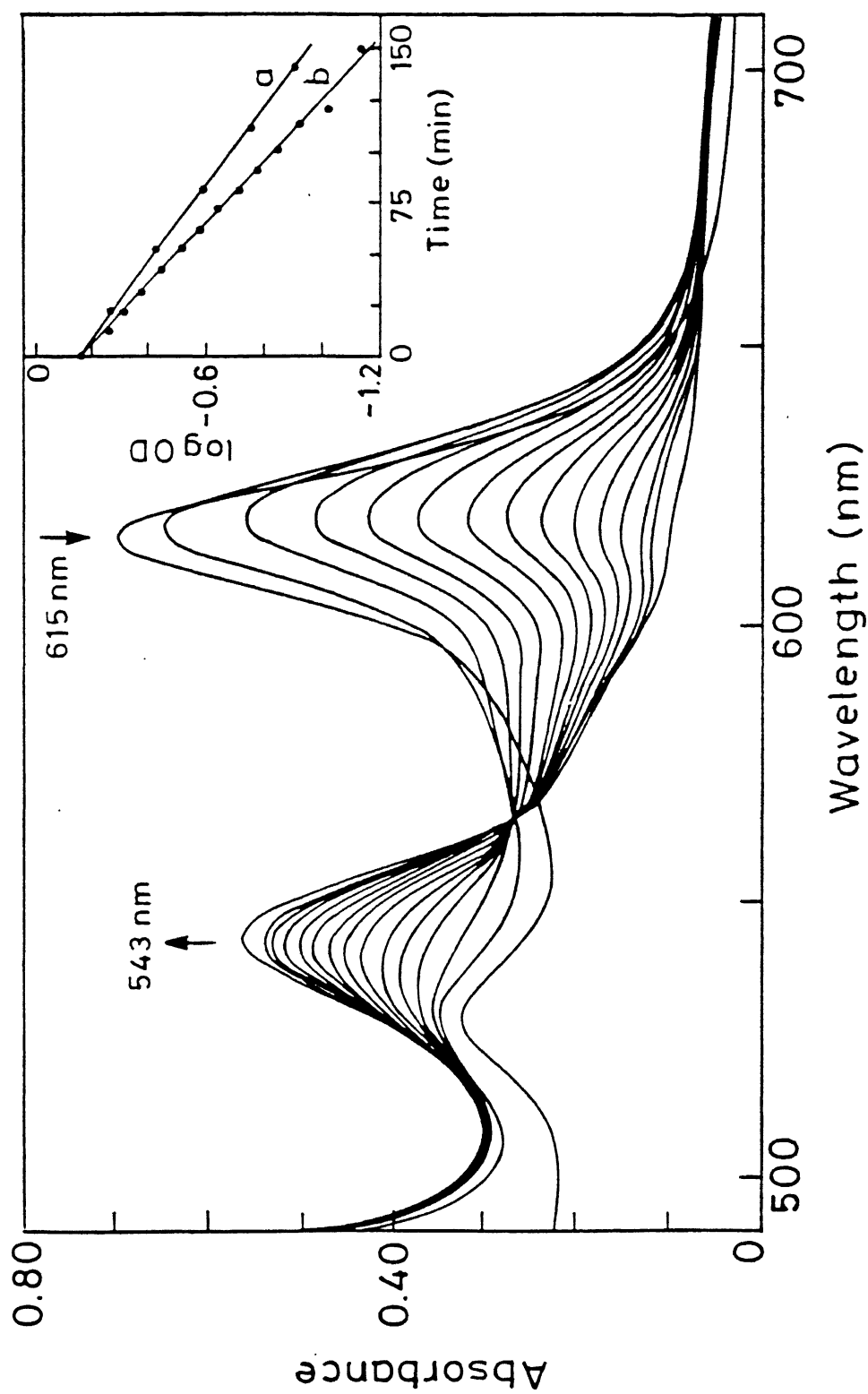
Fig. 3.3 Absorption changes of Co(II)TPC (5.05×10^{-5}M) in the presence of BFO (3.86×10^{-3}M) in $CHCl_3$ with time (0-150 min at ~ 10 min intervals). The insert shows the plot of log OD Vs time (min) (a) CoTPC:BFO (1:50), (b) CoTPC:BFO (1:75).

characterised by two Q-bands; a strong band at 615 nm and a weak band at 528 nm and a Soret band at 410 nm. The observed changes upon interaction with BFO are (i) a gradual decrease in the absorbance at 615 nm (ii) an increase in the intensity at 528 nm and (iii) a red shift of the 528 nm band to 543 nm with time. These changes were followed with varying amounts of BFO since the effect (iii) was dependent on the amount of BFO present in solution. When the ratio of CoTPC:BFO is (1:10), effects (i) and (ii) are dominant, while effects (i) and (iii) are dominant when the ratio of CoTPC:BFO is increased to 1:50 and 1:75. The intensity decrease at 615 nm and simultaneous increase in the intensity of the 528 nm band is consistent with the oxidation of the chlorin ring where cobalt(II)TPC is transformed to Cobalt(II)TPP. A further red shift of the 528 nm band to 543 nm reflects metal ion oxidation from Cobalt(II)TPP to $[Co(III)TPP]^+$. The rates of oxidation derived from a plot of the change in optical density with time [Fig. 3.3 insert] are 6.44×10^{-5} s^{-1} (1:10), 1.95×10^{-4} s^{-1} (1:50) and 2.43×10^{-4} s^{-1} (1:75). These values are consistent with those reported previously for similar systems.[29,31] It is known that the oxidation of the porphyrin ring becomes progressively easier as the macrocycle becomes more saturated since the energy of the highest occupied π-orbital increases with saturation of the porphyrin skeleton.[110] The oxidation of the chlorin ring prior to the metal oxidation in the present study is consistent with the above observation. Thus the oxidation scheme for cobalt(II) TPC can be represented as

$$Co(II)TPC \Longrightarrow Co(II)TPP \Longrightarrow [Co(III)TPP]^+ \qquad 3.5$$
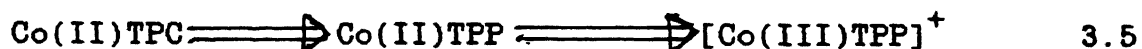
3.3.3 ESR studies of cobalt(II) porphyrins:

The oxidation state and the electronic environment of Co^{2+} ion in cobalt porphyrins were found to be affected by the method of sample preparation. At room temperature no ESR signal was observed due to a short spin-lattice relaxation time.[111] The $^{59}Co^{2+}$ ion having a nuclear spin of 7/2 should give eight hyperfine lines due to the magnetic interaction of the unpaired electron with the nucleus. The odd electron in Co^{2+} ion is found to be in $a_1(d_z2)$ orbital. Thus, unlike Cu^{2+} and VO^{2+} porphyrins, the study of cobalt porphyrins by ESR offers the possibility of looking closely at the a_1 (d_z2) orbital. It has been shown[112] that the ESR parameters, particularly the g-tensors depend strongly on the relative levels of a_1 (d_z2) orbital. In presence of a solvent, particularly a σ - donating Lewis base, there is a possibility of axial co-ordination which effects the energy level of $a_1(d_z2)$ orbital.

The theoretical treatment of Co porphyrins are much complicated than Cu and VO porphyrins because the electrostatic repulsions between the seven d-electrons have to be taken into account. Theoretical expressions for $g_\parallel$, $g_\perp$, $A_\parallel$ and $A_\perp$ applicable to Co porphyrins were first derived by Griffiths[113] and by McGravey.[114] The inadequacy in these equations lies in the fact that $g_\parallel$ can never be greater than $g_\perp$ and hence they are not applicable to solvent coordinated complexes. However, there are some recent theories for cobalt porphyrins which account for wide range of $g_\parallel$ and $g_\perp$ values.[115-117]

In the present study the treatment of Assour[118] was followed. The first order g-tensors can be written as,

$$g_{||} = 2.0023 \qquad\qquad\qquad 3.6$$

$$g_{\perp} = 2.0023 \pm 6\ \xi/\triangle \qquad\qquad 3.7$$

and for second order calculations,

$$g_{||} = 2.0023 - 3\ (\xi/4)^2 \qquad\qquad 3.8$$

and $\quad g_{\perp} = 2.0023 + 6\ (\xi/4) - 6\ (\xi/4)^2 \qquad 3.9$

where $\triangle$ is the energy difference between a_1 (d_{z^2}) and e states and ξ is the spin-orbit coupling constant for Co^{2+}. The hyperfine constants derived from first order calculations are

$$A_{||} = p[4/7 - K - 18/7\ (\xi/\triangle)] \qquad\qquad 3.10$$

$$A_{\perp} = p[-2/7 - K + 51/7\ (\xi/\triangle)] \qquad\qquad 3.11$$

Here $A_{||}$ and $A_{\perp}$ are found to be positive and K is negative.

The ESR spectrum of $CoTPP(OCH_3)_4$ recorded at 100K in toluene-ethanol (3:1) consists of two separate sets of hyperfine lines (Fig. 3.4a). The low field set of eight lines corresponds to $g_{\perp}$. These hyperfine lines are not equally spaced and this progressive splitting of the hyperfine lines is due to the substantial second order effect. The high field lines that belong to $g_{||}$ are composed of eight lines with unequal spacings. The value of $g_{\perp}$ is calculated from the spectrum by measuring the field at the mid point of the 4th and 5th line in the low field region (perpendicular region). Similarly the $g_{||}$ values were calculated by measuring the field at the midpoint of 4th and 5th parallel line in the high field region of the spectrum. The hyperfine constants were calculated from the expanded spectrum.[119]

3.3.4 ESR Spectra of Cobalt porphyrin and BFO Complex

The changes occuring in the ESR spectrum of $CoTPP(OCH_3)_4$ with time on interaction with BFO are shown in Fig. 3.4. ESR
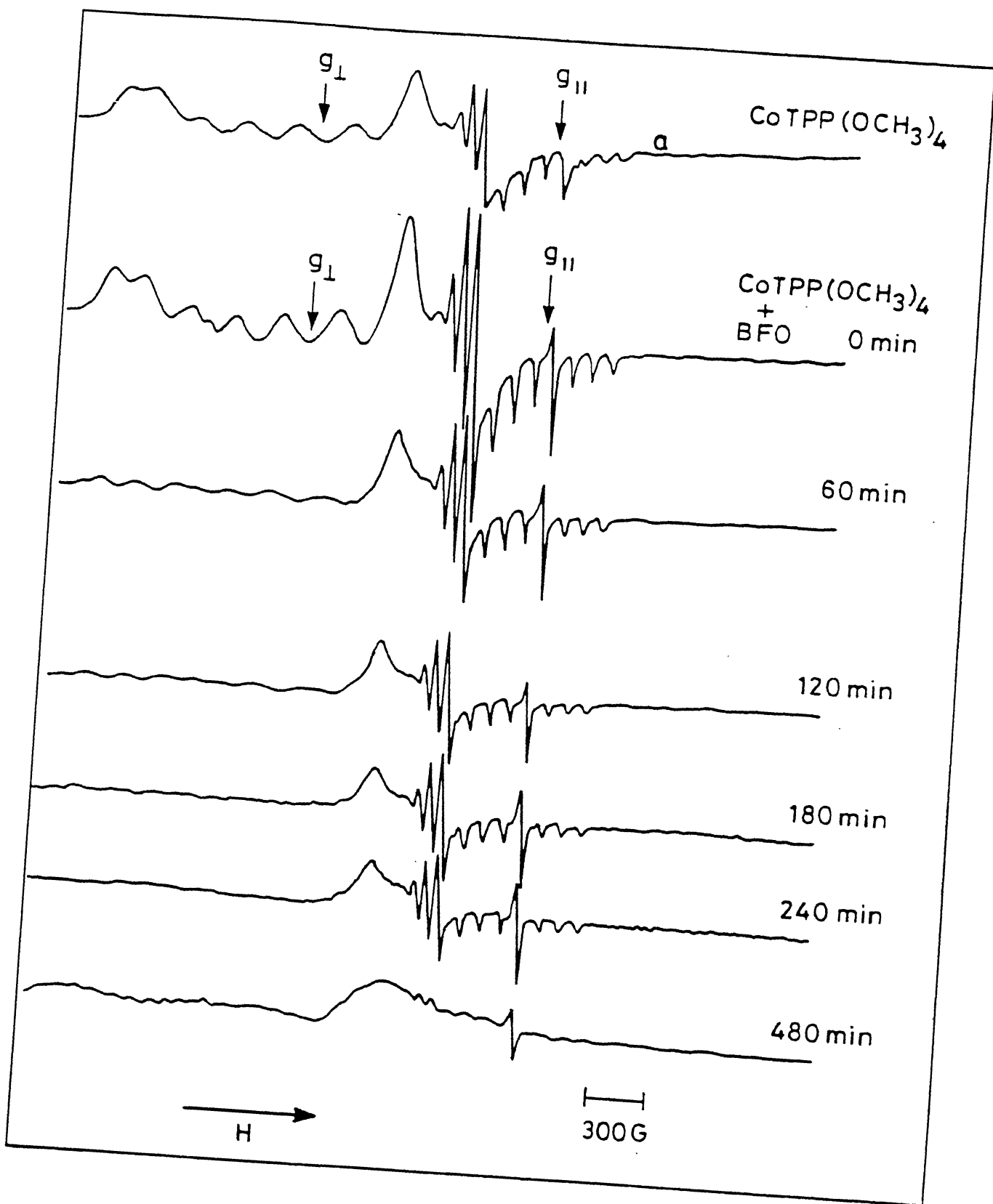
Fig. 3.4 ESR spectral changes of [CoTPP(OCH$_3$)$_4$] ($\sim$1x10^{-3}M) in presence of excess BFO with time.

parameters derived from the spectra are listed in table 3.3. The changes observed immediately following mixing with BFO are (i) the spectrum becomes better resolved, (ii) $g_{||}$ and $g_{\perp}$ values change slightly giving a small increase in magnetic anisotropy $(g_{||}^2 - g_{\perp}^2)$, and (iii) a marginal increase in the $A_{\perp}^{Co}$ value is found. The magnitude of the magnetic anisotropy value before and after complexation has been used to distinguish between the molecular complexation and axial ligation by coordinative interaction.[120] If the coordinative type of interaction prevails in solution the magnitude of magnetic anisotropy is expected to be lowered while the reverse is true for the molecular complexation. Thus the observed changes are consistent with the formation of a molecular complex. However with time the 8 line pattern due to the Co^{+2} (I=7/2) complex is reduced by about 80% upon interaction with BFO and a weak free radical signal in the g=2 region is generated. In the presence of air there is a drastic reduction in g and A values and the ESR spectrum is typical of a cobalt(II) porphyrin: O_2 adduct.[121] Addition of BFO to this solution results in the gradual loss of ESR signal due to the adduct and appearance of a weak free radical signal in the g=2 region. Fig. 3.5 shows the decrease in intensity of ESR signals [2 lines in parallel region and 2 lines in the perpendicular region] of Cobalt(II) species with time. The radical signal is weak probably due to the decomposition of BFO^- formed. When the solvent was changed from $CHCl_3$ to $CHCl_3:CH_3OH$ (1:9), the ESR signal due to the cobalt(II)-O_2 adduct was lost immediately after addition of BFO indicating that the cobalt(II) species has been oxidised to its cobalt(III) derivative consistent with the absorption data. To make sure that the free
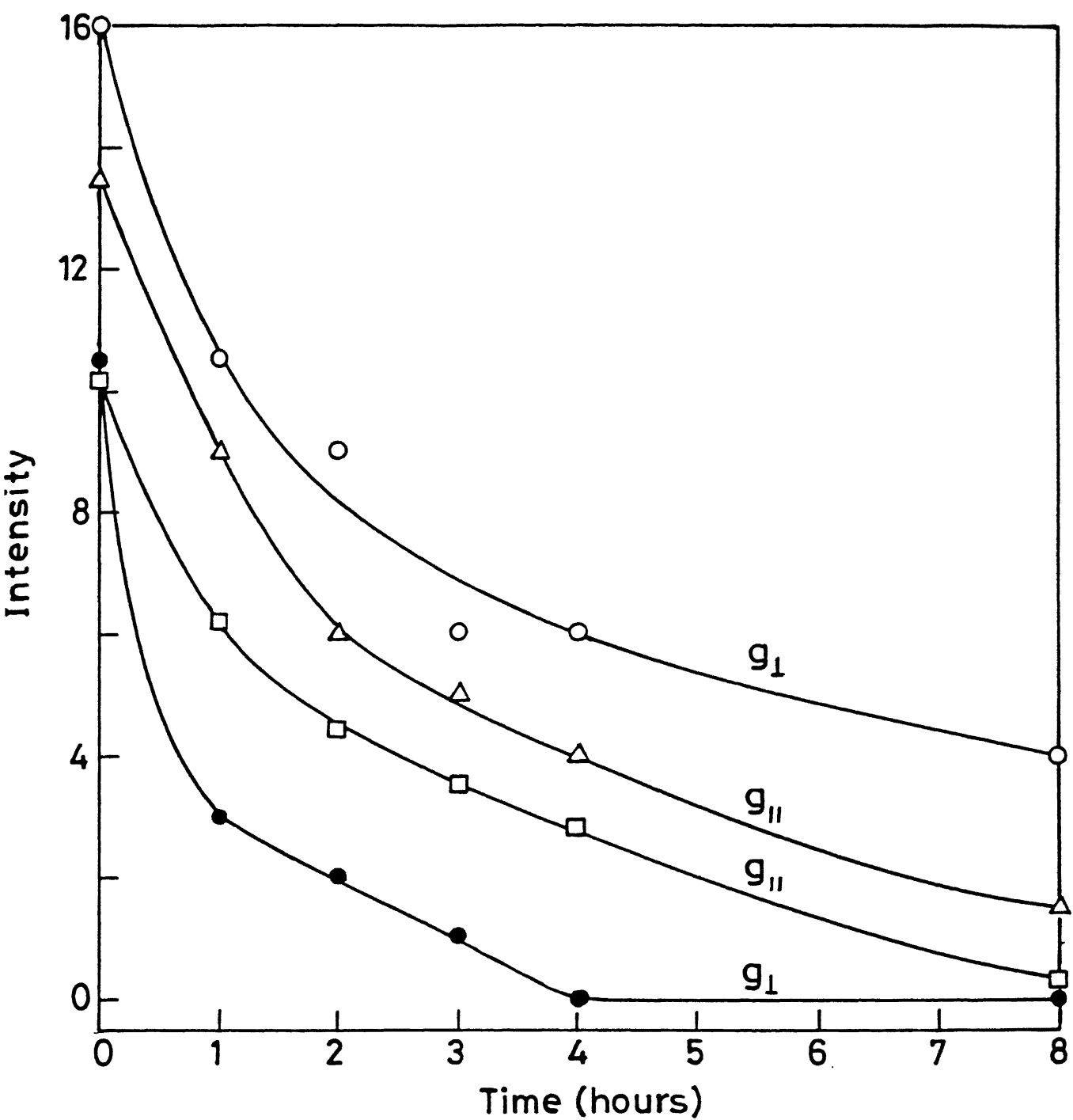
Fig. 3.5 Variation of intensity of ESR signals upon interaction
with BFO as function of time.

Table 3.3: ESR parameters for Cobalt and copper porphyrin:BFO complexes and free radicals.

Porphyrin	$g_{\parallel}$	$g_{\perp}$	g_{iso}	$A_{\parallel}^{Co}$ $10^4 cm^{-1}$	$A_{\perp}^{Co}$ $10^4 cm^{-1}$	Line width (G)
Co(II)TPP(OCH$_3$)$_4$	2.057	3.277	-	245.0	95.0	-
[a]Co(II)TPP(OCH$_3$)$_4$ + BFO	2.062	3.291	-	247.7	95.0	-
[b]Co(II)TPP(OCH$_3$)$_4$ + BFO	-	-	2.0434	-	-	20.33
[b]Co(II)TPP + BFO	-	-	2.0032	-	-	21.00
[b]Co(II)OEP + BFO	-	-	2.0042	-	-	21.89
[c]BFO$^-$	-	-	2.0043	-	-	23.07

	$g_{\parallel}$	$g_{\perp}$	$A_{\parallel}^{Cu}$ $10^4 cm^{-1}$	$A_{\perp}^{Cu}$ $10^4 cm^{-1}$	$A_{\parallel}^{N}$ $10^4 cm^{-1}$	$A_{\perp}^{N}$ $10^4 cm^{-1}$
CuTPP	2.185	2.047	208.1	31.5	14.7	15.7
CuTPP + BFO	2.179	2.038	206.66	32.82	15.72	16.81

a) immediately after mixing

b) after 24 hours of mixing

c) chemically reduced anion of BFO

radical signal observed was due to the anion radical of the acceptor, BFO was chemically reduced with potassium metal in dimethoxyethane. At room temperature, the ESR signal is well resolved with 15 hyperfine lines (Fig. 3.6) due to two nitrogens and two protons [a_N = 8.5G and a_H = 3.1G]. However, at low temperature these lines merge to give a single broad line. The g-values and the line widths of the radical signals obtained with the cobalt(II) porphyrin:BFO complex compare well with the free radical signal (table 3.3) supporting the conclusion that the BFO$^-$ radical is formed. Furthermore, the cyclic voltammogram of BFO in CH_2Cl_2 shows one irreversible reduction wave at $E_{1/2}$ = - 0.070V. This value compares well with those of conventional aromatic π- electron acceptors which are known to form molecular complexes.[121]

3.3.5 ^{1}H NMR Studies:

The ^{1}H NMR spectra of cobalt porphyrins were recorded in CDCl$_3$ using TMS as an internal standard. The ability to observe narrow, well resolved lines can be traced directly to the presence of efficient electron spin relaxation such that $T_{1e} \gg J_r$ (T_{1e} = electron spin relaxation time, J_r = rotational tumbling time of the complex). The ^{1}H NMR spectra of low spin cobalt porphyrins are well understood. The review by Lamar and F. Ann Walker[119] gives the details of the studies done on the low spin Co(II) porphyrins.

The ^{1}H NMR data of the cobalt(II) porphyrins investigated in the present study and their complexes with BFO are listed in table 3.4. The resonances of paramagnetic cobalt(II) porphyrins are expected to be broad and down field shifted because of the
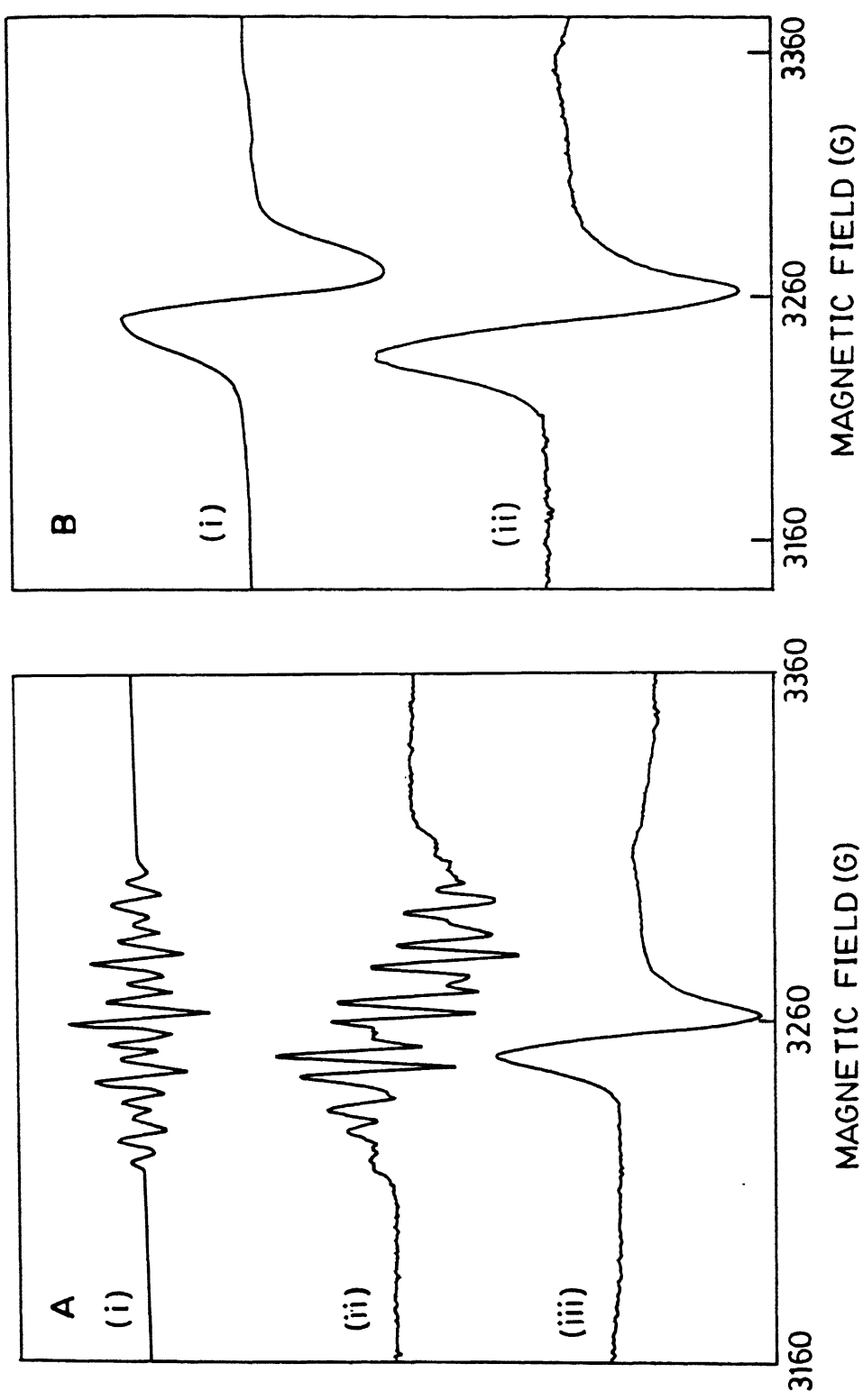
Fig. 3.6 ESR spectra of BFO anion radical (A) (i) Simulated at R.T., (ii) Chemically reduced BFO at R.T., (iii) Chemically reduced BFO at 100K. (B) (i) Signal obtained from CoTPP: BFO Complex at 100K. (ii) Chemically reduced BFO at 100K.

Table 3.4: ^1H NMR Chemical Shifts (ppm) and line widths (Hz) of Cobalt Porphyrins in the presence and absence of BFO.

Porphyrin	Phenyl		β-Pyrrole	P-OCH$_3$
	Meta	Ortho		
Co(II)TPP(OCH$_3$)$_4$	9.43(s)[18.6]	13.07(s)[58.8]	15.96(s)[74.3]	5.25(s)[10.8]
Co(II)TPP(OCH$_3$)$_4$ + BFO	7.19(m)	7.65(m)	9.37(s)[5.0]	3.99(s)[7.4]
Co(II)TPP(OCH$_3$)$_4$ + Py	7.17(m)	7.694(m)	9.48(s)[6.0]	4.03(s)[6.0]
Co(III)TPP(OCH$_3$)$_4$Cl	7.41(d)	8.17(d)	9.35(s)[5.5]	4.11(s)[5.5]
	J_{AB}=8.5 Hz	J_{AB}=8.5 Hz		
Co(II)TPP(d$_{20}$)	-	-	15.8(s)[173.4]	-
Co(II)TPP(d$_{20}$) + BFO	-	-	9.39(s)[5.6]	-
Co(II)TPP(d$_{20}$) + Py	-	-	9.12(s)[5.6]	-
[a]Co(III)TPP(d$_{20}$)Cl	-	-	9.32(s)[6.2]	-
Co(II)TPP(F$_{20}$)	-	-	15.31(s)[179.0]	-
Co(II)TPP(F$_{20}$) + BFO	-	-	9.04(s)[6.0]	-

The numbers in paranthesis corresponds to line width in HZ

a: in CD$_3$OD

presence of the odd electron in $d_z{}^2$ orbital with $^2A_1$ ground state.[119] The resonances of the oxidised product are expected to be sharp, consistent with the formation of low spin Co(III) derivatives. The ^{1}H NMR spectrum of BFO in $CDCl_3$ consists of resonances centered around 9.15 ppm and 8.85 ppm corresponding to the H^7 and H^5 protons (Fig. 3.1), respectively. In the presence of cobalt(II) porphyrins, these resonances become broad and experience a down field shift consistent with the formation of molecular complex.[120] From the concentration dependence of these shifts equilibrium constants have been calculated.[105] The effect of interaction with BFO on the ^{1}H NMR resonances of cobalt(II)TPP (d_{20}) is shown in Fig. 3.7. For comparison the ^{1}H NMR of Cobalt(III)TPP (d_{20})Cl in CD_3OD is also included. It is apparent from Fig. 3.7 that the broad resonance of cobalt(II)TPP is lost upon interaction with BFO and is replaced by sharp, upfield-shifted resonance. The chemical shift and the line width of the CoTPP:BFO complex are in good agreement with that of Cobalt(III)TPPCl consistent with the oxidation of a cobaltous derivative to cobaltic derivative. The chemical shift and line width data also compare well with those given by cobalt(II) porphyrin- pyridine complexes where it is known that the presence of axial base facilitates oxidation.[29,31]

The proton NMR of Co(II)OEP show three resonances at 29.5 ppm (s, 126 Hz), 8.79 ppm (s, 35 Hz) and 6.1 ppm (s, 22 Hz) due to meso hydrogens, $-CH_2$ protons and $-CH_3$ protons of the ethyl groups respectively. In the BFO complex all the three resonances are shifted upfield to 9.3 ppm (s, 7.4 Hz), 4.2 ppm (m) and 1.93 ppm (m) indicating the oxidation. The ^{1}H NMR spectrum of Cobalt(II)TPC is characterized by a broad singlet due to pyrrole
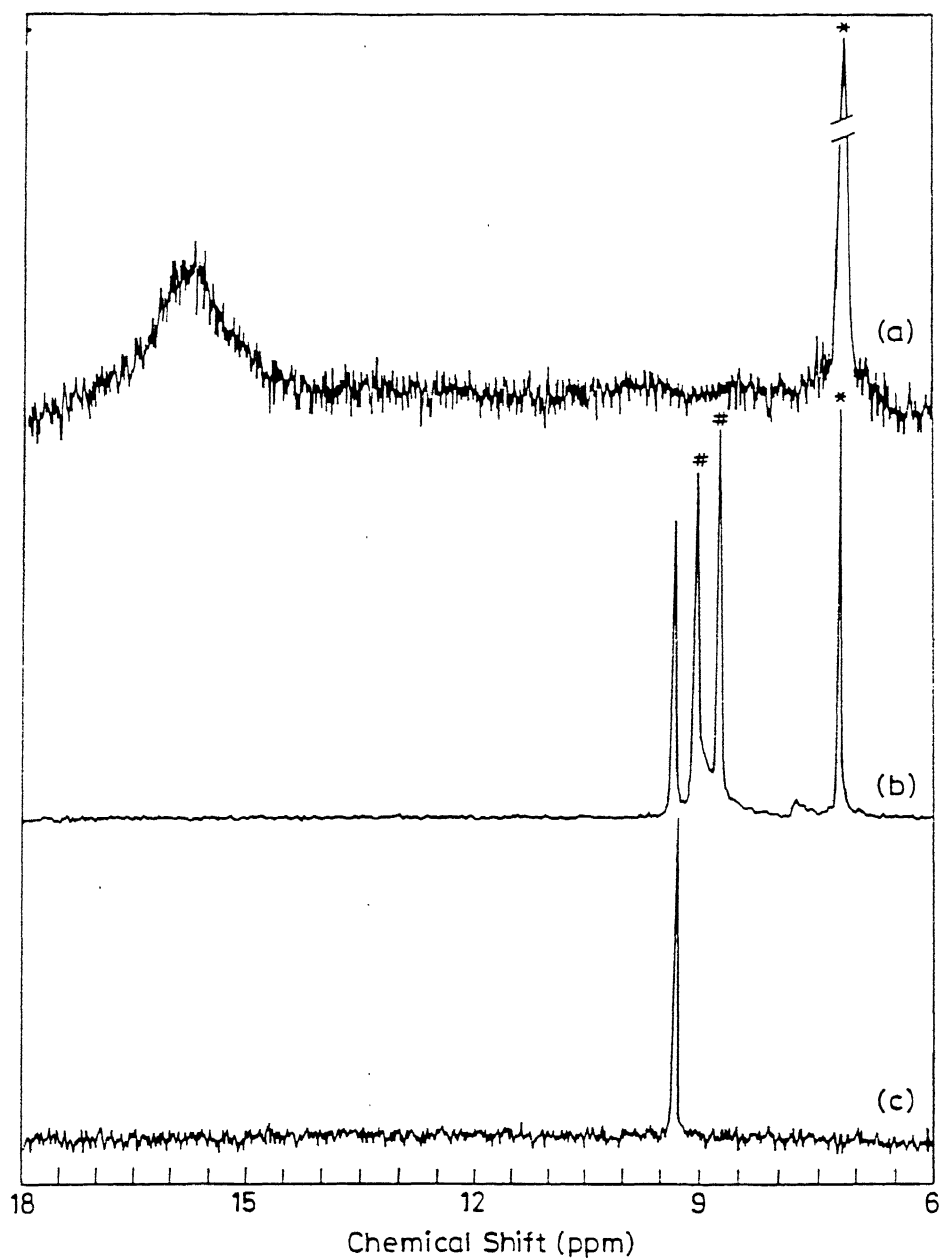
Fig. 3.7 ^{1}H NMR spectra of (a) CoTPP(d_{20}) (b) CoTPP(d_{20}) containing excess BFO (after 24 hours of mixing) in CDCl$_3$ and (c) Co(III)TPP(d_{20})Cl in CD$_3$OD (The concentration of Co porphyrins ~1x10^{-3}M). The (*) Corresponds to CDCl$_3$ signal and (#) corresponds to BFO protons (see text).

protons at 15.9 ppm (117.7 Hz) while the ortho hydrogens of the phenyl groups gives a singlet at 13.07 ppm (99 Hz). The meta and para hydrogens resonate at 9.68 ppm (44 Hz) while the β-CH_2 of the saturated ring gives a singlet at 7.59 ppm (43 Hz). The NMR spectrum was recorded as a function of time in the presence of BFO. The spectrum recorded after about 3 hrs of mixing shows the absence of the β-CH_2 signal at 7.59 ppm, while the spectrum recorded after 10 hours of mixing shows a sharp singlet at 9.39 ppm (6 Hz) and a multiplet centered around 7.6 ppm for the phenyl protons. This is consistent with chlorin ring oxidation followed by metal oxidation as observed in the optical spectrum.

3.3.6 ^{19}F NMR Studies:

^{19}F NMR spectra of pentafluorinated Co(II)TPP both in the presence and absence of BFO were recorded. Figure 3.8 shows a comparison of Co(II)$TPPF_{20}$, in the presence and absence of BFO along with diamagnetic Zn(II)$TPPF_{20}$. The Co(II)$TPPF_{20}$ shows three relatively broad resonances (typical of paramagnetic Co(II) porphyrins) at -133, -160.14 and -150.41 ppm (with external reference CF_3COOH at -76.5 ppm) attributed to ortho, meta and parafluorines of phenyl rings. These assignments were made on the basis of ^{19}F NMR of pentafluorinated benzene[122]. Upon interaction with BFO the spectrum was well resolved as in diamagnetic Zn(II) derivative and all the fluorine resonances experienced an upfield shift [-137.55, -161.70 and -152.84 ppm, J_{o-m} 19.5 Hz]. These chemical shifts and coupling constants are comparable to that of the diamagnetic Zn$TPPF_{20}$ [-137.49, -162.67 and -153.015 ppm and J_{o-m} 19.53 and J_{m-p} 19.5 Hz] indicating the formation of diamagnetic Co(III) derivative.
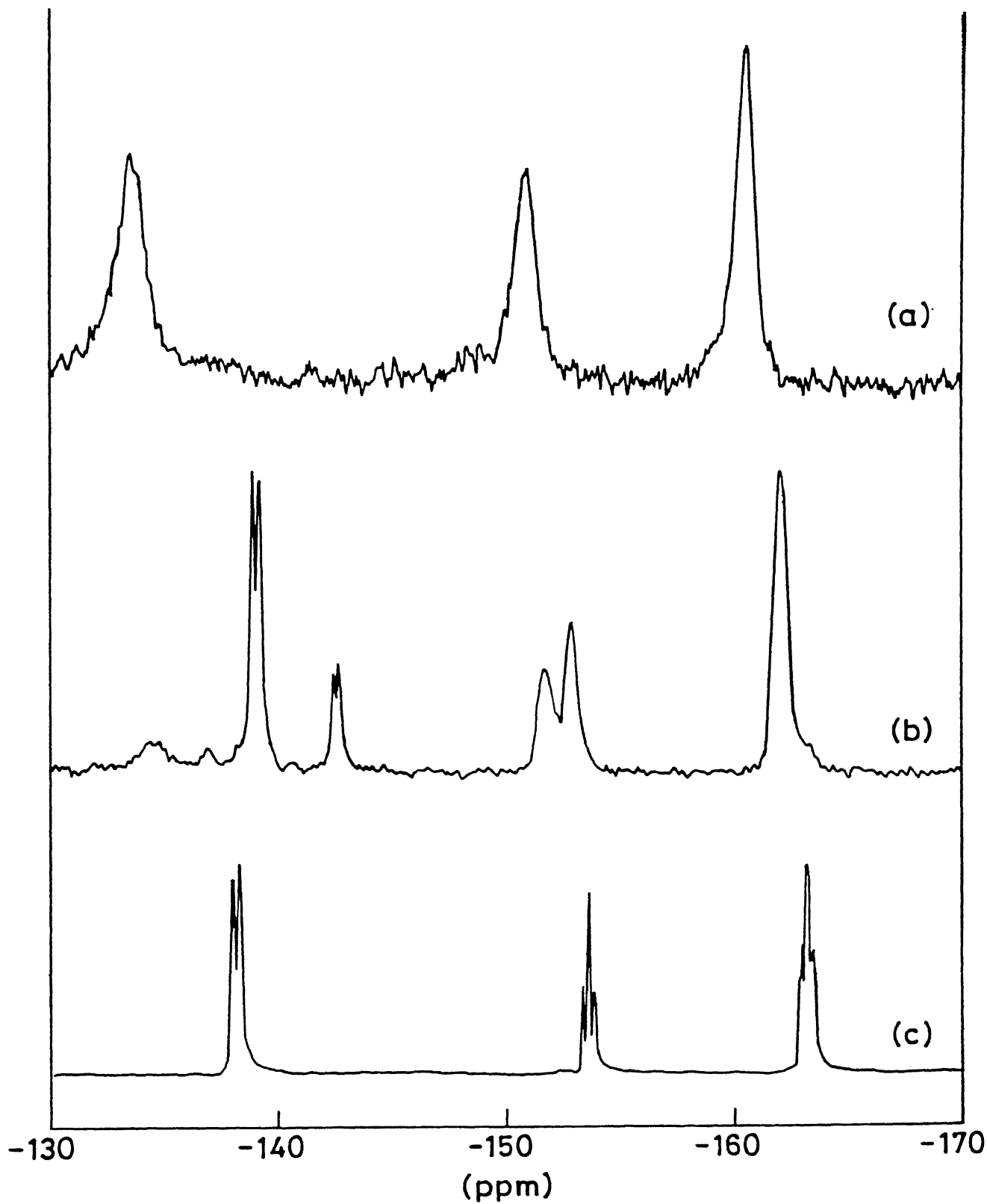
Fig. 3.8 ^{19}F NMR spectra of (a) CoTPPF$_{20}$, (b) CoTPPF$_{20}$ containing BFO (spectrum recorded after 48 hours of mixing) and (c) ZnTPPF$_{20}$ in CDCl$_3$.

The formation of a peroxobinuclear cobalt dimer of the type [(S)PCo(O$_2$)CoP(S)] was also considered because of the known existence of such complexes in aprotic, non-coordinating solvents.[31] The existence of this type of peroxodimer in the present study was ruled out on the basis of the following experimental observations; (i) the presence of an ESR signal in the g=2 region assigned to the anion radical of BFO. (ii) It is known that Co(III)TPPCl releases its chloride upon dissolution in methanol and yields [Co(III)(CH$_3$O)(CH$_3$OH)].[90,103] The resemblance of both optical and ^{1}H NMR spectra of Cobalt porphyrin – BFO complexes to those of Co(III)TPPCl strongly suggests the formation of mononuclear Co(III) species in solution. (iii) The similar magnitudes of chemical shifts and coupling constants of Cobalt porphyrin -BFO complexes of cobalt porphyrin-pyridine adducts indicated the formation of diamagnetic Co(III) porphyrins (Table 3.4). (iv) The magnitude of the Soret band shift was used previously to distinguish between the formation of a binuclear peroxodimer and mononuclear Co(III) porphyrin.[32] The observed magnitude of Soret shifts (Table 3.2) are consistent with the formation of mononuclear Co(III) porphyrins.

3.4 CONCLUSIONS:

The results obtained herein, indicate that the BFO forms predominantly 1:1 complex with Zn^{2+} and Cu^{2+} porphyrins. The NMR and ESR data are helpful in arriving at a possible geometry of the complexes in solution. The fact that both the H^7 and H^5 protons of BFO experience similar magnitude of downfield shift upon increasing addition of porphyrin solution imply that these

two protons are experiencing the similar ring current effect from the porphyrin ring. This is possible when BFO and porphyrin π-planes are essentially parallel. Thus, two possible geometries of the complexes in solution are visualized (Fig. 3.9) as (a) BFO can be positioned above one of the pyrrole rings at Van der Waals distance such that one of the NO_2 groups of BFO is pointing towards metal ion. Alternatively (b) BFO can be positioned above the porphyrin plane such that the aromatic ring of the BFO lies exactly above the center of the porphyrin core facilitating the π-π interaction. Similar solution structures have been proposed earlier.[120] In the absence of X-ray structural evidence it is difficult to decide among the two alternative structures proposed here.

In the case of Co(II) porphyrins, it has been clearly shown that all the Co(II) derivatives undergo metal centered oxidation to Co(III) derivatives. While in the case of Co(II) chlorin, first the ring oxidation followed by metal oxidation occurs upon interaction with BFO. The redox products have been characterized using various spectroscopic methods.
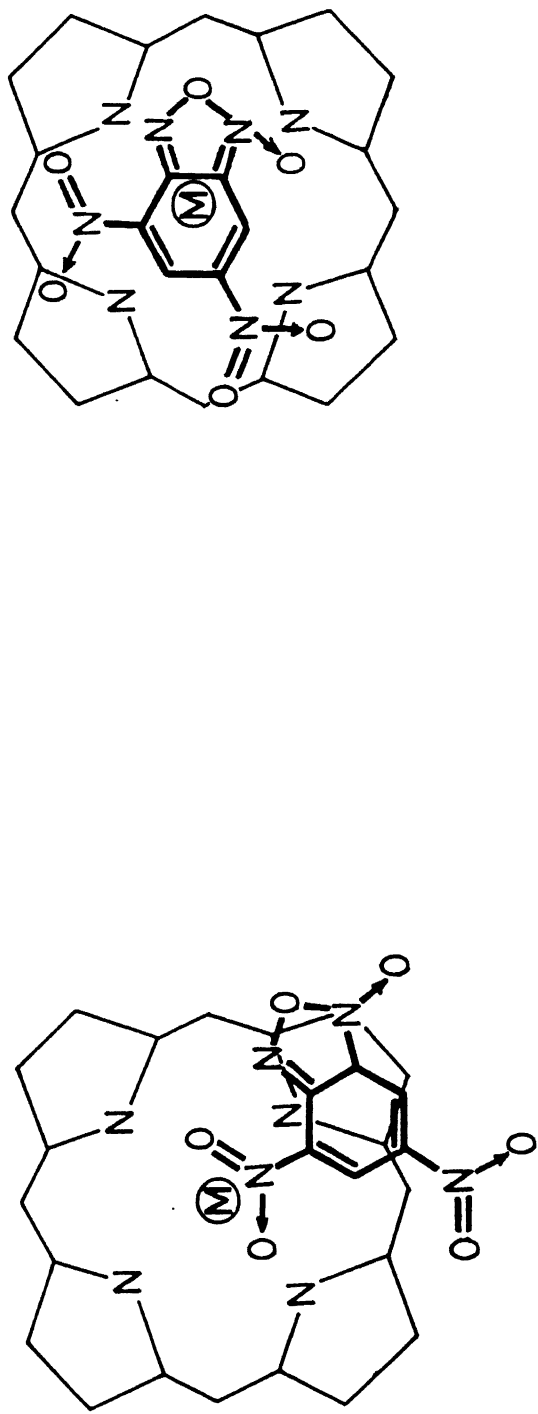
Fig. 3.9   Possible overlap structures of Metallo porphyrin and BFO in solution. For clarity, the double bonds and the substituents on porphyrin are omitted.

INTERACTION OF WATER SOLUBLE METALLOPORPHYRINS WITH NUCLEIC ACID BASES

4.1 INTRODUCTION:

In the previous chapter, it has been shown that the interaction of various metalloporphyrins with an electron acceptor (BFO) results in the formation of molecular complexes as well as the charge separated species D^+ and A^- (where D is the porphyrin donor and A is the acceptor). It has been well known that[105,120] in the presence of strong π-donors, metalloporphyrins act as acceptors in general appear to be much weaker than in which they act as π-donors. Hill et al[123] observed only very weak complex formation between π-donors and Mn(III) meso-porphyrin IX dimethyl ester at room temperature. Walker[124,125] has studied the complexation behaviour of number of amine and other nitrogen bases towards metalloporphyrins by ESR spectral method and has concluded that the amines and bases axially coordinate to the metal ions forming five/six co-ordinate complexes. There have been[126-128] number of studies in literature on the thermodynamics and kinetics of axial ligation of metalloporphyrins. These studies indicate that the basicity of porphyrins are considerably affected by the nature of the axially ligating molecules. Baker et al[129] from their extensive studies have shown that metalloderivatives of number of porphyrins form higher coordinate complexes with ligands such as pyridine, imidazole etc. Studies on low spin Co(II) porphyrins have received considerably more attention because of their capacity to bind molecular oxygen reversibly.[130-132]

Recently it has been shown that the water soluble tetra-cationic porphyrins and metalloporphyrins form molecular complexes with DNA and DNA constituents such as nucleosides, and nucleotides[133]. It is interesting to note that the nucleic acid bases (Adenine, cytosine, Guanine, and Thymine) have donor co-ordinating sites but they prefer to form a π-π stacking type complex with water soluble metalloporphyrins rather than binding axially to the metal center. A perusal of literature indicate very little studies on the interaction of nucleic acid bases with metalloporphyrins. In this chapter we have chosen to study the interaction between the water soluble metal tetrakis (4-N-methylpyridyl) porphyrin [MTMPyP, M = Cu^{2+}, Zn^{2+}] (Fig. 4.1) with an aim of evaluating the stability, Stoichiometry and structure of molecular complexes. Such a study would help to delineate any site specific interaction that may prevail in such complexes. The nucleic acid bases chosen for the study are adenine, cytosine, Guanine and Thymine. Electronic absorption method has been used to evaluate association constants (K) and ESR measurements were helpful in assessing the axial perturbation in the metal upon complexation.

4.2 EXPERIMENTAL:

Meso-tetrakis (4-N-methylpyridyl) porphyrin [H_2TMPyP] procured from Strem chemicals, USA, was used without any further purification. The nucleic acid bases were obtained from Sisco Research Laboratories, Bombay (India) and were used as received.

Solvents employed in the synthesis and spectral measurements were purified as described in chapter 2.
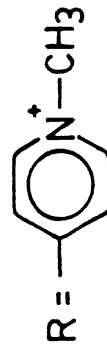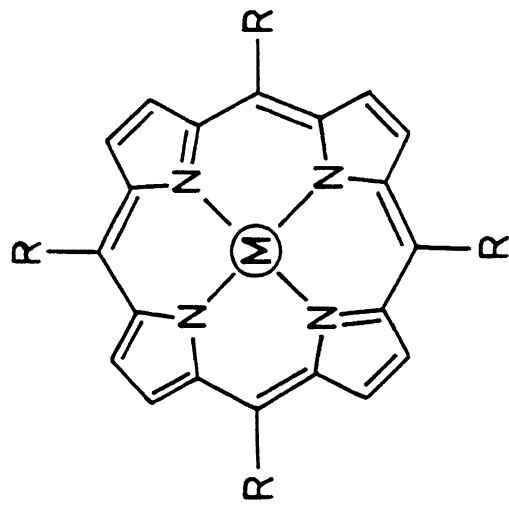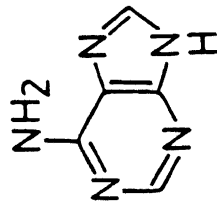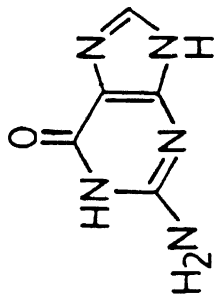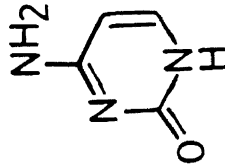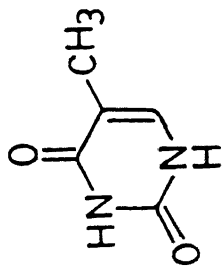
Fig. 4.1 Molecular structures of MTMPyP and Nucleic acid bases.

The electronic absorption method employed for the evaluation of association constants involved the measurement of absorbance of Soret band of the metal porphyrin on increasing addition of different bases. The concentration of the porphyrins were held constant ($\sim 10^{-6}$M) and the range of concentration of the bases employed were $\sim 5 \times 10^{-4}$ to 2×10^{-3}M.

The description of the Instruments used are given in chapter 2.

4.2.1 Prepation of metallo tetrakis (4-N-methylpyridyl) porphyrins (MTMPyP):[134]

Metallo derivatives of H_2TMPyP have the two central imino hydrogens replaced by a metal ion. The metallation step can be represented as

$$H_2TMPyP \underset{+2H^+}{\overset{-2H^+}{\rightleftharpoons}} TMPyP^{2-} \underset{-M^{2+}}{\overset{M^{2+}}{\rightleftharpoons}} MTMPyP.$$
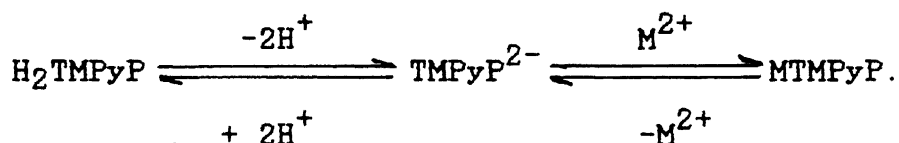
Cu^{2+}, Zn^{2+} and Co^{2+} derivatives of TMPyP prepared as following procedures.[134]

4.2.1a Preparation of Cu^{2+}TMPyP

H_2TMPyP (150 mg) was dissolved in 100 ml of DMF and 100 mg of Cu(II) acetate (in 10 ml of DMF) was taken in a 250 ml round bottomed flask. After adding few drops of glacial acetic acid the mixture was refluxed for 6 hours. The solvent was removed under reduced pressure. The pure Cu(II) TMPyP was obtained after recrystallization from Chloroform-methanol (1:1). Yield: 130 mg (83%).

λ_{max}(nm) : 424 ($\mathcal{E}$ = 2.31 x $10^5 M^{-1} cm^{-1}$).

4.2.1b   Preparation of Zn^{2+}TMPyP:

A mixture of H_2TMPyP (150 mg) in 100 ml of DMF and 100 mg of Zinc acetate in 10 ml of DMF was taken into a 250 ml round bottomed flask. The mixture was refluxed for 1 hour after adding few drops of acetic acid. The solvent was removed under reduced pressure. The crude product was recrystallized from chloroform-methanol (1:1) gave pure ZnTMPyP. Yield 140 mg (89%).

λ_{max}(nm) = 437 ($\mathcal{E}$ = 2.04 x $10^5 M^{-1} cm^{-1}$).

4.2.1c   Preparation of Co(II)TMPyP:

Co(II) TMPyP was prepared by refluxing H_2TMPyP (100 mg) and Co(II) acetate (100 mg) in methanol (100 ml) containing a drop of acetic acid for about 6 hours under nitrogen atmosphere. The solvent was removed under vacuum and the crude product was recrystallized from 1:1 mixture of chloroform: methanol (1:1). The purity was checked by absorption spectrum. Yield: 80 mg (77%).

λ_{max} : 429 nm and 543 nm.

4.3 RESULTS AND DISCUSSION:

4.3.1 Optical absorption studies and evaluation of association constants:

The metal derivatives of TMPyP exhibits intense absorption bands in the visible region the position of which depends on the nature of the metal ion in the porphyrin cavity. There is some controversy regarding the aggregation state of this porphyrin[135].

But Pasternack et al.[133] have shown that H_2TMPyP exists as monomer in solution upto about 40 mM. In the present study the concentrations of porphyrin used were less than 40 mM and we presume that H_2TMPyP exists as monomer in solution.

Addition of nucleic acid base to the porphyrin solution decreased the absorbance and in some cases a red shift of the absorption maxima is also observed. Fig. 4.2 shows the effect of addition of adenine, guanine, cytosine and thymine on the absorption spectra of CoTMPyP. It is clear from the figure that in all the cases the absorbance of the porphyrin decreased upon addition of nucleic acid bases and a considerable red shift of both the soret band [429 nm to 438 nm] and Q-band [543 nm to 552 nm] was observed upon addition of adenine. The Zn and Cu derivatives of porphyrin also shows the same behaviour but no red shift of the absorption bands was observed on addition of adenine. To evaluate the binding constants the absorption spectrum of the metalloporphyrin in the (Soret) region was further followed as a function of increasing base concentration (Figs. 4.3 and 4.4). The observed effects are: (i) a gradual decrease in the absorbance of the metal porphyrin with increasing concentration of base, (ii) a slight broadening and a small red shift (< 2 nm) of the absorption bands. This is consistent with the formation of molecular complexes between metalloporphyrin and the base[105, 120, 133].

The electronic absorption method developed by Nash[136] has been used to evaluate the association constant (K) as follows. The equilibrium reaction between an electron donor (D) and an acceptor (A) resulting in the formation of a 1:1 donor acceptor complex (DA) can be represented as,
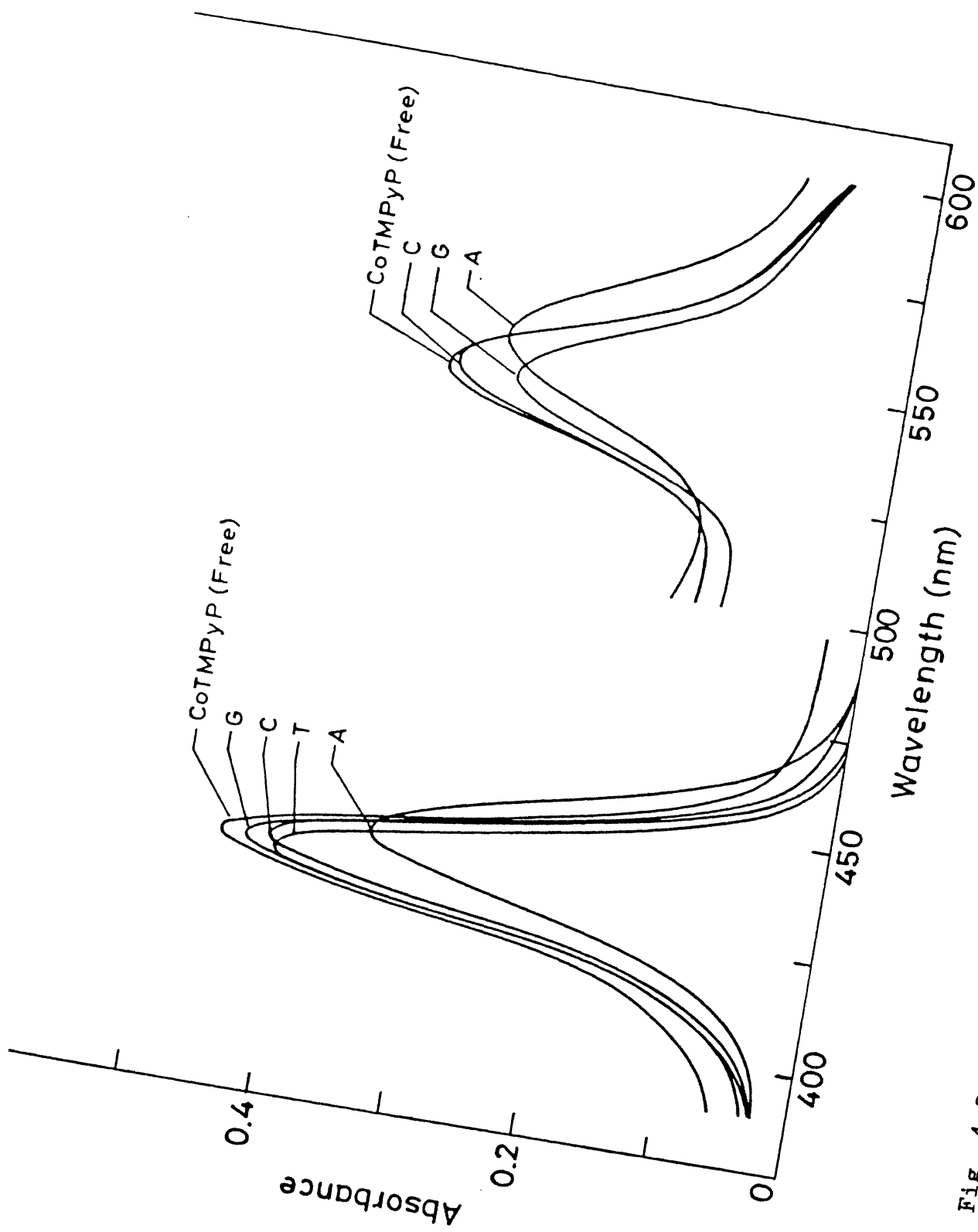
Fig. 4.2 Effect of addition of nucleic acid bases (A, adenine; T, thymine; C, cytosine; and G, guanine) on the visible absorption spectra of CoTMPyP.
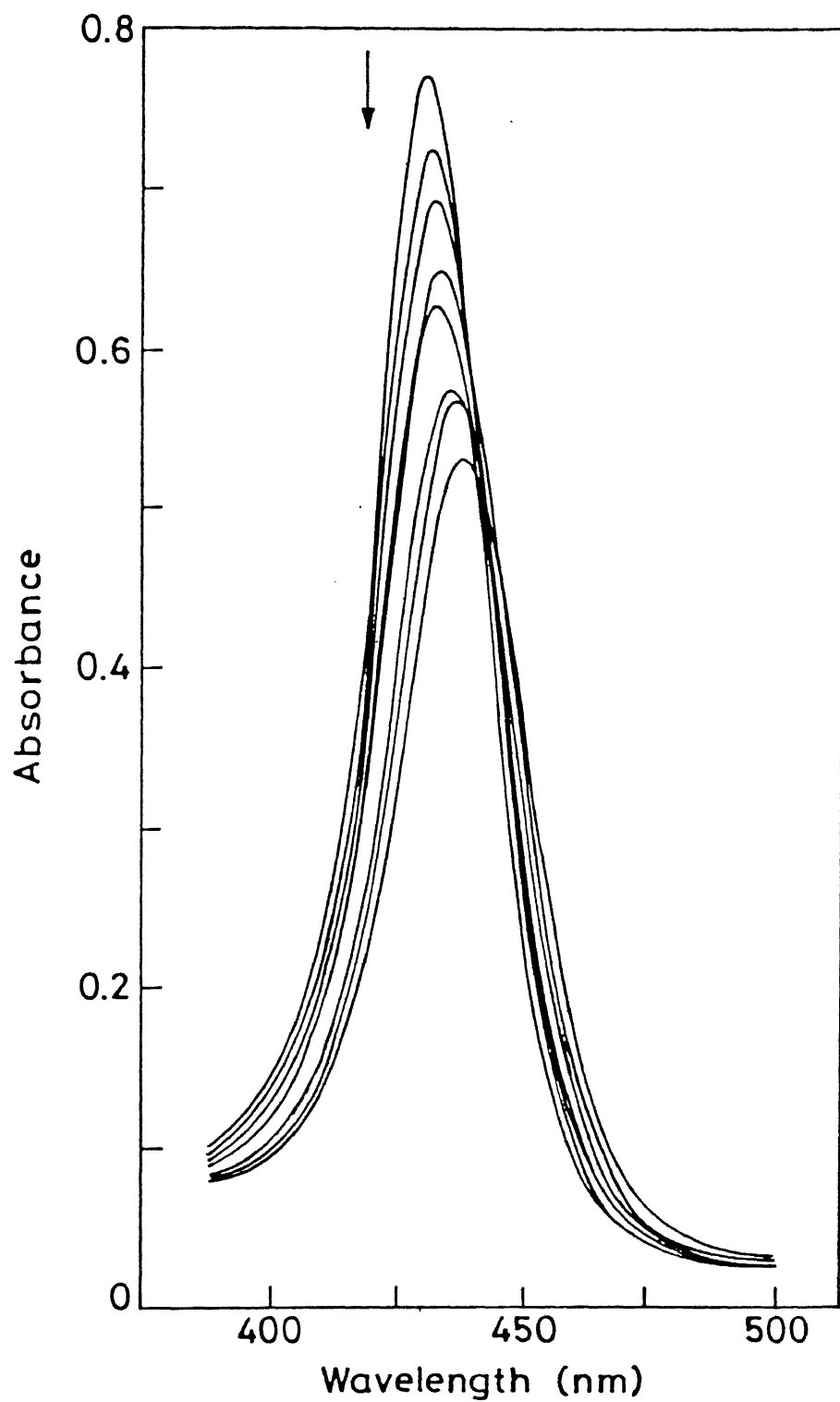
Fig. 4.3   Visible   absorption spectrum of CoTMPyP [1.22 x 10^{-5}M]
containing   increasing   concentration   of   adenine [6.04   x
10^{-5} to 2.42 x 10^{-3}M].
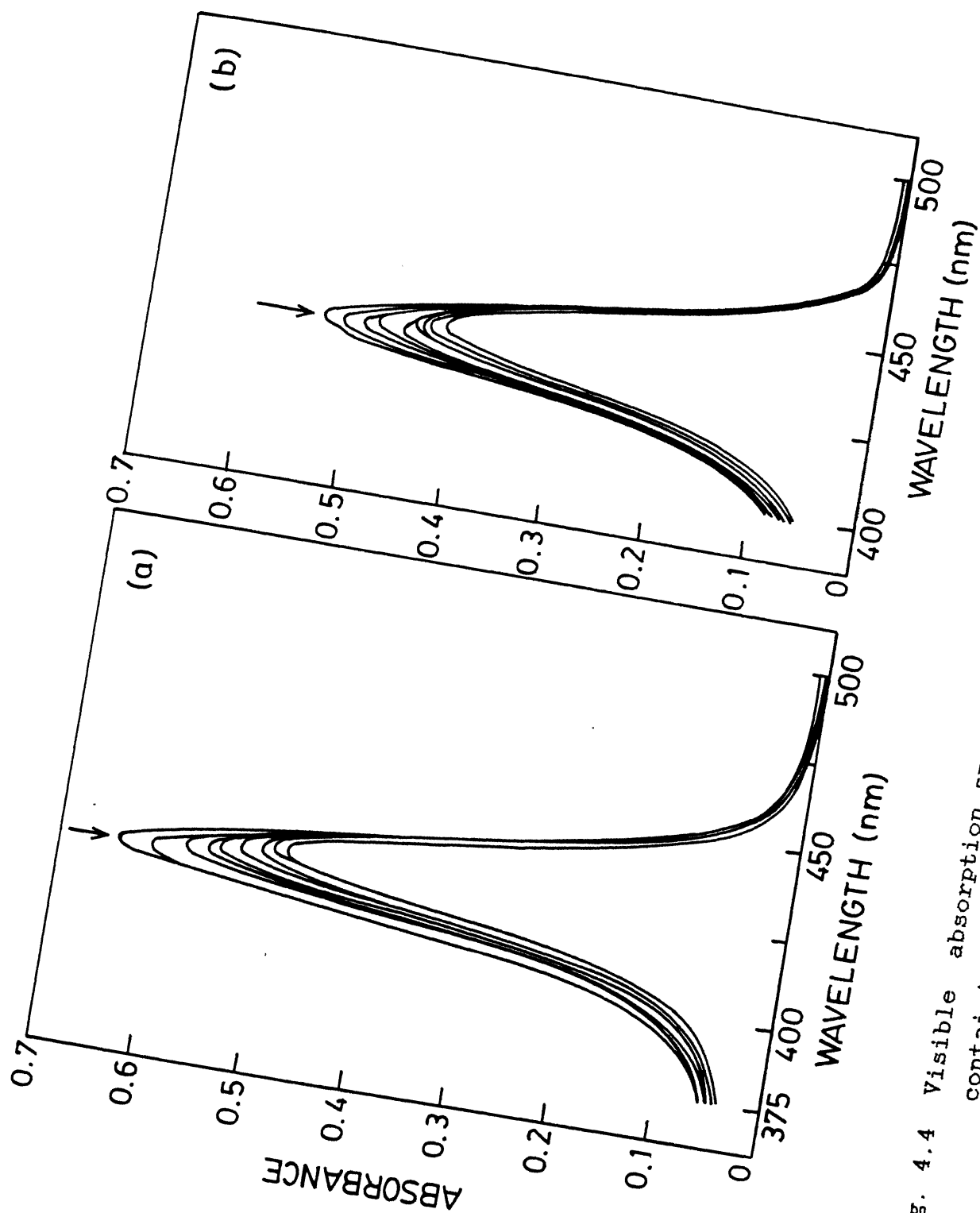
Fig. 4.4 Visible absorption spectrum of (a) CuTMPyP [1.32 x 10⁻⁵M] containing increasing concentration of adenine (1.21 x 10⁻⁴ to 3.02 x 10⁻³M). (b) ZnTMPyP (1.6 x 10⁻⁵M) containing increasing concentration of adenine (1.21 x 10⁻⁴ to 3.62 x 10⁻³M).
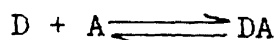
$$D + A \rightleftharpoons DA \qquad \dots 5.1$$

The equilibrium constant for this equation in the concentration units is given by,

$$K = C_{DA}/C_D C_A \qquad \dots 5.2$$

where C_{DA}, C_D and C_A represent the equilibrium concentrations of the complex, donor and acceptor respectively. For this equilibrium Nash had derived an equation of the form

$$1/C_A = d^o/(d^o-d)[(K - \varepsilon_{DA}/\varepsilon_D)] - K \qquad \dots 5.3$$

where d^o is the optical density of pure donor, d is the total optical density of the complex and the donor. The physical significance of this equation is quite clear when the reciprocal acceptor concentration is plotted against $[d^o/(d^o-d)]$. The intercept of the straight line should be negative of the equilibrium constant and the slope is related to the molar absorptivity of the complex. This equation is made use of in the present study to evaluate the association constants.

The absorption bands (Soret) were monitored to evaluate the association constants for MTMPyP. The linearity of the plots of d^o/d^o-d Vs $1/C_A$ (Fig. 4.5) indicated that the predominant species that exists in solution is 1:1 complex. The possible existence of 1:2 (metalloporphyrin: base) complexes in solution was then analysed using the method of Bent and French[137]. The slopes of the logarithmic plots yielded values in the range from 1-1.7 indicating the existence of higher order complexes. It was difficult to quantify the binding constants of these higher order complexes as they were present in only very low concentrations.
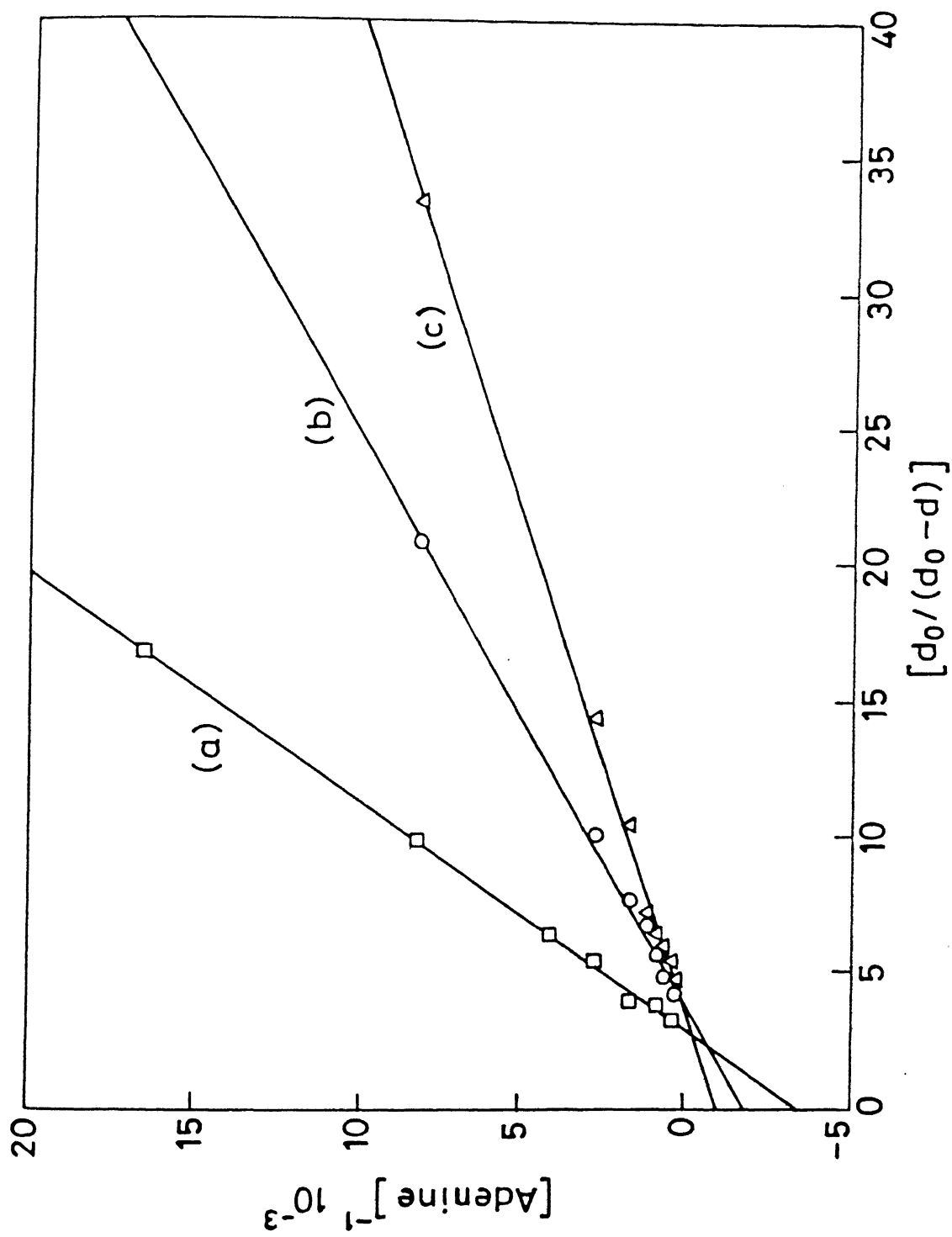
Fig. 4.5 Plots of d^o/d^o-d versus $1/C_A$ for the interaction of (a) CoTMPyP-adenine; (b) CuTMPyP-adenine and (c) ZnTMPyP-adenine at 30^oC.

However, the presence of these complexes did not alter the magnitudes of K-values calculated for 1:1 complexes appreciably. The interaction of the nucleic acid bases with metalloporphyrin could also be of coordinative type where they can bind to the metal axially forming strong complexes like in pyridine or imidazole[138,139]. If such kind of interaction exists, then a large red shift of the soret band as well as the Q-bands is expected in all the cases because of the formation of five/six coordinate complexes. The failure to observe the expected red shift in all the cases at least in the soret region indicates that the interaction between the macrocycle and the nucleic acid base is of the stacking type with $\pi-\pi$ interaction. A similar observation is made recently by Saterlee et al. for the interaction of uroporphyrin with quinine[140].

It has been shown in the previous chapter that the Co(II) porphyrins in the presence of molecular oxygen and amine ligands undergoes oxidation to Co(III) porphyrins[31,32]. The red shift observed in the case of CoTMPyP-adenine could be due to the oxidation of $Co^{II}TMPyP$ to $Co^{III}TMPyP$ in presence of molecular oxygen and adenine. The position of the absorption maxima also agree well with this observation. The peak at 429 nm in the soret region is characteristic of the $Co^{II}TMPyP$ while that peak is shifted to 438 nm which is characteristic of $Co^{III}TMPyP$[141]. This observation is also supported by the ESR studies where the signals due to the paramagnetic Co^{II} (I = 7/2) is lost upon addition of adenine in presence of molecular oxygen. However, it is not yet clear why only in the case of adenine the shift in the absorption maxima was observed while in the case of cytosine, guanine and thymine no shift was observed.

The binding constants evaluated from the optical data are listed in Table 4.1. For comparison the K-values obtained by Pasternack et al.[133] for the corresponding monophosphates are included in the table. It is seen from the table that the K-values obtained in the present study are of comparable magnitude to those determined by Pasternack et al. for the nucleosides and nucleotides. The binding constants for CuTMPyP is higher than those observed for ZnTMPyP for both cytosine and adenine. The values observed for CoTMPyP are higher than those observed for Cu and Zn complexes. It is difficult to quantify the data obtained for CoTMPyP since it is undergoing oxidation to Co^{III}TMPyP. However, the higher value of binding constant for CuTMPyP relative to ZnTMPyP for both adenine and cytosine could be explained by considering the structure of the macrocycle. It is known that all the metalloporphyrins possess a rigid structure and the positive charges are located on the alkylated pyridine residue of the porphyrin. The pyridinium ring is out of the plane with respect to porphyrin plane. The CuTMPyP shows little tendency to bind axial ligands and exists as a 4-coordinate species in aqueous solution while the ZnTMPyP is five coordinate with the axial water and Zn is out of plane of the porphyrin core[142]. Since the complex formation is of stacking type with $\pi - \pi$ interaction the presence of axial ligand on the metal hinder the $\pi - \pi$ interaction and this is reflected in the magnitude of binding constants.

4.3.2 ESR spectra of complexes:

The ESR spectral studies on paramagnetic Cu(II)TMPyP and Co(II)TMPyP were carried out to estimate the extent of axial

Table 4.1: Binding constants $K[dm^3 mol^{-1}]$ of MTMPyP complexes with nucleic acid bases (pH 6.5; temp. $30^{\circ}C$)

Metal porphyrin	$K \times 10^{-3}$ ($dm^3 mol^{-1}$) with			
	Adenine	dAMP[*]	Cytosine	dCMP[*]
CoTMPyP	3.45	–	7.50	–
CuTMPyP	1.85	1.80	0.81	1.00
ZnTMPyP	1.03	0.90	0.45	0.30

* Data taken from ref. (134).

perturbation and the changes in the electronic structure of the metal ion on complexation.

4.3.2a ESR spectra of Cu(II)TMPyP:

The ESR spectra of copper porphyrins have been extensively studied[143,144]. The electronic ground state of a Cu(II) porphyrins is $^2B_1$ with configuration $(b_2)^2$ $(e)^4$ $(a_1)^2$ $(b_1)^1$ [$b_1(dx^2-y^2)$, $a_1(dz^2)$, $e(d_{xz}, d_{yz})$ and $b_2(d_{xy})$].

The ESR spectra of CuTMPyP and its 1:1 complex with adenine are shown in Fig. 4.6 at 100 K in water- glycerol (3:1) mixture. The ESR spectrum of CuTMPyP consists of two sets of metal hyperfine lines corresponds to parallel ($g_\parallel$) and perpendicular ($g_\perp$) regions. The metal hyperfine lines in perpendicular region of ESR spectrum are further split by the superhyperfine interaction with four nitrogens of pyrrole rings, permitting the calculation of $g_\parallel$, $g_\perp$, $A_\parallel{}^{Cu}$, $A_\perp{}^{N}$. The third component of the copper parallel line is merged with much stronger perpendicular lines to some extent while the fourth line in parallel region is completely overlapped. The spectrum of the frozen solution was interpreted with the spin Hamiltonian for axial symmetry[144b].

$$
\begin{aligned}
H = \beta\,[& g_\parallel\,(H_zS_z) + g_\perp\,(H_xS_x + H_yS_y) \\
 & + A_\parallel{}^{Cu}(I_zS_z) + A_\perp{}^{Cu}(A_xS_x + A_yS_y) \\
 & + A_\parallel{}^{N}(I_z{}^{N}S_z) + A_\perp{}^{N}(I_x{}^{N}S_x + I_y{}^{N}S_y)]
\end{aligned}
\qquad 5.
$$

where $(z, \parallel)$ and $(x, y, \perp)$ refer to, parallel and perpendicular directions respectively to the central copper axis. S, I^M and I^N refer to the electron spin, copper nuclear spin and Nitrogen nuclear spin respectively. H is the applied magnetic field and β is the Bohr magneton.
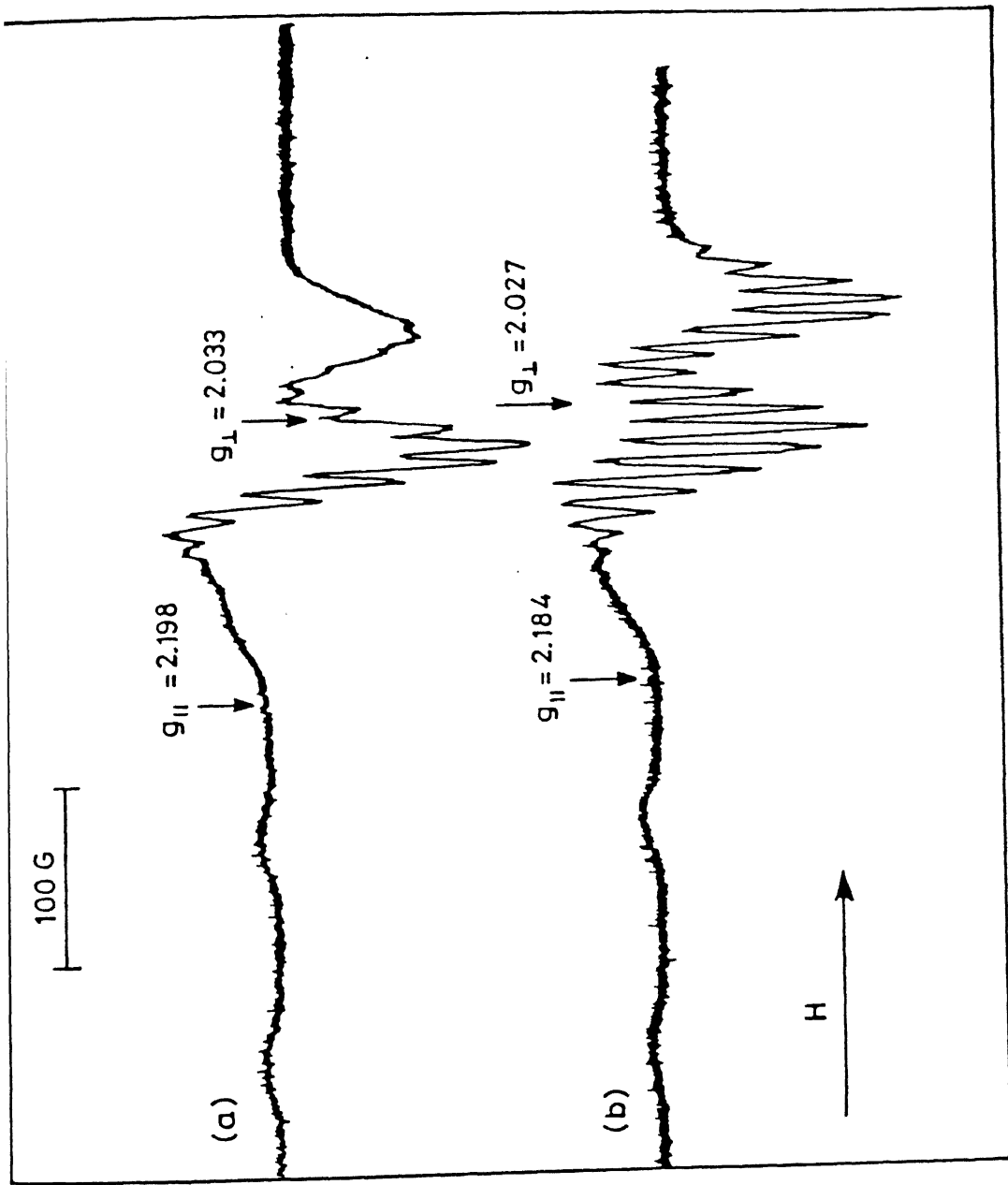
Fig. 4.6 ESR spectra of (a) CuTMPyP and (b) 1:1 complex CuTMPyP: adenine in 3:1 water-glycerol mixture at 100K.

The $g_{||}$ values in the present study were calculated by measuring the field at the mid point between the second and third copper parallel lines. In the high field region of the spectrum (perpendicular region) there are 18 lines which are almost equally separated by ~15 Gauss. The value of $g_{\perp}$ was calculated by measuring the magnetic field at the 8th line of 18 lines allow in $\perp$ region. In the present study, the values of $A_{11}{}^{Cu}$ and $A_{\perp}{}^{N}$ were calculated as described in literature.

The bonding parameter (α^2) which is a measure of covalency of the inplane σ- bonding of the Cu-N bond was calculated using an expression[145] based on the copper hyperfine tensor A_{11} as,

$$\alpha^2 = -[(A_{||}/P) + (g_{||} -2) + 3/7(g_{\perp} -2) + C]$$

where 'C' is the constant and P (P = 0.0354 cm^{-1}) is a constant term proportional to the d-orbital radical integral.

The ESR parameters are listed in the Table 4.2. Upon inspection of the Table 4.2 the following effects are observed upon complexation with nucleic acid bases are: (i) a small decrease in $g_{||}$ and $g_{\perp}$ and $A_{||}{}^{Cu}$ values and (ii) a small increase in the $A_{\perp}{}^{Cu}$ and $A_{\perp}{}^{N}$ values. These effects are consistent with the formation of the molecular complexes[146]. The manifestation of such effects arise from relatively small change in the distribution of π-electron levels of porphyrin π-system as a consequence of $\pi - \pi$ interaction. Such $\pi - \pi$ interaction causes a change in the electron distribution over the porphyrin core affecting the electronic energy levels of the central metal ion. The perturbance of electronic levels of Cu is seen in the slight decrease in the value of the covalency factor (α^2) of the (Cu-N) σ-bond. This decrease in α^2 signifies that the σ-

Table 4.2: ESR parameters[a] for the interaction of CuTMPyP with nucleic acid bases

Complex	$g_{\parallel}$	$g_{\perp}$	$10^4 A_{\parallel}^{Cu}$ (cm^{-1})	$10^4 A_{\perp}^{Cu}$ (cm^{-1})	$10^4 A_{\perp}^{N}$ (cm^{-1})	α^2
CuTMPyP[b]	2.198	2.033	182.03	29.67	14.83	0.7264
CuTMPyP-adenine	2.184	2.027	175.50	31.06	15.53	0.6913
CuTMPyP-cytosine	2.185	2.028	176.77	30.83	15.41	0.6965
CuTMPyP[c]	2.197	2.033	175.61	28.53	14.26	0.7077
CuTMPyP-Adenine	2.191	2.028	174.15	32.34	16.17	0.6948

(a) The estimated errors are 0.001 for g and $\pm\ 1 \times 10^{-4} cm^{-1}$ for $A_{\parallel}^{Cu}$ $\pm\ 0.1 \times 10^{-4} cm^{-1}$ for $A_{\perp}^{N}$ values. $A_{\parallel}^{N}$ could not be determined due to poor resolution of the spectrum. The $A_{\perp}^{N}$ values were determined from partially enlarged spectrum.

(b) In 1:3 glycerol-water.

(c) In DMSO.

bonding is slightly more covalent in the complex relative to the free CuTMPyP. A similar observation was made by Iwaizumi et al.[146a] for the molecular complexes of Cu-porphyrins with π-acceptors.

The ESR spectrum of CoTMPyP was not resolved well and is characteristic of a typical oxygenated Co complex[147]. Also the lines were very weak and did not allow any accurate determination of ESR parameters. Upon addition of adenine the signal was completely lost and a weak free radical signal at g = 2 was observed. This is consistent with the oxidation of paramagnetic Co^{II} to diamagnetic Co^{III}TMPyP. The identity of the free radical signal is not yet determined with certainty but it resembles like a spectrum of superoxide.

4.4 CONCLUSIONS:

The spectral data obtained in the present study provides some insight into the proposition of possible overlap structures of porphyrin and nucleic acid base in solution. The failure to see any expected red shift both in Q-band region and soret band region (CuTMPyP and ZnTMPyP) upon addition of increasing amounts of nucleic acid bases suggest the absence of coordinative interaction. Thus, it is reasonable to presume that the major stabilization for the complex arises from the π-π interaction of the porphyrin and nucleic acid base. Based on 1:1 stoichiometry, a structure could be perceived by juxtapositioning the base over the porphyrin keeping the intermolecular distance at van der Waals interaction level. CPK models indicate that one can visualize a structure interms of a plane to plane overlap such that the aromatic ring of the bases placed over the center

of the porphyrin core promoting $\pi-\pi$ interaction. Such a stacking type interaction has been proposed earlier for the interaction of uroporphyrin I with Quinine based on the spectral data.[140]

However, the red shift observed for both soret and Q-bands of Co(II)TMPyP upon addition of adenine suggest a co-ordinative type of interaction. A plot of $log[A^{o}-A^{c}/A^{c}-A^{\infty}]$ versus log[Adenine] [where the A^{o}, A^{c} and A^{∞} are absorbance of CoTMPyP in absence of base (A^{o}), in the presence of base (A^{c}) and at maximum concentration of base (A^{∞})] gives straight line with a slope of 1, indicating that the stoichiometry (Fig. 4.7) of Co(II) porphyrin to adenine is $1:1$[139]. It has been shown in the earlier chapter that the Co(II) porphyrins has the tendency to co-ordinate amine ligands in the presence of molecular oxygen resulting in the formation of Co(III) porphyrins. Thus it is possible that CoTMPyP binds adenine at one of the axial sites with the 6th co-ordinate side occupied by molecular oxygen undergoes oxidation to Co(III)TMPyP. The position of absorption maxima aggrees with the Co(III)TMPyP formulation. The disappearance of ESR signal due to Co(II) species upon addition of adenine is also consistent with this formulation.
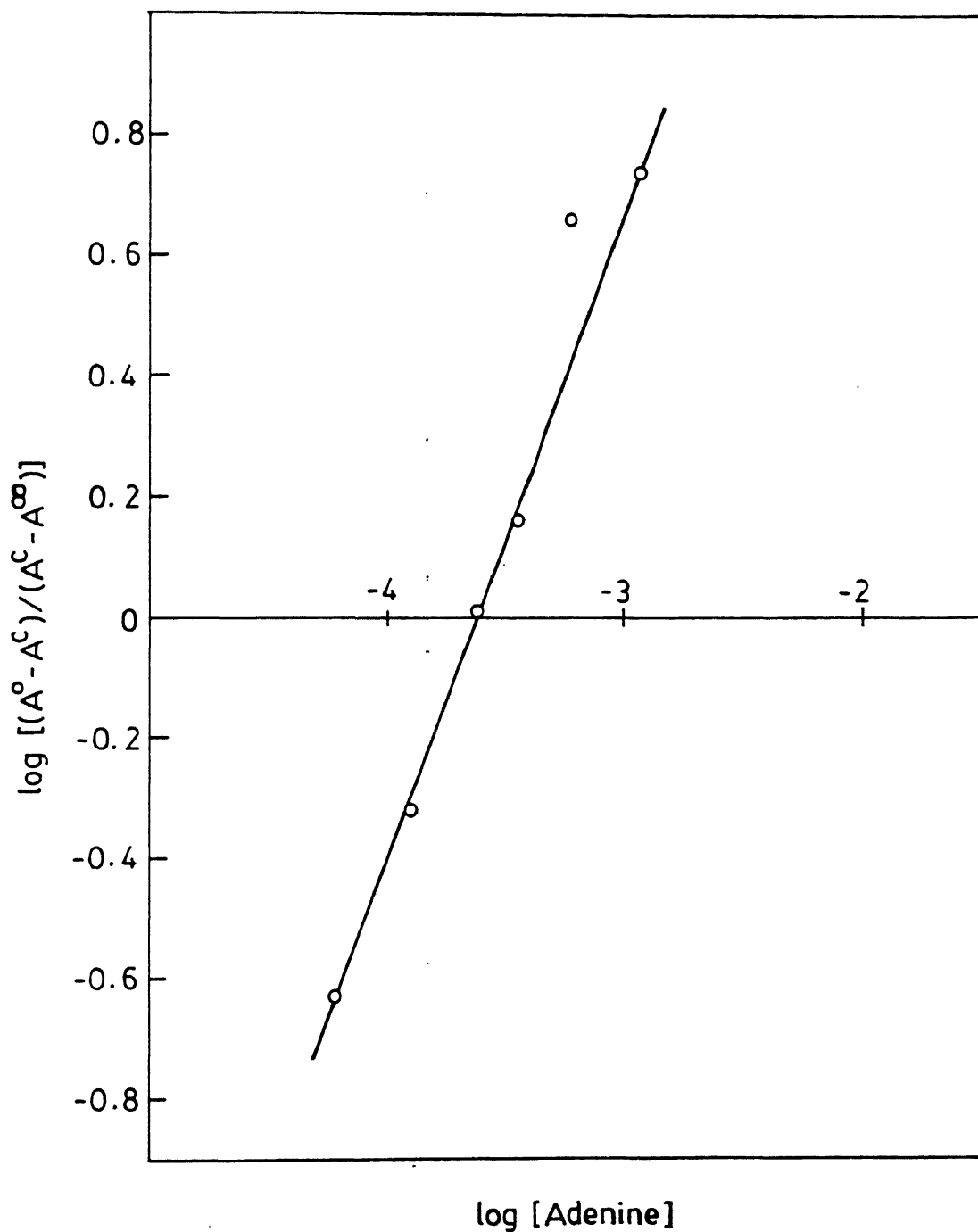
Fig. 4.7   Plot of log [Adenine] versus log $[(A^O-A^C)/(A^C-A^\infty)]$ of CoTMPyP-adenine complex.

CATION AND SOLVENT INDUCED DIMERIZATION OF METALLOTETRACROWNED
PHTHALOCYANINES

5.1 INTRODUCTION:

In earlier chapters 3 and 4, the discussions were confined to interaction between a porphyrin unit and an electron acceptor/donor. It is also possible that the two porphyrins/ phthalocyanines which are oriented in a face to face geometry can exhibit electronic coupling because of interaction between themselves, which result in large changes in the spectral characteristics. This chapter describes studies on interaction of two phthalocyanine rings containing crown ether voids.

Recent studies on photosynthetic systems have revealed the involvement of dimers and higher aggregates of chlorophyll molecules in the photosynthetic pathway.[59b,148] Also, the X-ray structure of the reaction center (RC) complex of R.viridis support the earlier observations that one of the components of the RC is a bacteriochlorophyll dimer [(B.Chl)$_2$][149].

Several spectral descriptions of the model systems directed towards mimicking those of bacteriochlorophyll dimer are available in literature.[150] The dimeric porphyrin based model systems thus far reported are by covalently linking of two monomeric units.[151] But it is well established that there is no covalent linkage between two chlorophyll molecules in bacterio- chlorophyll dimer [(B.Chl)$_2$]. To get an insight into the structure and properties of these chlorophyll dimers and higher aggregates research has been focussed on the synthesis and study of aggregates of chlorophyll like molecules such as metallo-

porphyrins[152] and phthalocyanines.[153]

Recently it has been reported that the dimerization can be induced in the porphyrins and phthalocyanine systems containing appended crown ethers.[153] In these systems, dimerization can be induced by addition of alkali cations to a dilute porphyrin solution ($CHCl_3$-CH_3OH). While this work was in progress, Lever et al reported the synthesis, characterization and dimerization of tetracrowned phthalocyanines and its Zn^{2+}, Cu^{2+} and Ni^{2+} derivatives.[153] In these systems, the cation induced dimerization were studied using optical and magnetic resonance methods. The spectral studies indicated a face to face dimer formation between two monomeric π-systems. The ESR studies on copper tetra crowned phthalocyanine, indicated that the separation between two Cu^{2+} centers is 4.1 A°. In this chapter we wish to report our studies on synthesis and dimerization of metallophthalocyanines appended with four crown ether voids at 3,4 positions (MtCRPc; M = VO^{2+} and Ag^{2+}). The optical and ESR studies indicated an electronic coupling between a pair of metallophthalocyanine moieties in a cofacial geometry, similar to the studies of Lever and coworkers.[153] Furthermore, the ESR studies allowed an estimation of distance between the two metal centers and the calculated metal-metal distance compare well with that reported for similar dimers.[154]

5.2 EXPERIMENTAL

5.2.1 Synthesis of 4,5 dibromobenzo-15-crown-5:[155]

A solution of bromine (1.93 ml, 5.97g, 37.3 mmol) in acetic acid (10 ml) was added dropwise into a solution of benzo-15-crown-5 (5g, 18.6 mmol) in acetic acid (30 ml) over 2 hours at

0°C and the reaction was further stirred for 24 hours at room temperature to yield a yellow precipitate. It was filtered and washed with petroleum ether (60-80°). The product was dissolved in ethanol (50 ml) and boiled inorder to expel bromine which was complexed in the crown ether ring. Cooling to room temperature gave the product as white needles. Yield: 3.76g, (60%): m.p. 80°C

^{1}H NMR (CDCl$_3$): δ 7.05(2H,s) and 3.8-4.1 (16H, m).

IR (KBr) : $\nu_{aromatic}$(C-Br). 650 cm^{-1}.

5.2.2 Synthesis of 4,5-dicyanobenzo-15-crown-5:[156]

A mixture of 3g (8.9 mmol) of 4,5-dibromobenzo-15-crown-5, 2.39g (26.7 mmol) of CuCN and 1 ml of pyridine in 50 ml of DMF was refluxed while stirring for 20 hours under an atmosphere of dry Argon. The mixture was cooled and poured into 200 ml of 25% aqueous NH$_3$ solution and stirred for 1 hour. The mixture was extracted with CHCl$_3$ (3 x 100 ml) and the combined organic extracts were washed with water (3 x 100 ml), dried over anhydrous Na$_2$SO$_4$ and solvent was evaporated, resulting solid was extracted with diethylether using Soxhlet extractor gave a colour less crystalline solid. yield 1.9g (67%). m.p.: 151-152°C

^{1}H NMR (CDCl$_3$): δ 7.15 (2H,s); 3.7-4.4 (16H,m)

IR (KBr) : ν(C$\equiv$N) 2225 cm^{-1}

5.2.3 Synthesis of free base tetra crowned phthalocyanine (H$_2$tCRPc):[155,156]

H$_2$tCRPc was prepared by refluxing 4,5-dicyanobenzo-15-crown-5 (1.9g, 5.98 mmol) in 2-(dimethylamino) ethanol (10 cm^3) for 24 hours, a dark green precipitate was separated. The reaction mixture was filtered and precipitate was washed with water, dried

over anhydrous Na_2SO_4 and then chromatographed on basic alumina. Initiall yellow band in $CHCl_3$ was discarded. The dark green band separated with Methanol-chloroform (2:98 V/V) as eluent gave pure product. Yield 0.4g (21.2%).

5.2.4 Synthesis of zinc tetra crowned phthalocyanine (ZntCRPc)[153]

H_2tCRPc (25 mg) and Zn acetate (100 mg) in 1:1 mixture of 1,2-dichloroethane (20 ml) and ethanol (20 ml) was refluxed for 24 hours. Solvent was evaporated under reduced pressure and resulting solid was washed with water (200 ml). The crude product was purified over basic alumina column using $CHCl_3$ and $CHCl_3$-MeOH as the eluents. Yellow band eluted with $CHCl_3$ was discarded. The light green band moved in $CHCl_3$-MeOH (98:2 v/v) was identified as the unreacted H_2tCRPc. The bluish green band eluted with $CHCl_3$-MeOH (95:5 v/v) gave the pure ZntCRPc. Yield: 15 mg (57%).

5.2.5 Synthesis of copper tetra crowned phthalocyanine (CutCRPc):[157]

H_2tCRPc (25 mg) and Cupric acetate (100 mg) in a mixture of 1,2-dichloroethane (20 ml) and methanol (20 ml) was refluxed for 24 hours. The solvent was evaporated under reduced pressure and resulting residue was washed with water. The crude product was purified by column chromatogrphy over basic alumina using $CHCl_3$ and $CHCl_3$-MeOH as the eluents. In chloroform the yellow material was eluted which was discarded. A light green band which moved in 2% CH_3OH was identified as unreacted H_2tCRPc and the final bluish green band was eluted with 5% CH_3OH was identified as pure CutCRPc. Yield 17 mg (65%).

5.2.6 Synthesis of Vanadyl tetra crowned Phthalocyanine (VOtCRPc):

H_2tCRPc (40 mg) and vanadyl sulphate (100 mg) in 100 ml of dry DMF was refluxed for 7 days. Solvent was evaporated under reduced pressure gave the dark green powder. The crude product was washed with excess water to remove unreacted $VOSO_4$ and was purified by basic Alumina Column using $CHCl_3$-MeOH (95:5 V/V) gave the pure green powder of VOtCRPc. Yield: 13 mg (30%).

5.2.7 Preparation of silver tetracrowned phthalocyanine (AgtCRPc):

H_2CRPc (20 mg), $AgNO_3$ (20 mg) and sodium acetate (20 mg) in a mixture of 1,2-dichloroethane (15 ml) and acetic acid (20 ml) was refluxed for 2.5 hours. The reaction mixture was filtered and resulting solid was washed with excess water. The crude product was dissolved in chloroform and subjected to column chromatography over basic alumina. A light green band was eluted with 2% CH_3OH was identified as unreacted H_2tCRPc. The bluish green band eluted in $CHCl_3$: MeOH (95:5 V/V) gave the pure AgtCRPc. Yield. 8 mg (40%).

5.2.8 Methods:

The details of instruments used in this chapter are described in chapter 2.

5.3 RESULTS AND DISCUSSION:

Synthesis of metallophthalocyanines (M = VO^{2+}, Ag^{2+}) functionalized at 3,4-positions with four crown ether voids (Benzo-15-Crown-5) are shown in Scheme 5.1, and the products were characterized using electronic and ESR spectral methods.

NC

NC

2-(dimethylamino) ethanol Δ

$\dfrac{DMF}{CuCN}$

Br

Br

$\dfrac{Br_2, Fe\ Powder}{CH_2Cl_2}$

$\dfrac{VOSO_4}{DMF, \Delta}$

VOtCRPc

$\dfrac{AgNO_3, NaOAc; \Delta}{C_2H_4Cl_2, CH_3CO_2H;}$ 2.5 hours

AgtCRPc
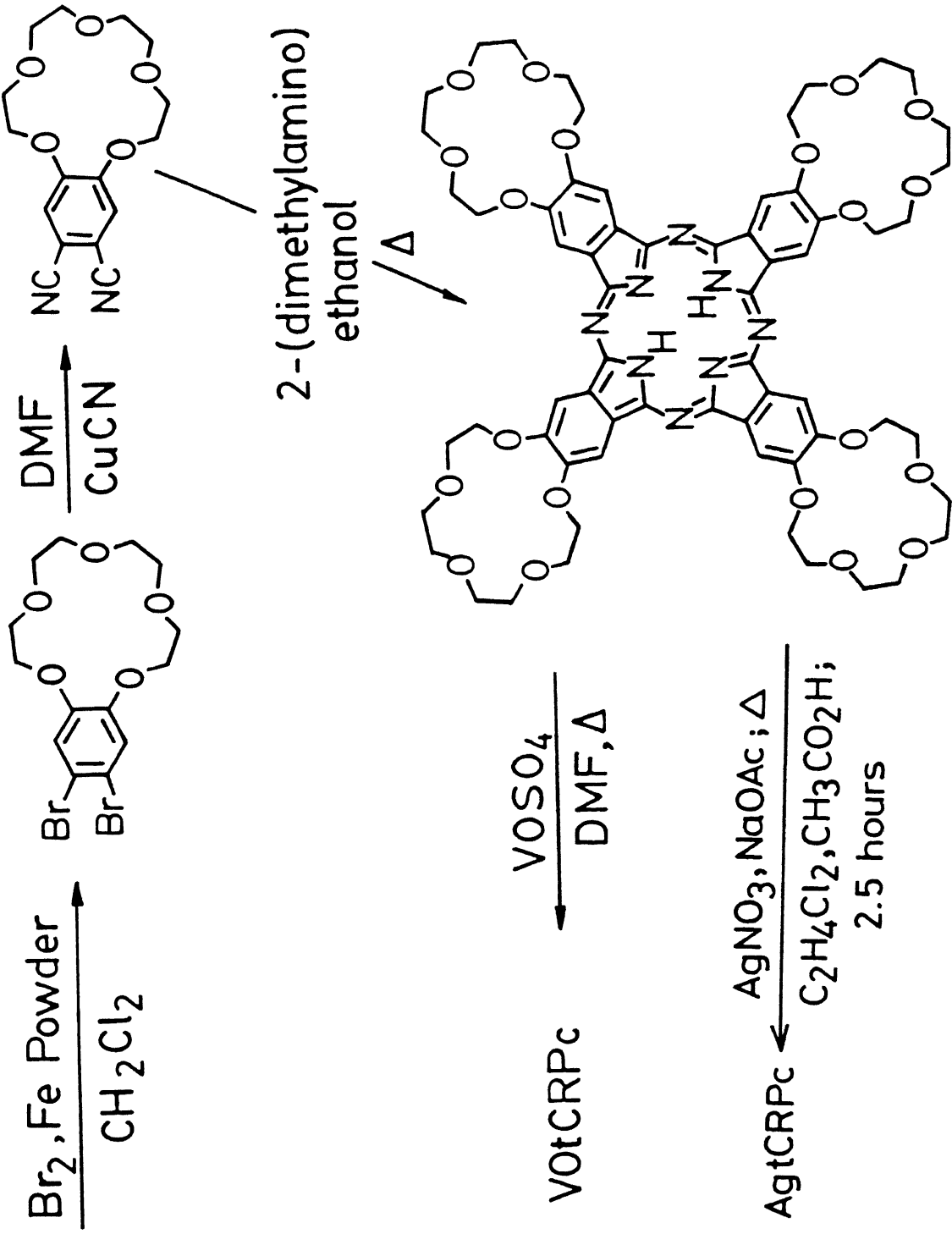
SCHEME 5.1

5.3.1 Electronic Spectra:

In chloroform solution ($\sim 10^{-5}$M) the metal tetra crowned phthalocyanine (MtCRPc; M = Zn^{2+}, Cu^{2+}, VO^{2+} and Ag^{2+}) exhibit spectra typical of monomeric metallo phthalocyanines[158] with a single intense $\pi - \pi^*$ transition in the range 665-700 nm, associated with higher energy vibrational components, commonly refered to as the Q bands and a second intense and broader $\pi - \pi^*$ transition at 300-360 nm called the Soret.[158] The metal free species (H_2tCRPc) is similar but shows two closely spaced Q-bands because of its lower (D_{2h}) symmetry. The absorption data of all the metal derivatives are listed in table 5.1.

The changes in the electronic spectra of MtCRPc (M = VO^{2+}, Ag^{2+}) in $CHCl_3$ solution containing 1% CH_3OH upon addition of increasing amounts of K^+ ions are shown in Fig. 5.1 and 5.2. Specifically the following changes were noted. (i) The Q-bands were shifted to blue (46 nm for VO^{2+} and 37 nm for Ag^{2+}) with broadening and reduction in absorbance. (ii) The soret bands also experienced a small blue shift (8-10 nm) with reduction of absorbance. These results suggest the existence of an equilibrium involving two species. Based on earlier findings from this laboratory[159] and literature[152,160], it is concluded that the two species involved here are monomer and dimer of MtCRPc. In the absence of cation, under our experimental conditions, all MtCRPc exists as monomer and addition of cation strongly drives the equilibrium to the dimer side facilitating the close approach of two phthalocyanine rings to form a dimer through a $\pi - \pi$ interaction.
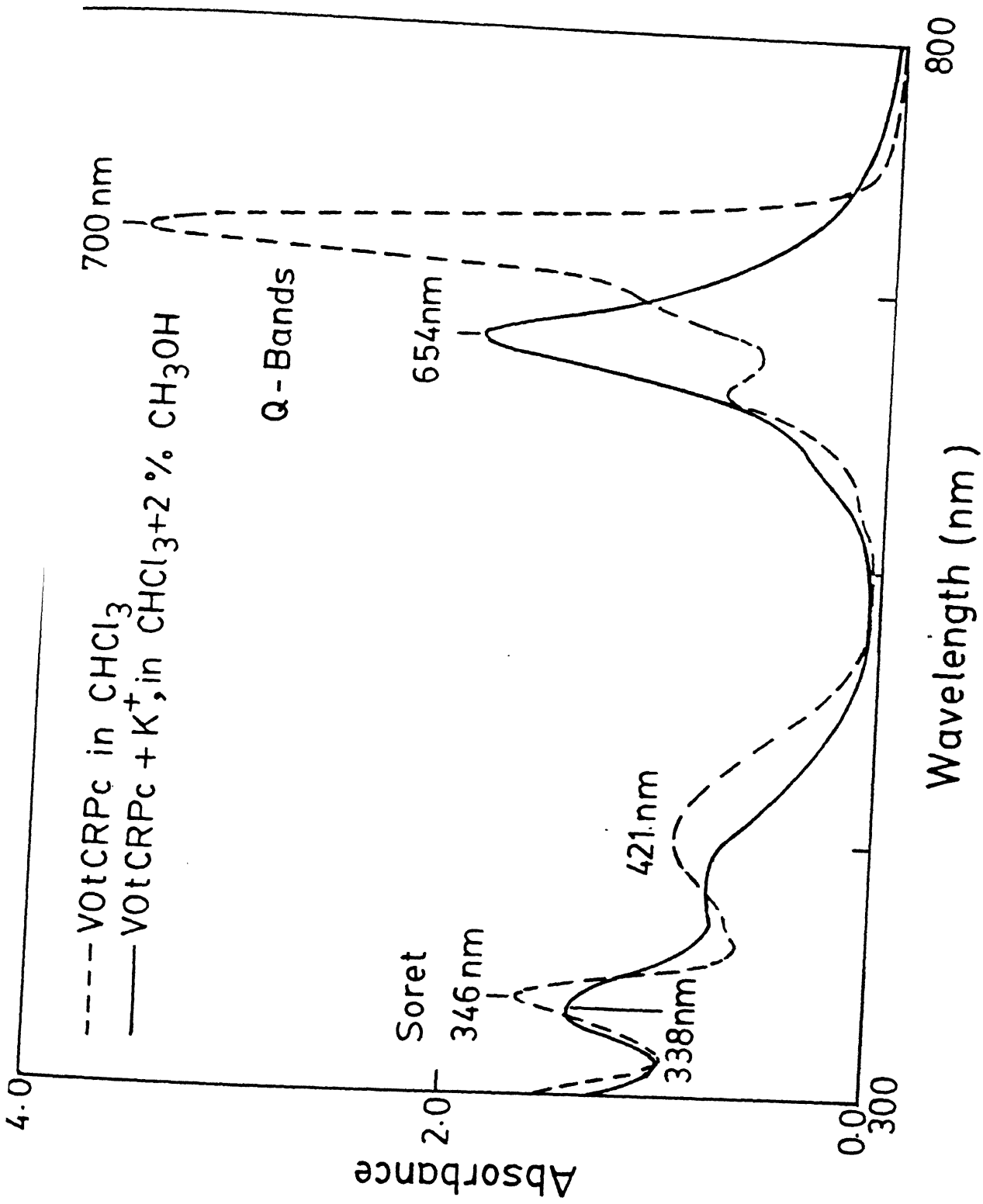
Fig. 5.1 Absorption spectra of VOtCRPc in the presence and absence of K+ ions.

Table 5.1: Optical data of monomers and dimers of tetracrowned phthalocyanines in $CHCl_3$

Compound	Q-bands λ_{max}(nm) ($\varepsilon \times 10^{-3}$)				Soret bands λ_{max}(nm) ($\varepsilon \times 10^{-3}$)		
AgtCRPc	674		642		342		287
	(12.82)		(9.45)		(12.32)		(12.39)
[AgtCRPc]$_2$K$_4^+$	637		–		339		284
[AgtCRPc]$_2$(NH$_4^+$)$_4$	636		–		343		282
[AgtCRPc]$_2$(Cs$^+$)$_4$	637		–		343		287
VOtCRPc	700		632		421	346	–
[VOtCRPc]$_2$K$_4^+$	654		–		–	338	–
H$_2$tCRPc	701	662	644	602	416	348	–
	(33.4)	(27.4)	(11.8)	(6.2)	(8.1)	(30.8)	
[H$_2$tCRPc]$_2$K$_4^+$	640.5	–	–	–	393.5	335	–
CutCRPc	677	–	646.5	613	408.5	341	–
	(129.4)			(31.2)	(23.3)	(57.4)	
[CutCRPc]$_2$K$_4^+$	635.5	–	–	–	338.0	333	–
ZntCRPc	677	–	–	611	–	355	–
	(96.7)			(17.3)		(61.2)	
[ZntCRPc]$_2$K$_4^+$	640	–	–	–	–	349.5	–

The insert in fig. 5.2 gives a plot of intensity changes of the Q-bands of AgtCRPc due to monomeric and dimeric species upon addition of increasing amounts of K^+ ions. The shape of the curve reveals that the process of formation of the dimer involves more than one step. Two types of dimers can be visualized upon addition of cation; a 'side-by-side' dimer of the type MtCRPc-cation-MtCRPc involving only one cation per dimer and a cofacial dimer which involves two or more cations per dimer. When K^+ ions are added to a solution of MtCRPc (M = VO^{2+}, Ag^{2+})[160], the intensity decrease (monomer peak) and increase (dimer peak) is sharp at lower concentrations of K^+ ions probably indicating the formation of a side-by-side dimer with a very high formation constant. At higher concentrations of K^+, a transformation of side-by-side dimer to a cofacial dimer occurs by encapsulating a second cation. Since two more sites are still available in the cofacial dimer for saturation, it is possible that the encapsulation continues at higher concentrations until the two phthalocyanine units bind four cations in the metallophthalocyanines. We believe that in this instance the cofacial dimer involves four cations per dimer.

In order to see whether different cations have different effects on dimer formation, optical spectra of solutions containing same amount of MtCRPc (7.96×10^{-6}M) and 1.6×10^{-5}M of KCl, $NH_4(CH_3COO)_2$, NaCl and CsCl were recorded. It was found that a complete dimerization was observed in the case of K^+ and NH_4^+ ions, while only ~70% dimerization was observed with Cs^+ ions. In the case of Na^+ ions no detectable dimerization was observed. Similar effects were observed for several crown ether linked porphyrins and phthalocyanines upon complexation with

alkali metal cations.[153,154,159a] This selectivity towards different cations varies with crown ether ring size and maximum effects were observed when the size of the crown ether cavity and ionic radii of the metal ions are comparable. Also, the nature of the complex (sandwich type or non sandwich type) depends on the crown ether cavity and cation size.[161] It is known that K^+, NH_4^+ form stable sandwich type complex with Benzo-15-crown-5 (cavity size 1.7-2.2 A^o) while the stability of sandwich complex formed by Cs^+ (ionic radii = 1.67A^o) with Benzo-15-crown-5 is much less compared to K^+ and NH_4^+ ions (ionic sizes are 2.66 and 2.86 A^o respectively). Na^+ ion (ionic size is 1.94 A^o) forms non sandwich type complex. Thus, the observed effects in the electronic spectra of crowned phthalocyanines is inline with this data.

5.3.1a Effect of Solvents:

The intensity and position of the Q-bands of MtCRPc (M = VO^{2+}, Ag^{2+}) are highly dependent upon the solvent used.[153] Fig. 5.3 shows the effect of various solvents on the absorption spectrum of AgtCRPc. It is observed from the fig. 5.3 that in $CHCl_3$ solution the absorption band at 674 nm and higher energy shoulder at 642 nm corresponds to the monomeric AgtCRPc. The intensity and position of these two bands are altered considerably when the solvent is changed; for example in polar solvents like ethanol and butane-1-ol, the monomeric band at 674 nm loses considerable intensity and a new band at ~630 nm gains intensity indicating the presence of dimeric and higher aggregates in solution. However in 100% methanol the band structure is completely lost and a featureless, broad absorption
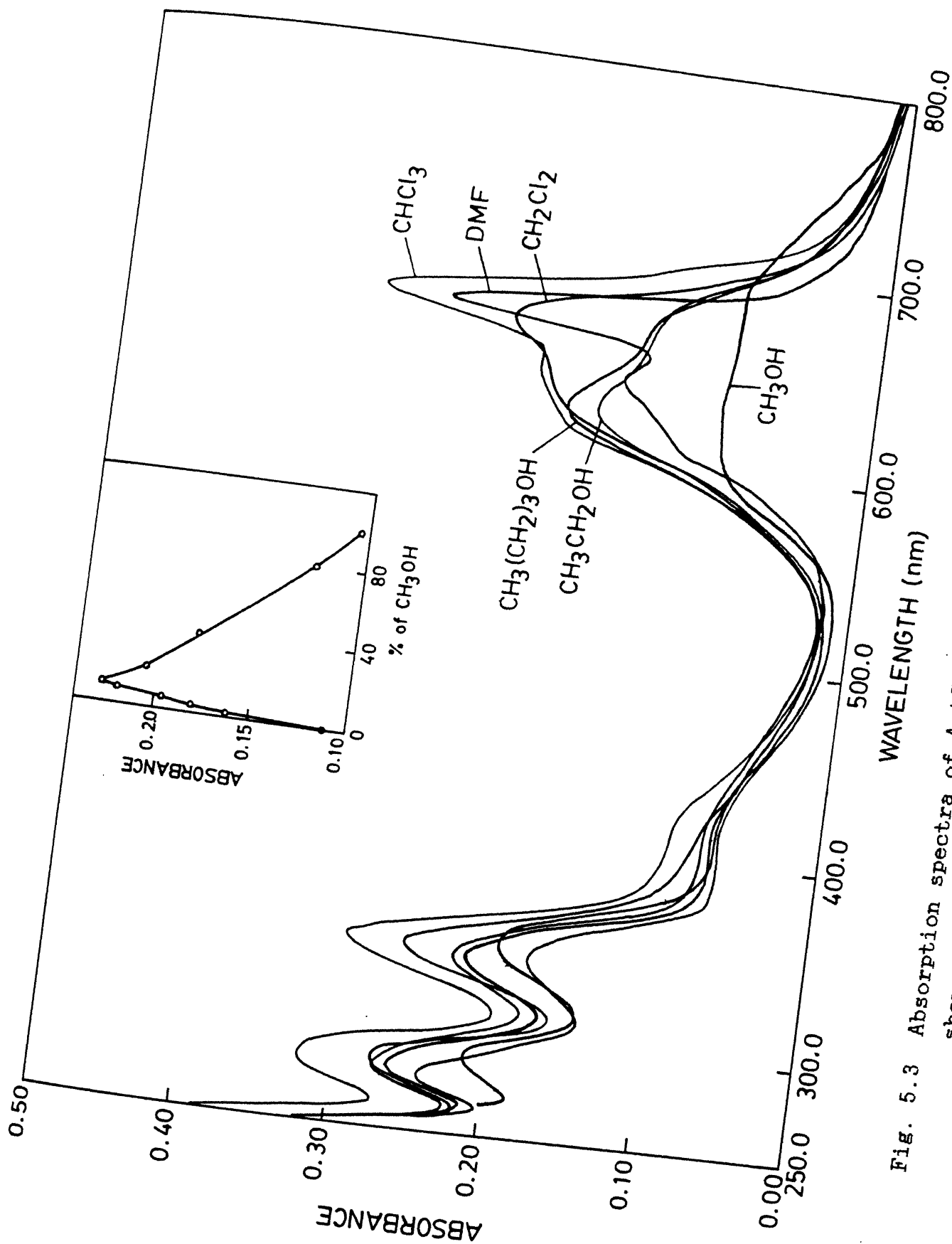
Fig. 5.3 Absorption spectra of AgtCRPc in different solvents. Insert shows the absorption changes at 633 nm (dimer peak) with increasing concentration of CH₃OH.

in the Q-band region clearly indicates the formation of oligomeric AgtCRPc in solution. However the Soret bands are not found to be highly sensitive to the changes in the solvent. Addition of small concentration of methanol to a $CHCl_3$ solution of AgtCRPc generates the dimeric species and the amount of dimeric species formed is found to be critically dependent on the concentration of the methanol used. Insert fig. 5.3 shows the effect of increasing methanol concentration of the dimeric species monitored at 633 nm (which is due to dimeric species). It is apparent from the plot that around 10% methanol concentration in chloroform solution, the maximum dimeric species is formed and any further increase in methanol concentration leads to the formation of higher aggregates. Thus at lower concentrations (less than 10%) the change in the absorption spectrum exactly parallels with that observed upon addition of alkali cations; this observation clearly suggests that the dimerization can be induced even by the solvent, at least in AgtCRPc by addition of various concentrations of methanol (less than 10%) in $CHCl_3$ solution. This is also in consistence with the observation of Lever[153], et al. for the crowned metallo-phthalocyanines.

Assuming a cofacial geometry of the two phthalocyanine rings, the spectral shift (blue shift) upon dimer formation can be explained using exciton theory.[162] The transition between $^1A_{1g} \longrightarrow {}^1E_u$ gives rise to Q-band absorption in metallo-phthalocyanines. The coupling of doubly degenerate excited states of two monomers give rise to two excited states, that are ^1E_g and ^1E_u. This is depicted in fig. 5.4. The nature of the coupling depends on the dimer geometry. In the case of cofacial

In-phase coupling

V

Out of-phase coupling

⟹ Allowed

⟹ Forbidden

V = Dipole – dipole exciton splitting

^1E_u

^1E_g

$^1A_{1g}$

DIMER D_{4h}

^1E_u Q,ES

Q – band

$^1A_{1g}$ Q,GS

MONOMER D_{4h}
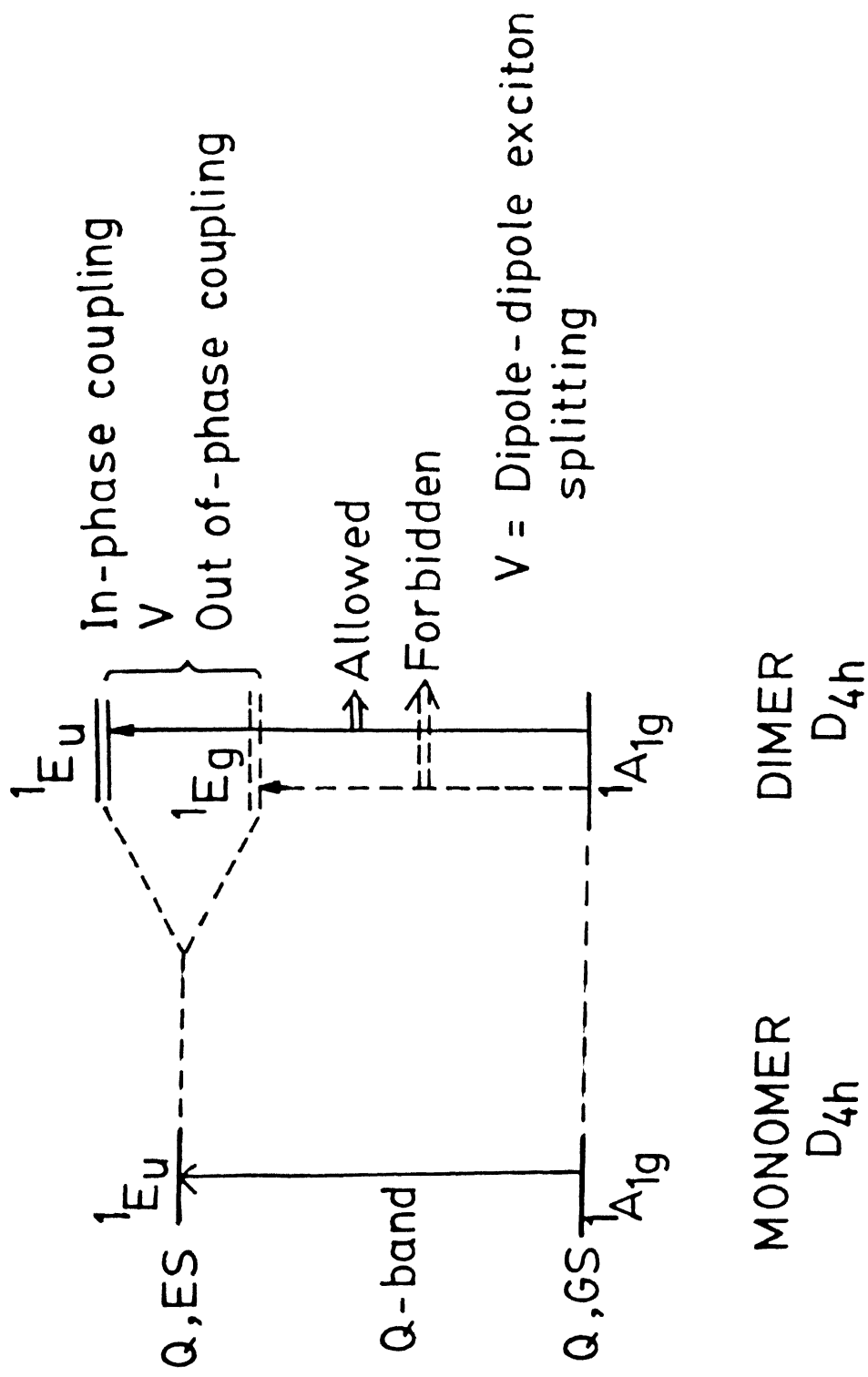
Fig. 5.4   Energy level diagram for Q-band absorption.

dimer, the higher energy degenerate state Eu ($^1A_{1g} \longrightarrow {}^1Eu$) is allowed to give rise to higher energy absorption (blue shift), where as the low energy Eg ($^1A_{1g} \longrightarrow {}^1Eg$) state is 'Laporte' forbidden. Thus the observed blue shifts upon dimerization is consistent with this. The exciton splitting parameter (V) estimated as twice the energy difference between the mononuclear Q-band and the dimeric Q-band peak energy are 1556 cm^{-1} for AgtCRPc and 2009 cm^{-1} for VOtCRPc. This compares very well with those observed[153] for NitCRPc (1760 cm^{-1}), CotCRPc (1960 cm^{-1}), CutCRPc (1910 cm^{-1}) and ZntCRPc (1960 cm^{-1}).

5.3.2 Electrochemical Studies:

The cyclic voltammetric experiments were conducted for H_2tCRPc and MtCRPc (M = Cu^{2+}, Zn^{2+}) in dichloromethane containing 0.1 molar TBAP as the supporting electrolyte. The free base and metal derivatives exhibit two reduction waves with the anodic and cathodic peak separation $\triangle(E_a-E_c)$ in the range of 60-120 mV. The anodic and cathodic peak current ratio (close to unity) indicates both the reduction steps involve one electron-transfer. The half wave potentials were calculated as the average of cathodic and anodic peak potentials and are listed in table 5.2.

A comparison of the reduction potentials of H_2tCRPc and MtCRPc (M = Zn^{2+}, Cu^{2+}) with tetrasulfonatophthalocyanine (Na_4H_2PTS) and its metal derivatives[163] (MPTS, M = Cu^{2+}, Zn^{2+}) are also given in table 5.2. An examination of table 5.2 reveals that the reduction potentials of H_2tCRPc and MtCRPc (M = Cu^{2+}, Zn^{2+}) occur at more negative potential than that of the corresponding H_2PTS and MPTS. It is well known that substitution

Table 5.2: Electrochemical data for crowned phthalocyanines

Compound	Redox Potentials (V) ($\Delta_{Epa-Epc}$)		
	I	II	III
H_2tCRPc	−0.944 (64 mV)	−1.40 (65 mV)	−
$ZntCRPc$	−1.085 (65 mV)	−1.402 (120 mV)	−
$CutCRPc$	−1.099 (60 mV)	−1.369 (120 mV)	−
Na_4H_2PTS[a]	−0.525	−0.970	−1.81
Na_4CuPTS[a]	−0.727	−1.110	−1.895
Na_4NiPTS[a]	−0.672	−1.165	−1.933

a   in DMSO

of electron donating groups ($-CH_3$, $-OCH_3$, $-OCH_2-$) at periphery of the porphyrin/phthalocyanine makes the macrocycle more basic, and potentials occur at more negative (lower) compared with that of unsubstituted tetraphenyl porphyrin.[164] Similarly on substitution of crown ether which is also an electron releasing group at the periphery of the phthalocyanine makes the phthalocyanine ring slightly more basic hence it is difficult to reduce these species relative to the unsubstituted phthalocyanines.

5.3.3 ESR Spectra:

5.3.3a VOtCRPc

The ESR spectrum of VOtCRPc in chloroform containing 2% methanol at 100K are typical of VO^{2+} ions (Fig. 5.5a). The ESR parameters of these crowned phthalocyanines do not show much variation upon crown ether substitution. Addition of cations to these crown phthalocyanines results in the encapsulation of four positive ions in the peripheral ether cavities. The ESR spectra of these compounds in solution do not show any marked changes, indicating that the unpaired electron in oxovanadium is essentially localized in the b_1 (dxy) orbital of the VO^{2+} ion.[154b].

The changes in the ESR spectra of vanadyl crown phthalocyanine observed on addition of K^+ is displayed in fig. 5.5b. The spectrum observed is typical of triplet state with axial symmetry, the hyperfine splitting indicating the presence of two equivalent interacting VO^{2+} nuclei.[154b] Interaction of two VO^{2+} ions with spin 1/2 will give rise to singlet (S = 0) and triplet (S = 1) states, the separation of which depends on the
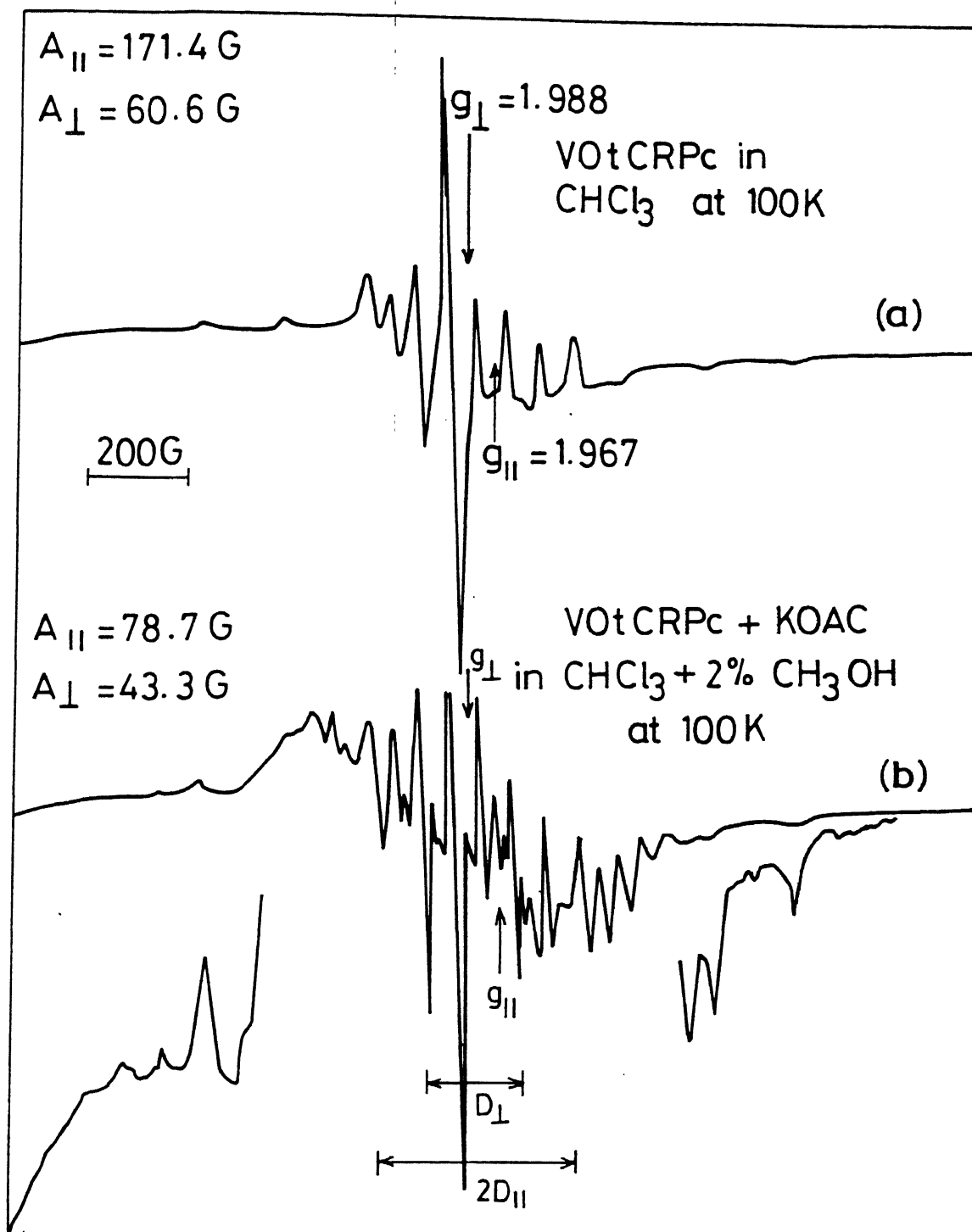
Fig. 5.5 ESR spectra of (a) VOtCRPc, (b) VOtCRPc + KOAc in CHCl₃: CH₃OH (98:2) at 100K.

magnitude of isotropic exchange interaction $-JS_1S_2$ while the separation of the levels within the triplet state is governed by the magnetic dipole-dipole interaction and anisotropic exchange terms. In the case of VO^{2+} and Cu^{2+} ions the isotropic exchange is considered small and the dominant contribution arises mainly from magnetic dipole-dipole interactions with negligible contribution from exchange terms with the assumption that the dimer is axially symmetric and the Z axis of the system and the direction of the applied magnetic field are parallel and coincide with V-V vector. The spin Hamiltonian can be represented as follows.[165]

$$H = g_{||} \beta H_z (S_{1z} + S_{2z}) + g_\perp \beta [Hx(S_{1x} + S_{2x}) +$$
$$Hy (S_{1y} + S_{2y})] + A (S_{1z}I_{1z} + S_{2z}I_{2z}) +$$
$$B(S_{1x}I_{1x} + S_{2x}I_{2x} + S_{1y}I_{1y} + S_{2y}I_{2y}) + H_D \qquad 5.1$$
$$H_D = (\beta^2/r^3)[g_x^2 S_{1x}S_{2x} + g_y^2 S_{1y}S_{2y} - 2g_{||}^2 S_{1z}S_{2z}] \qquad 5.2$$

where H_D is Hamiltonian for dipolar interaction. The zero-field splitting within the triplet state arises from the dipolar terms. With this brief background, the ESR spectra can be analyzed. The eight line pattern arising from both the parallel and perpendicular regions is now decomposed due to the zero-field splitting into two sets of each containing fifteen lines corresponding to a total spin of 7 (I = 7/2 for VO^{2+} ion). The sets of lines in the perpendicular region are separated by the zero-field parameter, 'D', while the parallel sets are separated by '2D'. Because of the similarity of $g_{||}$ and $g_\perp$ values, the lines from both the parts are superimposed. It is found that the parallel lines are equally spaced while those from the perpendicular part are distributed with more spacing in the high-

field region rather than in the low field region.

The appearance of a weak transition (ΔMs = $\pm$ 2) arising from the triplet state (S = 1) in the half field region, g = 4, provides a strong support for the existence of dimers in solution. The ESR parameters evaluated from the spectrum are listed in table 5.3.

Also, the hyperfine splitting $A_{\parallel}^{VO}$ and $A_{\perp}^{VO}$ values of these dimers are roughly half of the hyperfine coupling values observed for the VO(tCRPc) alone. Further the g values found in the dimers are similar in magnitude to those of the vanadyl crowned phthalocyanines, indicating that the coordination environment of the VO^{2+} ions in the dimer is identical with that of the vanadyl phthalocyanine alone. The values of D observed in both parallel and perpendicular regions are used to calculate the inter atomic distance (V-V) in the dimers with use of the following expression.[166]

$$R = [3/4 \ g^2 \ \beta^2 \ \frac{1-3 \ \cos^2 \theta}{D}]^{1/3} \qquad\qquad 5.3$$

For an axial dimer

$$R = [0.65 \ g^2/D]^{1/3} \qquad\qquad 5.4$$

The R-values calculated are given in table 5.4. For comparison the ESR spectra of vanadyl tetra crowned porphyrin (VOtCP) and its dimer are shown in Fig. 5.6 which is known to form the dimer. The 'R' value calculated for VOtCRPc dimer using zero-field splitting parameter (D), both in parallel and perpendicular region of the spectrum indicated the two VO^{2+} ions are separated

Comparison with VO^{2+} crowned porphyrin

A$_{||}$ = 166·66 G
A$_\perp$ = 58·73 G

g$_\perp$ = 1·995

g$_{||}$ = 1·97

VOTCP

(a)

400 G

A$_{||}$ = 84·44 G
A$_\perp$ = 27·77 G

VOTCP DIMER

(b)

D$_\perp$

2D$_{||}$

Magnetic Field (G)
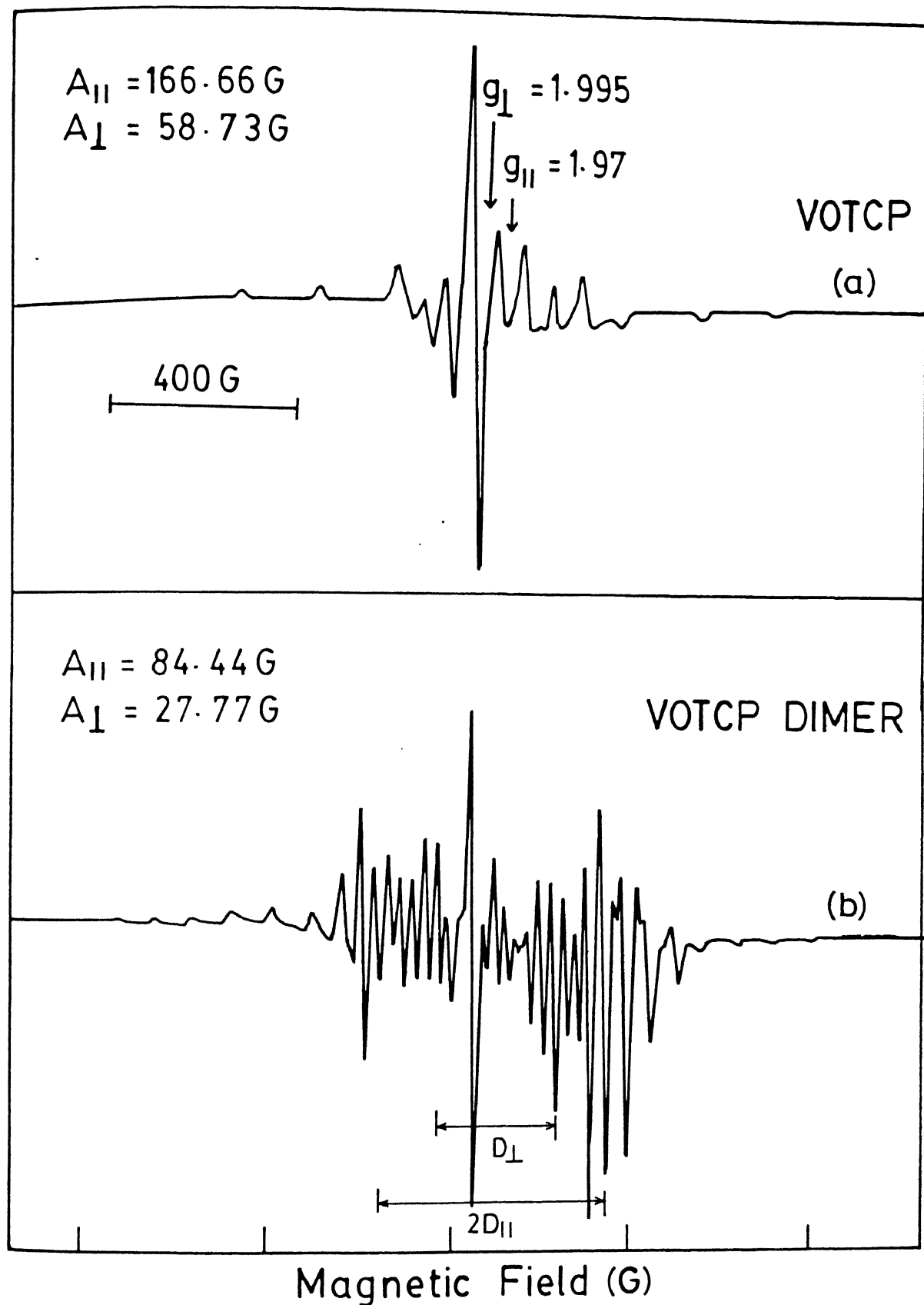
Fig. 5.6   ESR   spectra of (a) VOTCP, (b) VOTCP + KOAC   in   CHCl$_3$:
CH$_3$OH (98:2) at 100K.

Table 5.3: ESR parameters of metallotetracrowned phthalocyanines

Compound	$g_{\parallel}$	$g_{\perp}$	$10^4 A_{\parallel}^M$ (cm^{-1})	$10^4 A_{\perp}^M$ (cm^{-1})	$D_{\parallel}$ (G)	$D_{\perp}$ (G)
AgtCRPc	2.147	2.042	–	–	–	–
AgtCRPc + KCl	2.144	2.052	–	–	240	250
VOtCRPc	1.967	1.988	159.5	56.9	–	–
VOtCRPc + KCl	1.964	1.984	73.7	40	230	230
[a]VOTCP	1.964	1.985	154.7	52.96	–	–
[a]VOTCP + KCl	1.967	1.987	77.15	25.98	268.5	261

a   data taken from ref. (154b)

Table 5.4: Metal-Metal Distances, R(M-M), in the Dimers of Different metal complexes[a]

System	R(M-M) A°	ξ,[b] deg	Ref
Vanadyl (++)-tartrate (50% water-glycol, 77K)	4.08 (4.08)	28 (28)	169 170
Vanadyl (±)-tartrate(50% water-glycol, 77K)	4.18 (4.35)	0-10 (3)	c 171
Vanadyl-tetrakis(aminomethyl)-methane complex	4.8	50±5	172
Vanadyl deuteroporphyrin IX dimethyl ester	3.4		173
Vanadyl deuteroporphyrin IX dibutyl ester	3.5		173
Vanadyl protoporphyrin IX dimethyl ester	3.5		173
Vanadyl tetrasulfonatophthalo-cyanine	4.5±0.1		168
Vanadyl octaethylporphyrin cation radical dimer	4.7		174
Vanadyl crown porphyrins	4.7		154b
Vanadyl tetracrowned phthalo-cyanine dimer	4.9		This work
Silver tetra crowned phthalo-cyanine dimer	4.8		This work

(a) The values in the parenthesis correspond to crystallo-graphic data.

(b) Angle of deviation from axial symmetry.

by 4.9 A$^\circ$.

5.3.3b AgtCRPc

The ESR spectrum of AgtCRPc in chloroform containing 1% methanol at -170°C is typical of Ag^{2+} ions (Fig. 5.7) containing hyperfine structure at high field region due to the hyperfine interaction with four nitrogens. The g and hyperfine values were calculated following the literature methods.[167] The g values are listed in table 5.3 ($g_\parallel$ = 2.147, $g_\perp$ = 2.042 and $A_\perp^N$ = 27 G is typical of monomeric Ag^{2+}, I = 3/2). On addition of KCl to the chloroform solution containing 1% methanol of AgtCRPc gives an additional lines in ESR spectrum, apart from ESR signal corresponds to monomeric species. These additional lines were due to the triplet state arised from the two interacting paramagnetic centers (Ag^{2+}). The zero-field splitting parameter (D) at parallel and perpendicular region were estimated. The 'D', and g values of monomer and dimer are listed in the table 5.2. The g values were not effected upon dimer formation indicates that there was no change in symmetry and co-ordination environment around the Ag^{2+}, upon going from monomer to dimer. The internuclear distance between two Ag^{2+} were calculated at parallel and perpendicular region using the expression[166] (equation 5.4) gives 4.8 A$^\circ$.

The R (V-V) and R (Ag-Ag) values obtained in the present study were compared with those of reported systems of axially symmetric dimers are given in table 5.4. The distances of different VO^{2+} dimers range from 3.4 to 4.8 A$^\circ$. Specifically the V-V distances calculated in the present study compared very well with those observed for VOTCP dimer[154b] and vanadyl tetra
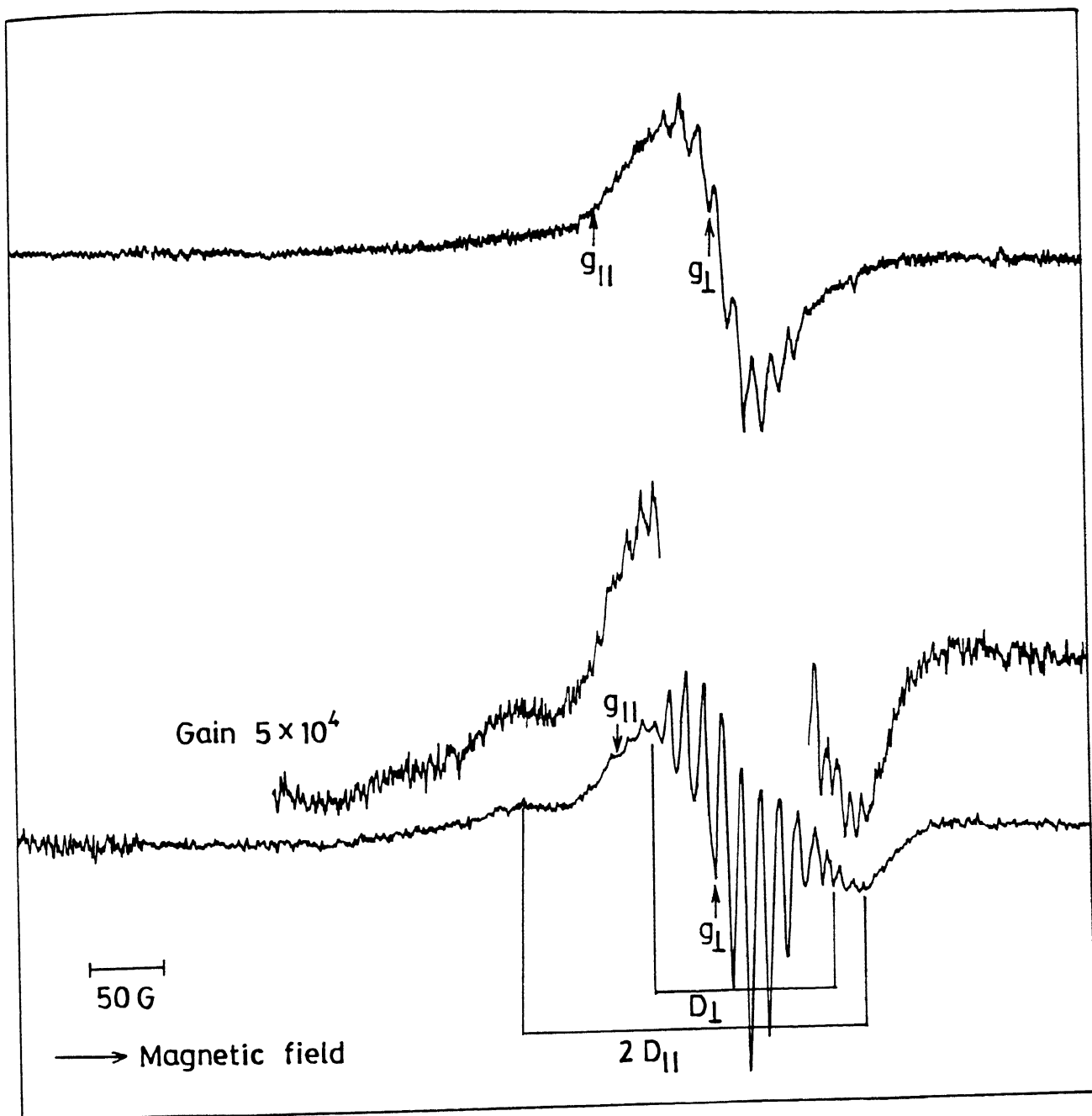
Fig. 5.7 ESR spectra of (a) AgtCRPc, (b) AgtCRPc + K^+ in CHCl$_3$:CH$_3$OH (99:1) at 170K.

sulfonatophthalocyanine[168] dimer probably indicating similar solution structures in these species. The Ag-Ag distance estimated in the present study [4.8 A$^\circ$] compares very well with the only reported to the (best of our knowledge) Ag-Ag distance of 5 A$^\circ$ for Silver mesoporphyrin dimethyl ester (AgMPD) dimer.

5.4 CONCLUSIONS

The solvent and cations have an influence on the aggregation behaviour of metallocrowned phthalocyanines (M = VO^{2+}, Ag^{2+}). The extent of aggregation of Silver tetracrowned phthalocyanine increases if the solvent polarity increases; the order of aggregation in different solvents follow as: $CHCl_3$ < pyridine < CH_2Cl_2 < 1-butanol < Ethanol < methanol. A similar behaviour was observed for the Cu^{2+} and free base crowned phthalocyanines[157,158]. The blue shift observed (~ 30 - 56 nm) in the absorption spectra of MtCRPc (M = VO^{2+}, Ag^{2+}) on addition of cations K^+, NH_4^+ and Cs^+, indicated the formation of dimeric species in solution. The driving force for the formation of dimer is the appended crown ethers will form the sandwich type of complexes with the cations and brings two phthalocyanine in close proximity promoting interaction between two π - systems. Also, the ESR studies shows that the formation of triplet ground state (S = 1) arising from an interaction between two paramagnetic centers (S = 1/2) in dimeric unit. The internuclear distance 'R' calculated from zero field splitting parameter (D) is ~ 4.8 A$^\circ$. Based on the spectroscopic data the possible geometry of the dimer (shown in the fig. 5.8) is cofacial (eclipsed). The similar solution structures proposed for Cu^{2+} and H$_2$CRPc on dimer formation.[153]

$M = VO^{2+}; Ag^{2+}$

$= K^+$
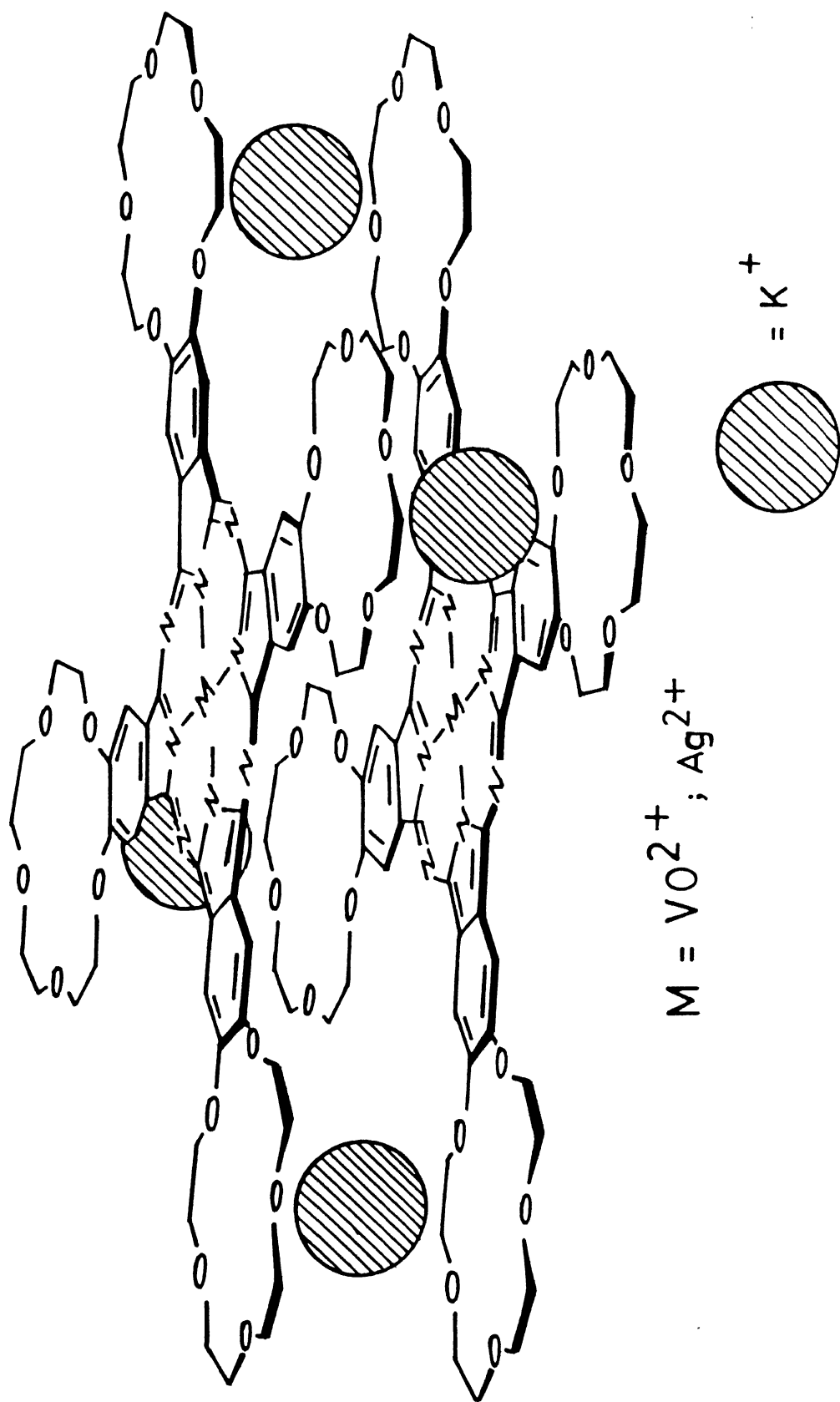
Fig. 5.8   Proposed Cofacial Dimer Structure.

CHAPTER 6

NONPLANAR PORPHYRINS; SYNTHESIS, CHARACTERIZATION, GROUND AND EXCITED STATE PROPERTIES

6.1 INTRODUCTION:

In the previous chapters the studies were confined to (a) the interaction of planar metalloporphyrins with electron acceptor/donor and (b) the interaction between two planar phthalocyanine units oriented in a face to face geometry. It is also well known in literature that the chemical and photochemical properties of porphyrins and metalloporphyrins can be influenced significantly by altering the planarity of the porphyrin core. Recently, in some cases, the biological function[175-178] of the porphyrin ring has been related to the nonplanar conformation. The spectroscopic studies on some nonplanar porphyrins and metalloporphyrins in the ground and excited states are described.

A brief review of biological importance of nonplanar porphyrins and related tetrapyrroles is given here. An excellent review by W.R. Scheidt and Y.J. Lee[48] has highlighted the importance of stereochemistry and their relationship to the function of heme proteins. It has been shown that the observed strong antiferromagnetic coupling between metal center and radical center of an Iron porphyrin has been attributed to the distorted conformation of the porphyrin ring.[48,49] Stolzenberg and co-workers in a recent series of papers have attributed the enhanced stability and unusual redox properties of oxidized products of metallochlorins and bacteriochlorins to the distorted

conformations of the tetrapyrrole rings[51]. Domed porphyrin macrocycles have been observed in the X-ray structure of heme proteins[57,58,179] and nonplanar macrocycles are found in crystal structure of bacterial photosynthetic reaction center.[59-180] Functional significance has been attached to the nonplanar tetrapyrrole conformations in the case of vitamin B_{12} and B_{12} dependent enzymes[176] and methyl reductase[177]. Methyl reductase contains cofactor F_{430} which is nothing but Ni(II) corphin derivative having all the four pyrrole rings and two of the four bridging meso carbon atoms reduced.[181] In the cases of both cofactor F_{430} and B_{12}, it is thought that the degree of planarity of the macrocycle can modulate axial ligation at the metal. The protein environment also exerts influence over the planarity of the macrocycle and in this way modulates ligand affinity and other properties.[178] In the case of ligand affinity, evidence for this mechanism has been found recently in studies of nickel reconstituted hemoglobin and myoglobin.[182-188] Very recently Shelnutt and co-workers have related the Raman frequencies observed for some planar and nonplanar Ni(II) porphyrins to their structural parameters.[175] Thus, recent research has focussed on the synthesis and characterization of nonplanar porphyrin systems to understand the structure- function relationship.

One of the ways of introducing distortion in the porphyrin skeleton is by steric crowding at porphyrin periphery.[189] This strategy has led to the synthesis and characterization of several unusual porphyrins such as crowned,[190] picketfence[191], strapped[192], capped[193] and basket handle porphyrins.[194] However, inspite of these efforts, significant structural

deformation in the porphyrin skeleton is observed only in "pyrrole strapped" porphyrins synthesized by Dolphin and co-workers[62] and "short chain basket handle porphyrins" synthesised by Walker and Co-workers[63]. In both the cases the presence of a "short bridging chain" was responsible for the observed distortion. In view of this we have taken up a systematic investigation on deformed porphyrin systems with the aim of relating the unusual spectroscopic and redox properties of these systems to the subtle structural changes. This chapter describes the synthesis, characterization and photo physical properties of basket handle porphyrins (Fig. 6.1) containing short para or meta phenylenedimethylenedioxy chain covalently linked at the ortho position of phenyl groups of 5,10,15,20 tetraphenyl porphyrin (H_2TPP). IsomerI of para derivative (PSI) and IsomerII and IsomerIII (MSII and MS III) of meta derivative has been characterized by various spectroscopic methods. Electronic and ^1H NMR spectral studies indicate significant distortion of the porphyrin skeleton in these derivatives. Protonation of free base derivatives results in a small blue shift of Q-bands and this has been attributed to the lack of conjugation between phenyl group and porphyrin plane because of restricted rotation of porphyrin-phenyl bond. The bridging phenylenedimethylenedioxy groups does not interfere with the axial ligation of metal derivatives (Co^{2+} and Zn^{2+}) of MSII & MSIII. Electrochemical studies indicate easier oxidations and harder reductions for free base derivatives relative to the corresponding unstrapped derivative. The easier oxidations are attributed to the loss of co-planarity due to the distortion and the harder reductions are attributed to destabilization of anions and dianions due to the

I

CROSS-TRANS-LINKED

II

ADJACENT-TRANS-LINKED

III

ADJACENT-CIS-LINKED

M = 2H ;   PSI

M = 2H ; MS II and MS III

M = Zn^{2+} ; ZnMS II and Zn MS III

M = Co^{2+}; CoMS II and Co MS III

(a) R = $-H_2C$—⟨benzene⟩—CH_2—

(b) R = $-H_2C$—⟨benzene⟩—CH_2—
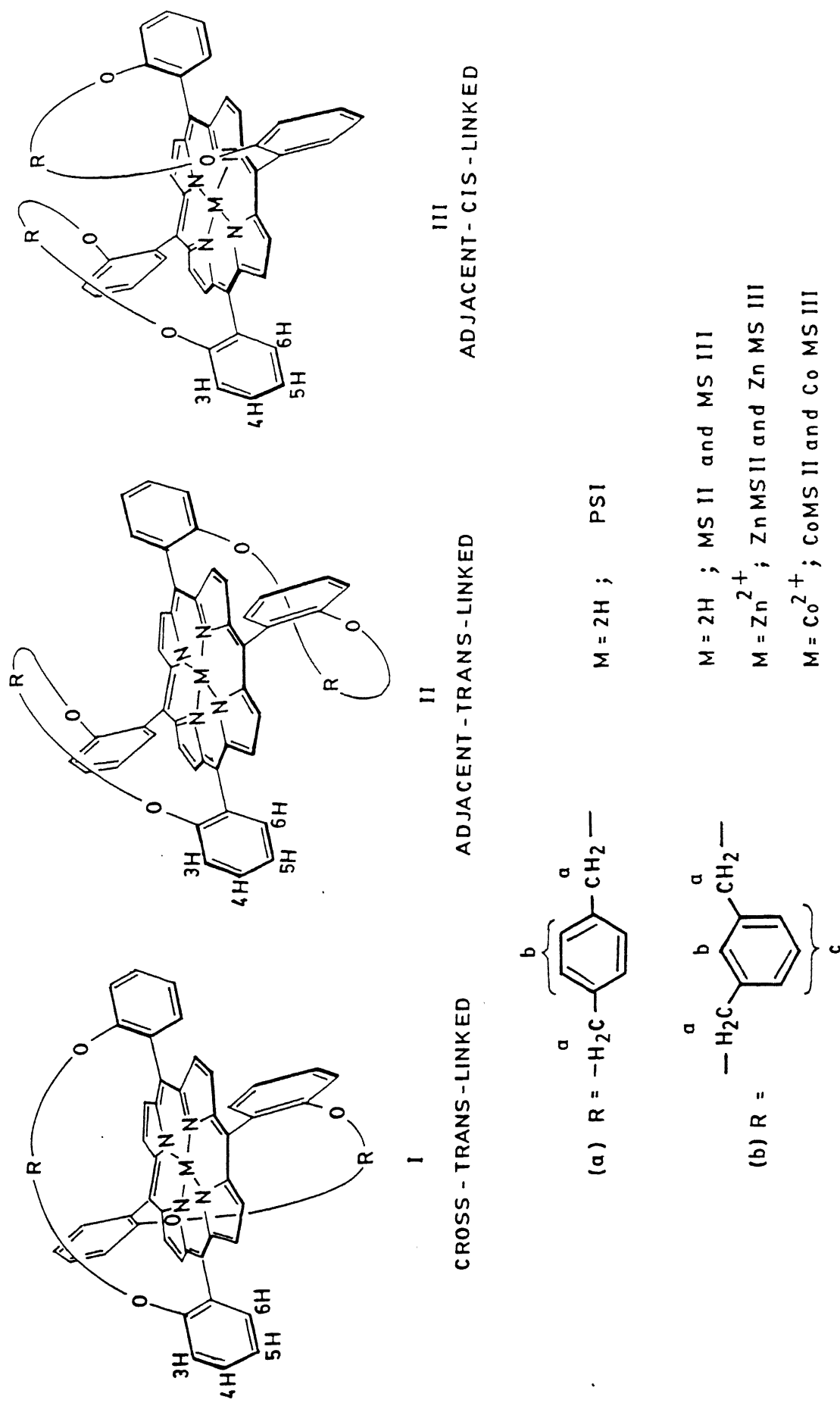
Fig. 6.1 Structures of free base short chain basket handle
porphyrins and their metal derivatives.

lack of solvation. The redox potential data for Co^{2+} derivative of MSII indicate that the metal centered molecular orbital $A_1(d_z2)$ is situated above filled A_{2u} orbital of the porphyrin ring.

The excited state properties of these compounds and their Zn^{2+} derivatives are determined by fluorescence and photoexcited triplet ESR methods. Fluorescence spectral studies indicate that the basket handle porphyrins are less fluorescent than the parent H_2TPP. This difference is ascribed to the enhanced rate of intersystem crossing (ISC) from $S_1 \rightsquigarrow T_1$ and increased natural radiative life times (T°). The rate of radiative fluorescent decay roughly follows the molar extinction coefficient of the lowest energy Q-band. The estimated excited state potentials suggest that the cross trans-linked isomer (PSI) is a better electron donor in the first singlet excited state. Zero field splitting parameters D and E of these isomers evaluated from photoexcited triplet ESR show small but significant differences and this has been attributed to the distortion of the porphyrin plane caused by introduction of short bridging groups. The electron spin polarization (ESP) pattern remains same as in H_2TPP indicating the usual spin-orbit coupling mechanism for Inter-system crossing.

6.2 EXPERIMENTAL

The synthesis of α, α' -dibromo meta and para- xylenes have been described in chapter 2.

The spectroscopic methods employed are described in chapter 2.

6.2.1 Synthesis of 2,2'-(m-phenylenedimethylenedioxy)dibenzaldehyde (1)

α, α'-m-xylene dibromide (15 g, 56.8 mmol) and anhydrous K_2CO_3 (23.5 g, 170.5 mmol) were added to 100 ml of dry DMF and the mixture was stirred for 5 min. Salicylaldehyde (13.8 g, 113.6 mmol) was added to the reaction mixture and stirring was continued for 4 hours at room temperature. The reaction mixture was poured into water (200 cm^3) and extracted with chloroform (3 x 100 cm^3). The organic layer was washed with $NaHCO_3$ (3 x 100 cm^3) and water (3 x 100 cm^3), dried over Na_2SO_4. Addition of diethyl ether (25 cm^3) to a concentrated organic layer afforded (1) as white crystalline solid (15.7 g, 80%), m.p. 115-117°C.

^{1}H NMR (CDCl$_3$): 5.17 ppm (s, O-CH$_2$), 7.33 ppm (m, m-xylyl); 6.93 and 7.73 ppm (m, phenyl), 10.37 ppm (s, -CHO)

6.2.2 Synthesis of 2,2'-(p-phenylenedimethylenedioxy)dibenzaldehyde (2)

α, α'-p-xylene dibromide (15 g, 56.8 mmol), anhydrous K_2CO_3 (23.5 g, 170.5 mmol) and salicylaldehyde (13.8 g, 113.6 mmol) were added to 100 ml of dry DMF. The reaction mixture was stirred for 5 hours at room temperature. Work up of the reaction mixture as above gave (2) as a white crystalline solid (14.7 g, 75%) m.p. 180-182°C.

^{1}H NMR (CDCl$_3$): 5.03 ppm (s, -CH$_2$), 7.42 ppm (s, p-xylyl), 7.0 and 7.72 ppm (m, phenyl), 10.47 ppm (s, -CHO).

6.2.3 Preparation of MS strapped porphyrin

Dibenzaldehyde (1) (12.5 g, 36.27 mmol) and pyrrole (4.86 g, 72.54 mmol) were dissolved in freshly distilled propionic acid

(1000 cm^3). The reaction mixture was refluxed for an hour and left at room temperature for 12 hours. The solvent was evaporated under reduced pressure after filtration. The crude product was purified and separated by column chromatography over silica gel (60-120 mesh) using benzene and benzene-diethyl ether (9:1 v/v) as the eluents. A pink fraction which was eluted with only benzene was identified as MSIII. This was rechromatographed again using silica gel (60-120 mesh) and the pure fraction was eluted with benzene (0.5 g, 2%) (FAB Mass; M$^+$ = 883). Another red fraction eluted with benzene-diethyl ether (9:1 v/v) was identified as MSII. This was rechromatographed again using silica gel (60-120 mesh) and the pure fraction eluted with benzene-diethyl ether (9:1 v/v) gave crystalline solid (0.75 g, 2.4%) (FAB Mass; M$^+$ = 883).

6.2.4 Preparation of PS strapped porphyrin

Dibenzaldehyde (2) (3 g, 8.7 mmol) and pyrrole (1.18 g, 17.56 mmol) were reacted in 500 ml of boiling propionic acid. The crude product was obtained as above was purified by repeated column chromatography using silica gel (60-120 mesh). A violet band eluted with benzene was identified as PSI. This was rechromatographed again using silica gel (60-120 mesh) and the pure fraction eluted with benzene gave crystalline solid (0.23 g, 3%) (FAB Mass; M$^+$ = 883). The other red fraction which was eluted with benzene diethyl ether (19:1 v/v) was identified as mixture of two isomers (PSII and PSIII) (0.15 g, 2%). A clear separation of these two isomers has not yet been achieved. It was surprising that the yield of cross trans linked isomer PSI was considerably more compared to other isomers (PSII and PSIII).

6.2.5 Preparation of CoMS III

MSIII (46 mg) was added to a mixture of DMF (10 ml), CH_2Cl_2 (10 ml) and pyridine (1 ml) and heated for 15 min. Cobalt(II) acetate (26 mg, dissolved in 5 ml of DMF) was added to this mixture. The reaction mixture was refluxed for 6 hours. Evaporation of the solvent under reduced pressure followed by a water wash gave crude product. This was purified over silica gel (60-120 mesh) using benzene gave the single orange band as CoMSIII (25 mg, 54%). A minor second fraction which was eluted with $CHCl_3$ was identified as pyridine coordinated Co^{III} porphyrin.

6.2.6 Preparation of CoMSII

MSII (30 mg) was dissolved in 75 ml of $CHCl_3$. Cobalt (II) acetate (60 mg) dissolved in 25 ml of methanol was added to the boiling $CHCl_3$ solution. The reaction mixture was refluxed for 90 min. and evaporation of solvent under reduced pressure followed by water wash afforded crude CoMSII. Pure CoMSII was obtained after recrystallization from 1:1 $CHCl_3$: methanol (25 mg, 80%).

6.2.7 Preparation of ZnMSIII

MSIII (30 mg) and Zn(II) acetate (30 mg) in a mixture of DMF (10 ml) and CH_2Cl_2 (10 ml) was refluxed for 8 hours: Evaporation of the solvent under reduced pressure followed by water wash gave the ZnMSIII (25 mg, 80%). The poor solubility of the product did not allow ^{1}H NMR and cyclic voltammetric studies.

6.2.8 Preparation of ZnMSII

MSII (50 mg) was dissolved in 100 ml of $CHCl_3$. Zn(II) acetate (100 mg) dissolved in 25 ml of methanol was added to the

boiling CHCl$_3$ solution. The reaction mixture was refluxed for 30 min. and the evaporation of the solvent under reduced pressure followed by water wash gave the crude ZnMSII. Pure ZnMSII was obtained after recrystallization from 1:1 CHCl$_3$ methanol (30 mg, 60%).

In this chapter results and discussion are divided into two parts; Part 'A' describes the synthesis and ground state properties of short chain basket handle porphyrins and Part 'B' describes the excited state properties of short chain basket handle porphyrins.

6.3 PART A: SYNTHESIS AND GROUND STATE PROPERTIES OF SHORT CHAIN BASKET HANDLE PORPHYRINS

6.3.1 RESULTS

The short chain basket handle porphyrins were synthesised following the method of Momenteau[194] by condensation of appropriate dialdehydes with pyrrole in propionic acid medium. The crude porphyrins which were obtained as mixture of isomers were separated by repeated column chromatogrphy. Only one isomer (PSI) was separated in pure form when the 'R' group used was para phenylenedimethylenedioxy derivative. The other two expected isomers (PSII and PSIII) came always as a mixture and their clear separation has not yet been achieved. Two isomers were separated in pure form (MSII and MSIII), when the 'R' group was meta phenylenedimethylenedioxy derivative. The other expected isomer (MSI) was not formed probably due to reduced chain length of the R group relative to para phenylenedimethylenedioxy derivative.

(a) ^{1}H NMR Studies

The ^{1}H NMR spectra of the free base basket handle porphyrins are highly characteristic and the integrated intensities of the proton resonances are in conformity with the proposed structure (Fig. 6.2). An inspection of the ^{1}H NMR data listed in table 6.1 indicate that for PS I isomer, all the eight pyrrole protons resonate as a sharp singlet; the eight protons of methylene chain are equivalent appearing as a singlet and experience an upfield shift (0.93 ppm) relative to the corresponding protons in free dialdehyde; the eight aromatic protons of two strapped phenyl rings are equivalent and appear as a singlet and compared to the corresponding protons in free dialdehyde are shielded (3.53 ppm) by porphyrin anisotropy. The NH protons are highly deshielded (2.32 ppm) relative to tetra (o-methoxy phenyl) porphyrin (TMPP).[195,196] The isomers MSII and MSIII show two resonances for pyrrole protons as expected considering the symmetry of the isomers. Also, the methylene chain protons appear as an 'AB' quartet with negligible shielding relative to the free dialdehyde, the phenyl protons of the strapping group are split and experience a small shielding (~0.45 ppm) relative to free dialdehyde. The NH protons also experience a small shielding in these two isomers in contrast to PSI isomer.

Momenteau et al.[194] have pointed that the chemical shifts of the 6H proton of mesophenyl ring and the NH-protons are dependent on the chain length of the bridging group and the magnitude of deshielding of these protons indicate the tension imposed on the porphyrin ring by the bridging group. Fig. 6.3 shows a plot of the magnitude of deshielding of 6H and NH protons of various cross trans linked isomers including PSI versus the number of
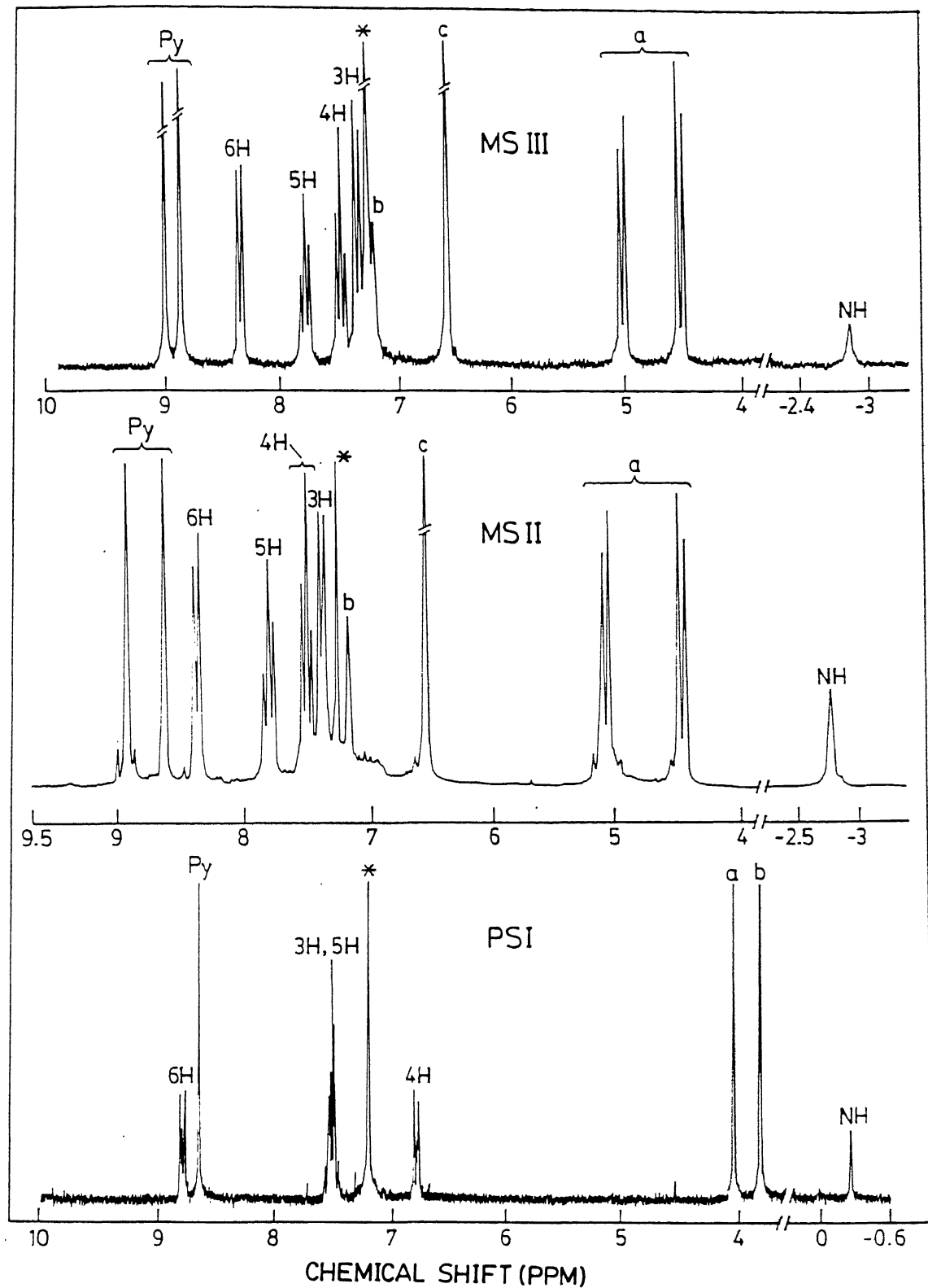
Fig. 6.2 ^{1}H NMR spectra of (a) PSI; (b) MSII; and (c) MSIII, in CDCl$_3$ (concentration of the porphyrins used is ~10^{-3}M). The asterisk corresponds to the CDCl$_3$ signal.
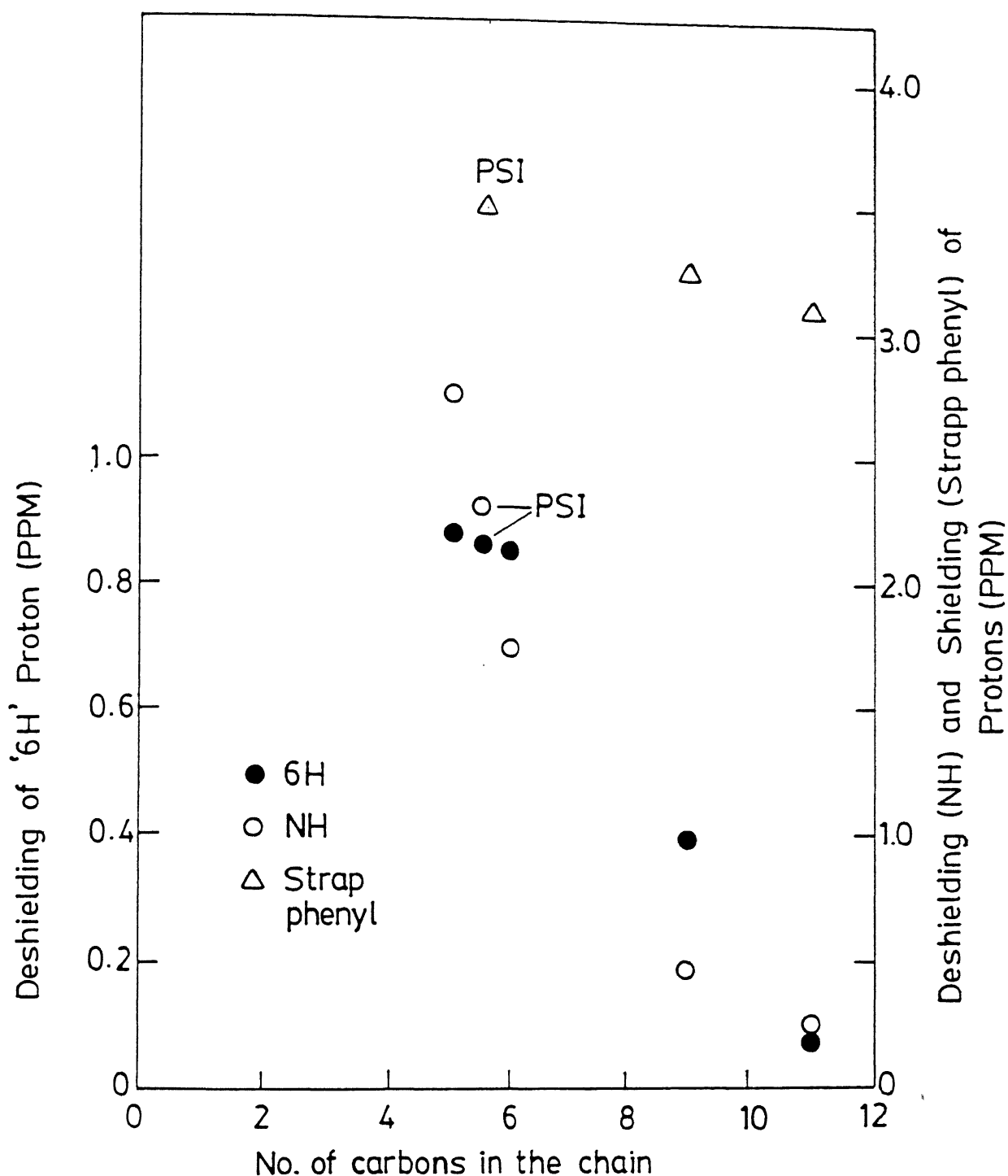
Fig. 6.3 Plot of deshielding of 6H and NH protons and shielding of strap phenyl protons versus chain length (see text for details) of various cross trans linked basket handle porphyrins.

Table 6.1: ^1H NMR data of short chain basket handle porphyrins (δ in ppm) in CDCl3 at room temperature

Compound	Pyrrole	Phenyl (Porphyrin)				Strap CH2	Phenyl (Strap)	-NH
		6H	4H	3H	5H			
TMPP	8.73	8.00	7.75	7.35	—	—	—	-2.58
PSI	8.71(s,8H)	8.85 (m,4H)	6.86 (m,4H)	—	7.58 (m,8H)	4.10(s,8H)	3.89(s,8H)	-0.27
PS Free dialdehyde	—	—	—	—	—	5.03(s,4H)	7.42(s,8H)	—
MS II	8.92(s,4H) 8.62(s,4H)	8.37 (d,4H)	7.49 (t,4H)	7.37 (d,4H)	7.80 (t,4H)	AB Quartet 5.06(d,4H) 4.45(d,4H) J_{AB}=9.97Hz	6.55(s,6H) 7.17(s,2H)	-2.77
MS III	8.86(s,4H) 8.99(s,4H)	8.34 (d,4H)	7.50 (t,4H)	7.35 (d,4H)	7.80 (t,4H)	AB Quartet 5.02(d,4H) 4.53(d,4H) J_{AB}=9.77Hz	6.57(m,6H) 7.19(s,2H)	-2.86
MS Free dialdehyde	—	—	—	—	—	5.17(s,4H)	7.33(m,8H)	—

s,d,t,m corresponds to singlet, doublet, triplet and multiplet respectively.
The numbers in the parenthesis corresponds to the number of protons.

carbons in the bridging chain. Also the magnitude of shielding of strapped phenyl protons for PSI isomer and the corresponding isomers of basket handle porphyrins synthesised by Momenteau et al.[194] $(-C_4.C_6H_4.C_4-)_2$, $(C_3.C_6H_4.C_3)_2$ isomers and Simonis et al.[63] (hexyl I and pentyl I isomers) are included in Fig. 6.3.

(b) Visible Absorption Studies

The absorption spectral characteristics of the free bases along with the corresponding dications generated by addition of a drop of trifluroacetic acid (TFA) in a benzene solution are shown in Fig. 6.4. The absorption spectral data are tabulated in table 6.2. A comparison of this with the unstrapped H_2TPP reveal some interesting features; (a) A considerable red shift of the soret band and Q-bands; (b) a drastic reduction in the intensity of both Soret and Q-bands; the magnitude of red shift and intensity decrease depends on the nature of the isomers and maximum effects are observed for PSI isomer. (c) Upon protonation, the Q-bands experience a blue shift in contrast to the large red shift observed for protonation of H_2TPP.[197] However, the effects observed parallels to those found for ortho substituted tetraphenyl porphyrins.[198]

The electronic absorption spectra of the basket handle porphyrins synthesised by Momenteau et al.[194] showed very little differences among the different isomers due to the lack of distortion in the porphyrin skeleton because of longer chain of bridging group. However, Simonis et al.[63] synthesised a series of basket handle porphyrins containing shorter chains and they found significant changes relative to corresponding unstrapped derivative in the absorption spectra of the different isomers. A
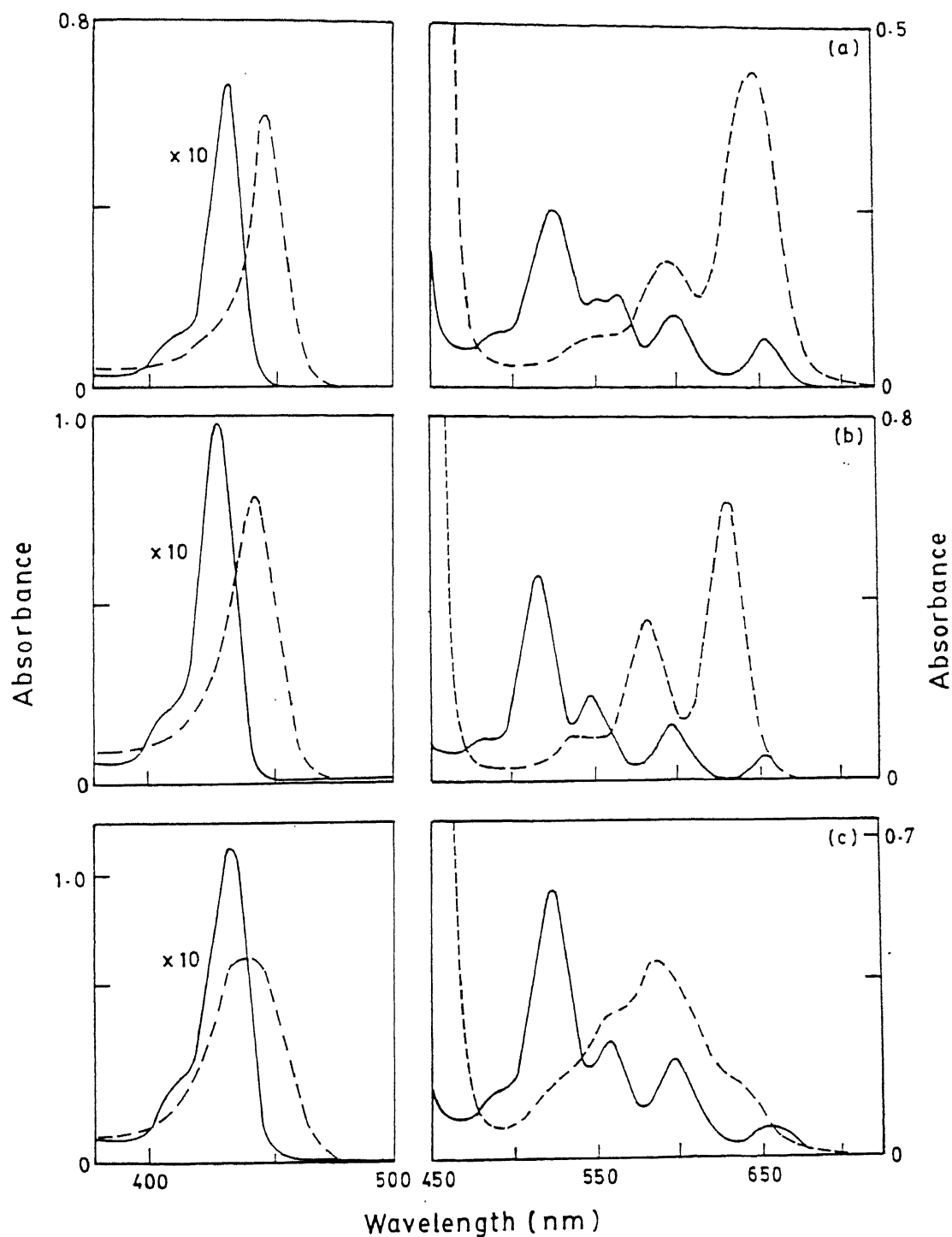
Fig. 6.4 Electronic absorption spectra of (a) MSII, (b) MSIII, and (c) PSI in benzene and their corresponding dications. Concentration for Q-bands $\sim 10^{-5}$M and for the Soret band $\sim 10^{-6}$M (Solid line corresponds to neutral form and dotted lines corresponds to dications).

Table 6.2: Electronic spectral data of short chain Basket handle porphyrins and their dications[*] in Benzene.

Porphyrin	Soret band $B(0,0)$ λ_{max}(nm) $(\epsilon \times 10^{-4})$	Q-bands λ_{max}(nm) $(\epsilon \times 10^{-3})$			
		$Q_y(1,0)$	$Q_y(0,0)$	$Q_x(1,0)$	$Q_x(0,0)$
PSI	433(22.21)	529(11.72)	566(5.16)	605.0(4.33)	663(1.24)
PSIH$_2^{2+}$	440(14.67)		566sh(6.34)	592.0(8.51)	646sh(3.07)
MSII	432(31.72)	526(12.09)	566(6.42)	601(5.14)	657(3.74)
MSIIH$_2^{2+}$	446(23.8)			599.0(6.98)	648(17.62)
MSIII	428(34.03)	520(16.09)	552(6.88)	602(4.79)	661(2.54)
MSIIIH$_2^{2+}$	442(21.54)		544sh(2.87)	586(9.78)	634(17.08)
H$_2$TPP	419(46.4)	515(18.7)	548(8.6)	592(5.5)	647(3.9)
H$_4$TPP^{2+}	448(43.6)			608(9.0)	659(50.9)

* Dications were generated by addition of dilute solution of TFA in benzene.

comparison of magnitude of red shifts and the intensity decrease for the different isomers of the present study with those synthesised by Simonis et al.[63] allowed us to distinguish isomer I from isomers II and III. Table 6.3 lists the magnitude of red shifts of Soret and Q-bands of various isomers relative to their unstrapped derivatives.

Metallation of MSII and MSIII by standard literature methods[199] afforded the metal derivatives (Co^{2+} and Zn^{+2}). Metallation of PSI was not achieved even under harsh conditions. It is apparent that the short chain strapping group causes steric hindrance to the metal, preventing the metallation of this isomer. The optical absorption data of metallo derivatives are collected in Table 6.4. Axial coordination of pyridine to the metal induces the expected red shift of Soret, α and β - bands with a change in the α and β -band intensity.[200] The magnitude of shifts are comparable to those observed for pyridine binding of ZnTPP. The axial ligation of CoMSII and CoMSIII results in hexacordinate Co^{3+} porphyrin with two axial pyridine ligands consistent with the oxidation of Co^{2+} to Co^{3+} in presence of pyridine.[201]

(c) Cyclic Voltammetric Studies

Representative cyclic voltammograms of free base PSI and MSII and metal derivatives (ZnMSII and CoMSII) are shown in Fig. 6.5. The free base and ZnMSII derivatives exhibit two oxidation waves and two reduction waves (with exception of free base MSIII which shows only one oxidation wave) with peak separation Δ_{Ec-Ea} in the range (50-80 mV). An analysis of the ratio of peak currents suggests one electron process for these waves. CoMSII
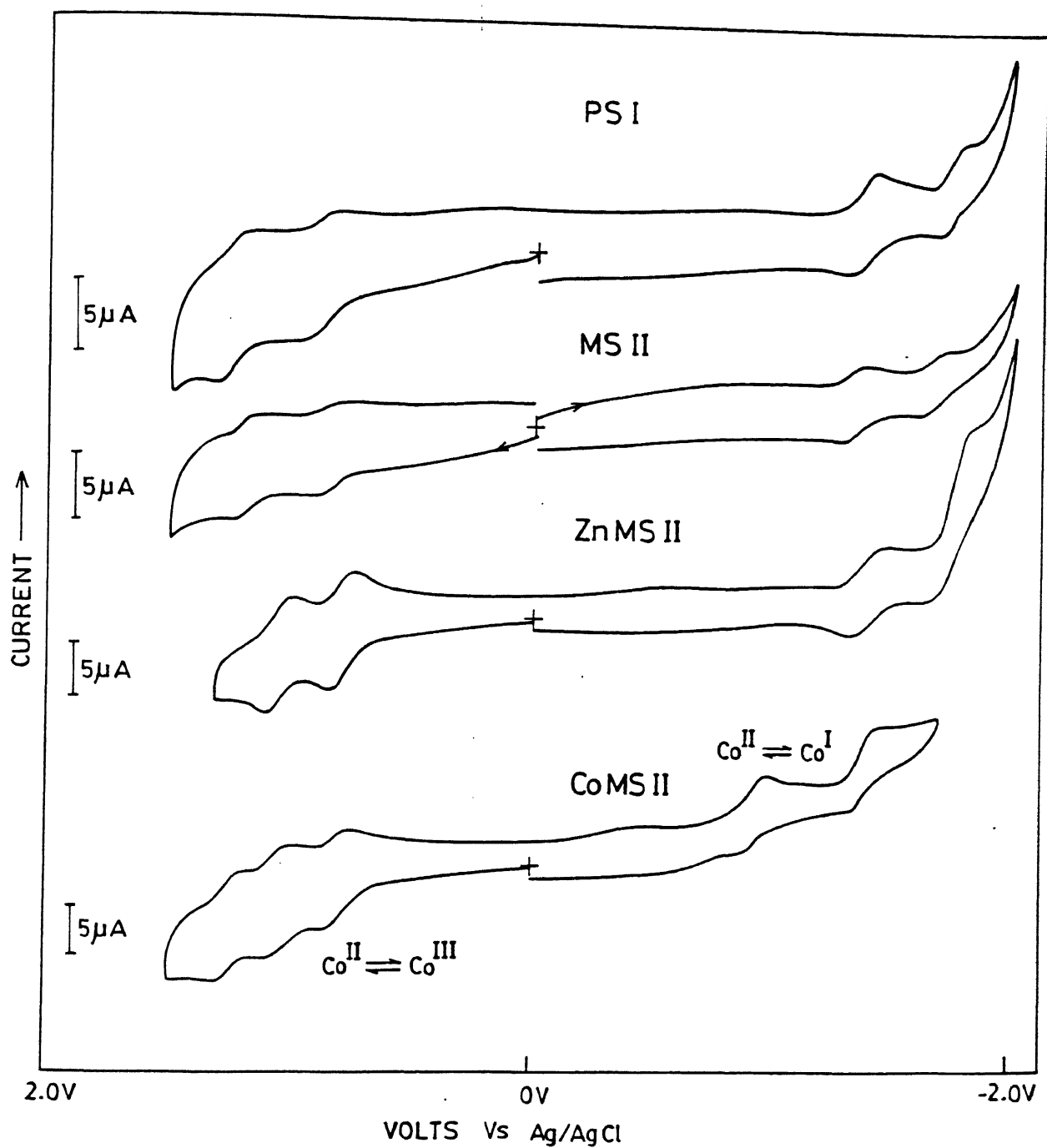
Fig. 6.5 Cyclic voltammograms of (a) PSI (1.47×10^{-4}M); (b) MSII (1.7×10^{-4}M), (c) ZnMSII (5.2×10^{-4}M) and (d) CoMSII (5.56×10^{-4}M) in CH_2Cl_2 containing 0.1 M TBAP at room temperature. The scan rate is 100 mV/sec.

Table 6.3: Comparison of red shifts (nm) of Soret and Q-bands of different isomers.

Porphyrin	Soret	Q-bands				Ref.
	$B(0,0)$	$Q_y(1,0)$	$Q_y(0,0)$	$Q_x(1,0)$	$Q_x(0,0)$	
*hexyl I	10	12	20	14	10	63
pentyl I	20	22	30	22	20	63
PSI	14	15	20	16	16	this work
hexyl II	2	2	2	4	-2	63
pentyl II	5	4	2	6	2	63
butyl II	8	6	10	16	14	63
MSII	14	12	20	13	9	this work
hexyl III	4	2	4	4	-2	63
pentyl III	6	6	6	6	0	63
butyl III	8	6	10	16	14	63
MSIII	10	6	6	14	13	this work

*The labeling of original publication has been retained.

Table 6.4: Electronic spectral data of metal derivatives of short chain Basket handle porphyrins in CHCl₃.

Porphyrin	Soret $\lambda_{max}nm(\epsilon x10^{-4})$	α $\lambda_{max}nm(\epsilon x10^{-3})$	β $\lambda_{max}nm(\epsilon x10^{-3})$
ZnMS II	427(25.0)	555(11.6)	596(2.4)
ZnMS II +Pyridine	439	572	615
ZnMS III	430(19.0)	559(7.8)	597(2.97)
ZnMS III +Pyridine	437	570	612
ZnTPP	419	548	589
ZnTPP +Pyridine	430	562	602
CoMS II	417(14.1)	532.5	–
CoMS II +Pyridine	437	549.5	585
CoMS III	418(8.1)	534(5.05)	–
CoMS III +Pyridine	438	550	–
CoTPP (p-methoxy)	414	529	–
CoTPP (p-methoxy) +Pyridine	440	553	593

shows three one electron reversible electro oxidations and two one electron reductions (Δ_{Ec-Ea} = 90 and 101 mV). The first oxidation and reduction process originate from the metal center corresponding to the formation of Co^{+3} and Co^{1+} porphyrin derivatives respectively.[202] The second and third oxidation steps are assigned to the formation of Co^{3+} porphyrin cation radical and dication respectively and the potentials for these species compare well with the similar reactions observed for corresponding CoTPP in CH_2Cl_2.[203]

6.3.2 DISCUSSION

(a) ^1H NMR

The identification of the three isomers shown in Fig. 6.1 was done by (i) using the symmetry concept proposed by Momenteau et al.[194] and (ii) comparing the NMR characteristics of the compounds synthesized in the present study with those of hexyl II isomer of Simonis et al. whose X-ray structure is known.[63] The cross translinked isomer is expected to show a relatively simple NMR spectrum because of the symmetry (D_{2d}) in which all the eight pyrrole protons, methylene chain protons and strapped phenyl ring protons resonate as three separate singlets indicating a highly symmetrical environment in this isomer. Also, since the methylene chain protons and strapped phenyl protons span the porphyrin ring current above and below the plane, they experience considerable upfield shift relative to the same protons in the free dialdehyde. The NMR data assigned for PSI are consistent with these observations indicating that PSI is a cross trans linked isomer.

The isomers MSII and MSIII show two pyrrole resonances and the magnitude of separation between these resonances has been used to distinguish between these two isomers. An analysis of the peak separation for isomer II (adjacent trans linked) and isomer III (adjacent cis linked) for the hexyl, pentyl and butyl bridged porphyrins of Simonis et al.[63] indicates that between these two isomers, always the adjacent trans linked isomer shows a larger pyrrole peak separation relative to adjacent cis isomer in a given series. The following data supports this observation.

hexyl II	0.22 ppm		hexyl III	0.09 ppm
pentyl II	0.38 ppm		pentyl III	0.02 ppm
butyl II	0.84 ppm		butyl III	0.44 ppm
MSII	0.30 ppm		MSIII	0.13 ppm

The X-ray structure of hexyl II isomer indicates that it has the adjacent trans structure. Interestingly, the basket handle porphyrins of Momenteau et al. also show a similar trend.[194] All these experimental data suggest that the compounds MSII and MSIII have adjacent trans and adjacent cis structure respectively.

The ortho protons (6H) of the phenyl ring experience a significant downfield shift (0.86 ppm) relative to TMPP in PSI suggesting a considerable strain on the porphyrin ring. It is obvious from the plot in Fig. 6.3 that this strain depends on the chain length and the strain increases with decrease in chain length. The NH protons also show a similar trend. The deshielding of NH protons suggests a large perturbation of the ring current at the central nitrogen atoms. However, the chemical shift of the pyrrole protons in these isomers is not

altered much, suggesting a very little disruption in peripheral ring current. The phenyl, pyrrole and NH resonances shifts observed for PSI are comparable in magnitude to the pentylI isomer of Simonis et al.[63] indicating a considerable static distortion of the porphyrin plane in this isomer.

The upfield shift of strap phenyl protons increases linearly with the decrease in chain length of the strapping group (Fig. 6.3). No detailed analysis of these shifts has yet been made to relate this to the conformation of the strap phenyl ring with respect to porphyrin plane. However, a detailed analysis of ^{1}H NMR and ^{13}C NMR shifts in Fe(II) basket handle porphyrin[63,204] and quinone capped porphyrins[205-206] have indicated that the capping group is essentially perpendicular to the porphyrin plane in both these compounds and free rotation of the capping group is possible. Qualitatively the ring current shifts of the strapping phenyl group and the direction of the NH proton shifts observed for PSI are comparable with these studies probably suggesting that the phenyl group is perpendicular to porphyrin plane. However we believe that because of the extreme shortness of the chain in PSI the chain is not flexible thus restricting the free rotation of the strapping phenyl group in PSI.

(b) Electronic absorption spectra

A theoretical account of the Soret and the Q-bands in the visible absorption spectrum of a porphyrin molecule, to a first approximation, are assigned to the transition between $A_{1u}(\pi)$ $\longrightarrow$ $E_g(\pi^*)$ and $A_{2u}(\pi)$ $\longrightarrow$ $E_g(\pi^*)$ molecular orbitals respectively.[207] In the free base porphyrins due to the symmetry

and the vibronic mixing, the Q-bands are further split in to $Q_x(0,0)$, $Q_y(0,0)$, $Q_x(1,0)$ and $Q_y(1,0)$. Thus, any change in the energy of these absorption maxima in free base basket handle porphyrins relative to the corresponding unstrapped derivative indicate changes in the energies of A_{1u}, A_{2u} and E_g orbitals which are involved in the transition. In PSI both the Soret band and Q-bands are affected significantly. Also, the magnitude of shifts of both soret band and Q-bands are comparable. This indicates that the energy of $E_g(\pi^*)$ orbital of the porphyrin macrocycle is affected most in this isomer due to the introduction of the strap. The direction of the shift indicates a slight lowering of the energy of $E_g(\pi^*)$ orbital thus decreasing the energies of transition.[63] Between isomers MSII and MSIII, the magnitude of shifts are comparable to those observed for the corresponding isomers of pentyl and butyl bridged derivatives of Simonis et al.[63] suggesting a slight distortion of the porphyrin plane in these isomers. This is attributed to the decreased chain length of the strap in meta isomers MSII and MSIII relative to para isomer PSI. This is also supported by the fact that $Q_y(0,0)$ band in these isomers are infact split further by about 6 nm (Fig. 6.4). The splitting of the $Q_y(0,0)$ band was also observed for the butyl bridged isomers II and III of Simonis et al.[63]

The intensity of the Q-bands are determined by the degree of degeneracy of the highest occupied molecular orbitals A_{2u} and A_{1u}. When these are exactly degenerate, the Q(0,0) band should have zero intensity and as the degeneracy is lifted the Q(0,0) bands gains intensity.[207(b),208] In free base H_2TPP, A_{2u} orbital is higher in energy. The fact that the intensity of the Q-bands

of PSI are reduced by more than 50% relative to the unstrapped tetraphenyl porphyrin (table 6.2) suggests a smaller energy gap between A_{2u} and A_{1u} orbitals. Thus, among the short chain strapped porphyrins (less than 6-carbons) it appears that the cross trans linked isomer is expected to show larger red shifts for both Soret and Q-bands with a significant decrease in intensity compared to other two isomers.

Protonation of unsubstituted or para substituted free base tetraaryl porphyrins generally results in a large red shift of Q-bands while the free base tetra alkyl porphyrins show a blue shift of Q-bands. This difference in behaviour is attributed to the increased resonance interaction between the aryl group and porphyrin ring in tetra aryl porphyrins due to the co-planarity of phenyl ring and porphyrin plane. X-ray structure of dication of H_2TPP supports this observation.[209] However, in the basket handle porphyrins synthesised in the present study restricted rotation around the porphyrin-phenyl bond because of substitution of strapping group at ortho position of phenyl ring may forbid any extension of conjugation between the phenyl groups and the porphyrin ring preventing resonance interaction. A similar effect was observed for the ortho substituted tetraphenyl porphyrins upon protonation.[198]

The metal derivatives of MSII and MSIII (Zn^{+2}, Co^{+2}) show a two banded 'normal' spectra in the visible region typical of a metalloporphyrin. The absorption bands of ZnMSII and ZnMSIII show a red shift of 7-11 nm (Table 6.4) relative to ZnTPP suggesting a slight distortion in these cases. However, the magnitude of shifts observed upon axial ligation of pyridine to form a penta co-ordinate complex are comparable to those of

ZnTPP. This observation clearly demonstrates that the strapping groups in these isomers essentially does not interfere with the incoming axial ligand which is in line with the X-ray structure of Zn^{+2} derivative of hexyl bridged isomer.[63] The oxidation of Co^{2+} porphyrin to its Co^{+3} derivative in presence of pyridine is well documented in literature and the observation made in the present study for pyridine binding to CoMSII and CoMSIII are consistent with literature reports.[29,32,201]

(c) Electrochemistry

The shifts in the redox potentials (Table 6.5) of the basket handle porphyrins are quite significant. Thus, the easier oxidations relative to H_2TPP are interpreted in terms of loss of coplanarity resulting in decreased electron delocalisation. Support for this also comes from the electrochemical behaviour and X-ray structure of the pyrrole strapped porphyrins.[210] The harder reductions relative to H_2TPP is attributed to the destabilisation of the porphyrin anions and dianions due to the lack of solvation caused by steric hindrance of the strapping group. The fact that the potential shifts for the formation of dianions are significantly larger (230 mV for PSI, 120 mV for MSII and MSIII) than those observed for the formation of monoanions (160 mV for PSI, 90 mV to MSII and 110 mV for MSIII) is in accordance with the increased charge in dianions. This is also consistent with the shifts observed for reduction in Fe(II) derivative of ether linked basket handle porphyrins.[211]

In CoMSII, the metal centered oxidation and reduction peaks occur at potentials less anodic to the corresponding porphyrin ring oxidation and reduction. This suggests that the first

Table 6.5: Electrochemical redox data of free base and metallo derivatives of short chain Basket handle porphyrins in CH_2Cl_2.

Porphyrin	Ring Oxidation		Metal redox data	Ring reduction	
	I $E_{1/2}$	II $E_{1/2}$		I $E_{1/2}$	II $E_{1/2}$
PS I	0.85	1.23	-	-1.39	-1.78
MS II	0.84	1.20	-	-1.32	-1.67
MS III	0.90	-	-	-1.34	-1.67
ZnMS II	0.78	1.04	-	-1.39	-1.75
CoMS II	1.05	1.24	0.80[Co(II)$\rightleftharpoons$Co(III)] -0.94[Co(II)$\rightleftharpoons$Co(I)]	-1.37	-
H$_2$TPP	1.03	-	-	-1.23	-1.55

Potentials in volts vs. Ag/AgCl.

oxidation and reduction occur from the metal centered molecular orbital $A_1(d_z2)$ in CoMSII is situated above the filled A_{2u} orbital and below the $E_g(\pi^*)$ orbitals of porphyrin ring. For ZnMSII, no reaction at the central metal are likely and both oxidations and reduction occur at the porphyrin ring in line with the general behaviour of Zn(II) porphyrins.[212]

6.4 PART B: EXCITED STATE PROPERTIES

6.4.1 RESULTS:

(a)Emission Spectra

The room temperature emission spectra of the basket handle porphyrins and their Zn^{2+} derivatives are shown in fig. 6.6 and the emission data evaluated from these are tabulated in table 6.6. The general features of these findings can be summarized as follows; (a) The fluorescence intensity of the basket handle porphyrins are quenched considerably and the emission maxima are shifted to red relative to the parent H_2TPP or ZnTPP. (b) The ratio of intensities of the emission bands $Q_{(0,0)}$ and $Q_{(0,1)}$ are noticeably different; the magnitude of red shift and the intensity decrease are dependent on the nature of the isomer and the maximum effects are observed for PSI. (c) The τ^o and K_f increases and decreases respectively for the free bases relative to H_2TPP with exception of MSII isomer and the magnitude of K_f is proportional to extinction coefficients of the lowest energy Q-bands and vary as MSII > MSIII > PSI (ε for MSII, MSIII and PSI are 3.74 x 10^3, 2.54 x 10^3 and 1.24 x 10^3 respectively). (d) The rate of intersystem crossing $S_1 \rightsquigarrow T_1$ increases more than three fold relative to H_2TPP. A comparison of the ground and excited state redox potentials of the basket handle porphyrins and their
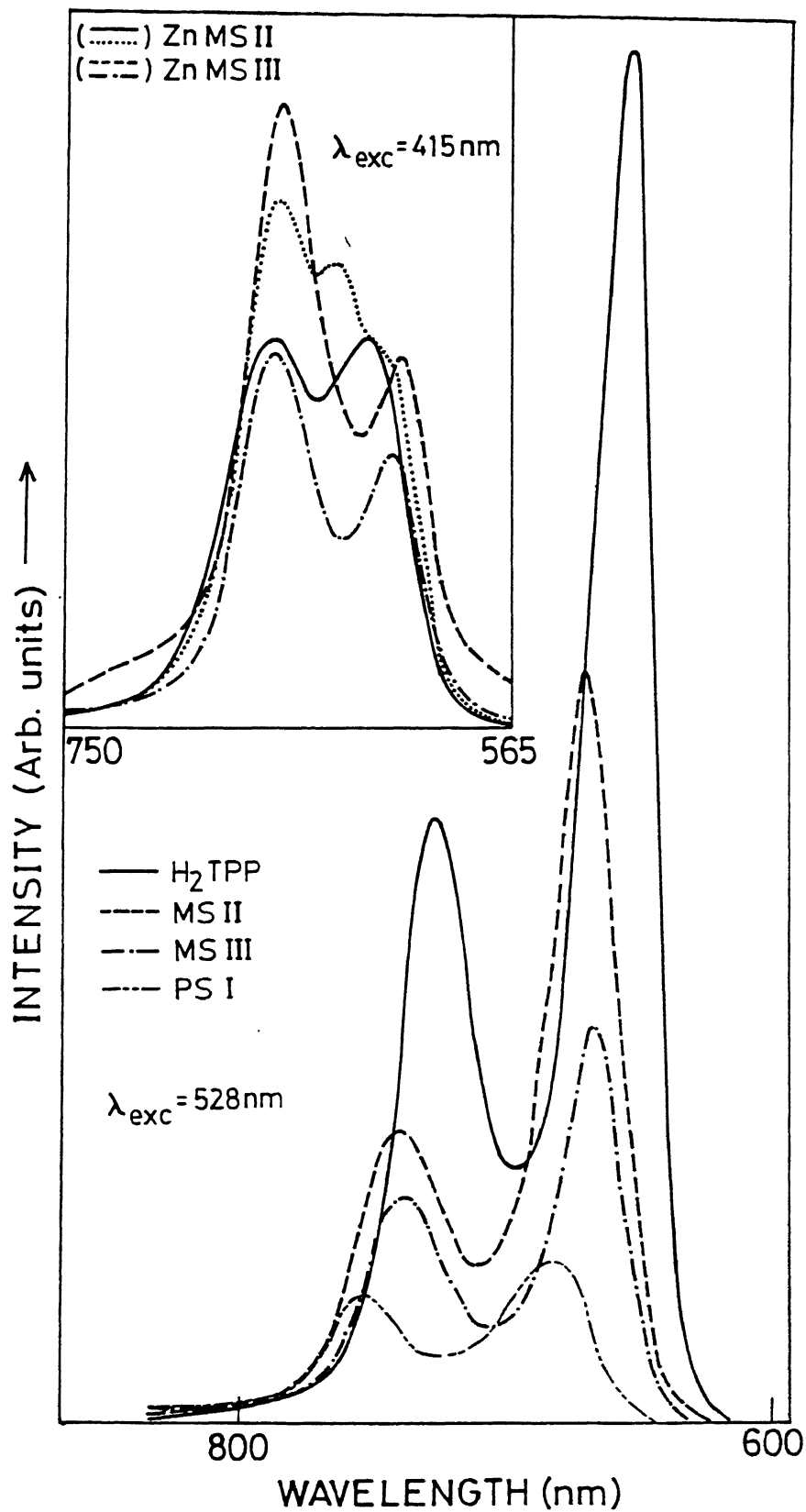
Fig.6.6 Emission spectra of H_2TPP ($1.76 \times 10^{-5}M$), MSII($1.47 \times 10^{-5}M$) MSIII ($1.36 \times 10^{-5}M$) and PSI ($2.04 \times 10^{-5}M$) in $CHCl_3$. Insert, ZnMSII ($3.59 \times 10^{-5}M$) (————); Zn MSIII (5.54×10^{-5} M) (—·—·—) in chloroform and ZnMSII ($4.85 \times 10^{-5}M$) (........), and ZnMSIII ($5.48 \times 10^{-5}M$) (— — — —) in Benzene.

Table 6.6: Singlet excited state parameters of basket handle porphyrins.

Porphyrin	Q(0,0) (nm)	Q(0,1) (nm)	ϕ_f	τ° (ns)	$10^{-7}K_f$ (s^{-1})	$10^{-8}K_{isc}$ (s^{-1})	E_{0-0} (P-*P) (eV)	$*E^\circ$ (P+/*P) (V)	$*E^\circ$ (*P/P-) (V)
H$_2$TPP	653.0	717.0	0.110	123	0.81	0.66	1.900	-0.870	0.670
MSII	665.0	727.0	0.039	88	1.14	2.81	1.864	-1.024	0.544
MSIII	663.0	727.0	0.032	143	0.70	2.12	1.870	-0.970	0.530
PSI	672.0	739.0	0.0116	284	0.35	2.99	1.845	-0.995	0.445
ZnMSII	621.0	662.0	0.0255	90	1.12	4.28	1.997	-1.217	0.607
	b618(sh),636.0	660.0	–	–	–	–	–	–	–
ZnMSIII	612.0	662.0	0.0371	119	0.84	2.18	2.03	–	–
	b610.0	660.0	–	–	–	–	2.03	–	–
ZnTPP[c]	b598.0	647.0	b0.033	57	–	–	2.07	-1.200	0.760

b – in benzene

c – from Ref. 43

Zn^{2+} derivative with H_2TPP are shown in Fig. 6.7. It is obvious from the figure that the free base derivatives are better oxidants and reductants in the first singlet excited state than their Zn^{2+} derivatives.

(b) Triplet ESR

Fig. 6.8 and Fig. 6.9 shows the low temperature high field ESR spectra of triplets of PSI, MSII and MSIII randomly oriented in Toluene: $CHCl_3(1:2)$ with and without modulation respectively. In general, the high field ESR spectrum of randomly oriented triplet state molecules consists of three pairs of symmetrically disposed lines, each pair corresponding to those molecules for which one of the magnetic axes is nearly parallel to the applied magnetic field.[213] The two lines in each pair correspond to the transition between high field spin states; $|0> \longleftrightarrow |+>$ and $|0> \longleftrightarrow |->$. The separation between the pairs of lines are given by $2D$ and $D \pm 3E$ where D and E are zero field splitting (ZFS) parameters.[214] Table 6.7 lists the values of the D and E parameters derived from the spectra shown in Fig. 6.8. Also, for comparision the ZFS parameters of the photoexcited triplets of H_2TPP, structurally related compounds H_2TPC (tetraphenyl-chlorin), H_2TCP (5,10,15,20-tetra crown porphyrin) and H_2TPPS (5,10,15,20-tetra(p-sulfonato)phenyl porphyrin are included in table 6.7. Our earlier ESR studies of the triplets of H_2TPPS with the magnetophotoselection technique established that the outer pair of lines (Z-peaks) are given by molecules oriented with the molecular plane perpendicular to the magnetic field direction.[215]
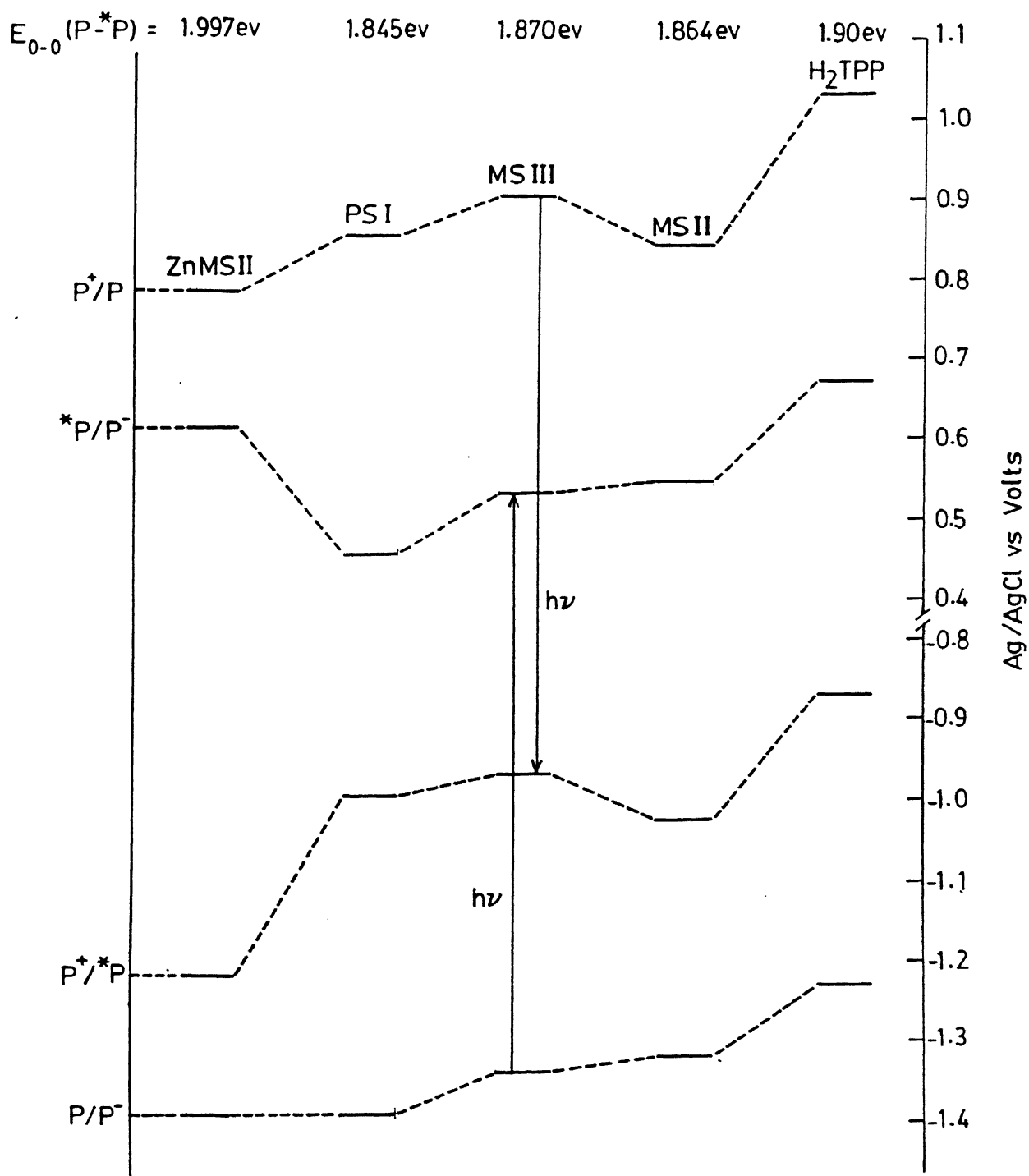
Fig. 6.7 Comparison of ground and excited state redox potentials
of basket handle porphyrins with H_2TPP.
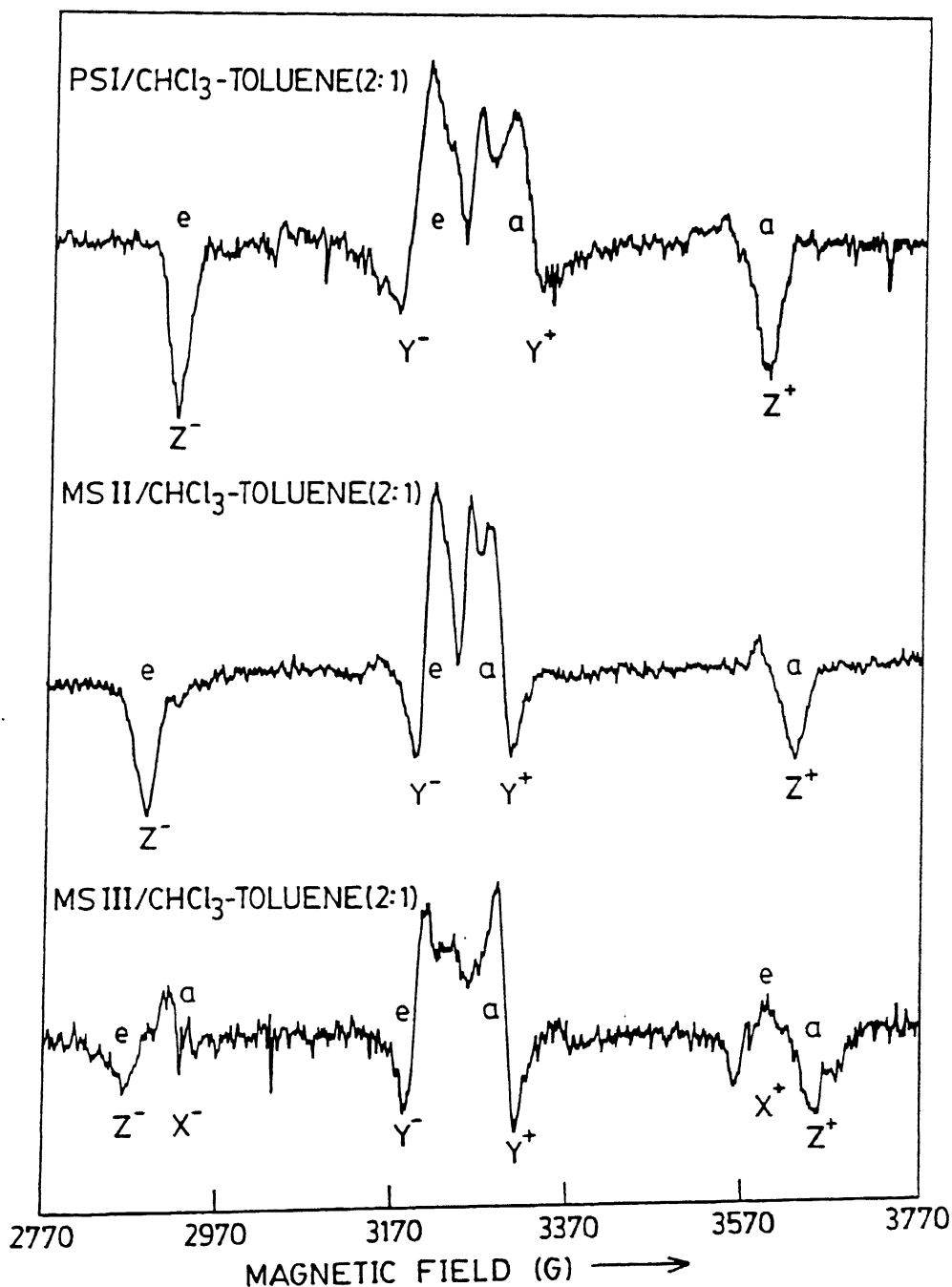
Fig. 6.8   Triplet   ESR spectra of PSI, MSII and MSIII in CHCl₃ – Toluene (2:1) at 100K.   Microwave power 5.0 mW,   <u>field modulation   20G (100 KHZ).   excitation with square   wave modulated   (83 HZ) light of an argon ion   laser   (514.5 nm.   0.5 W)</u>.   Absorption and emission peaks   have   been labelled a and e, respectively.   Approximately ~1x10⁻⁴M solution was used for recording the spectra.
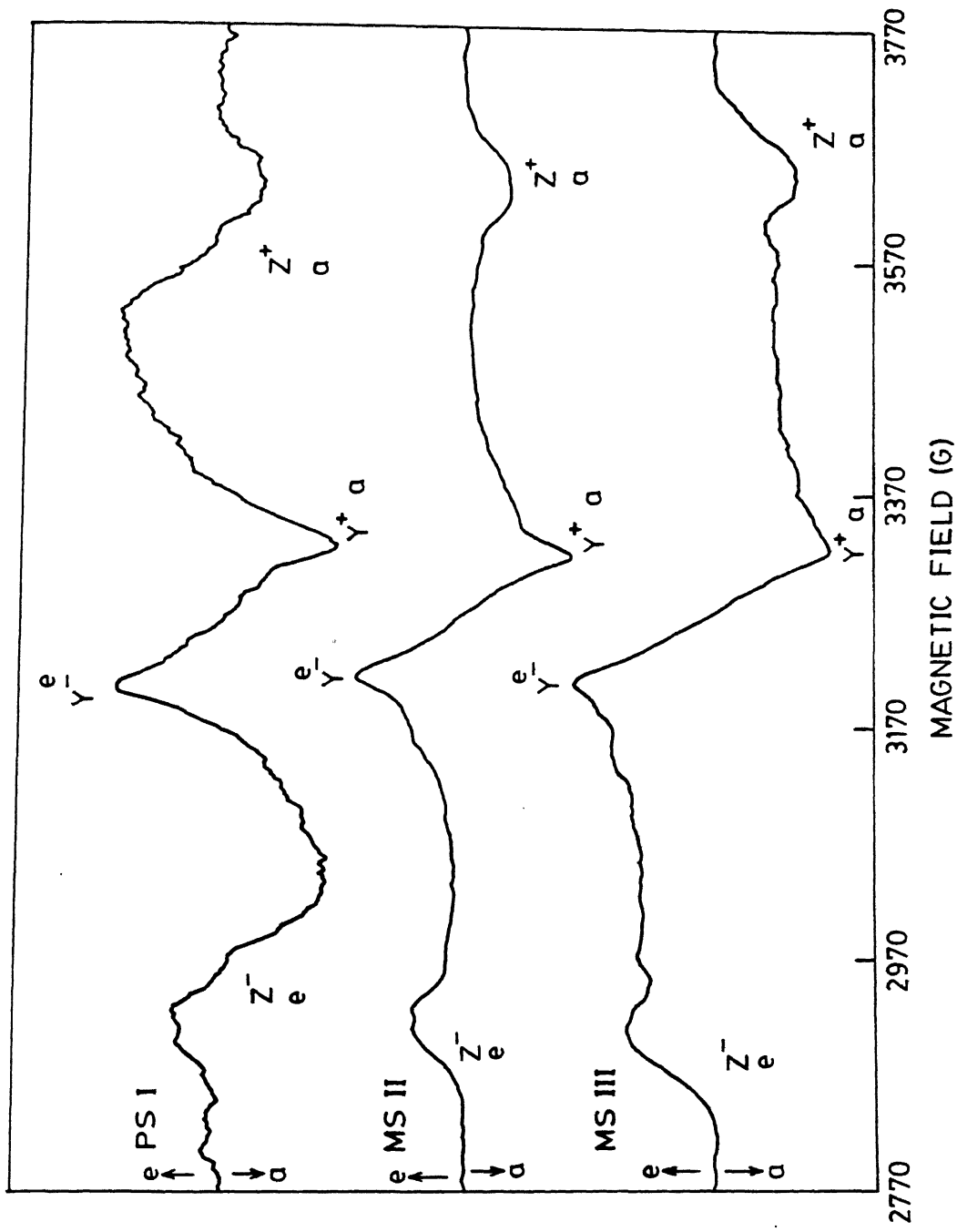
Fig. 6.9 Triplet ESR spectra of PSI, MSII and MSIII in CHCl$_3$ – Toluene (2:1) at 100 K. Microwave power 5.0 mW, and without field modulation and excitation with pulsed laser (560 nm). Absorption and emission peaks have been labelled a and e respectively.

Table 6.7: Zero field splitting parameters (10^{-4} cm^{-1}) of various basket handle porphyrins

Porphyrin	D	E	X	Y	Z	Ref.
PSI	317	66	171	40	-211	this work
MSII	347	90	206	25	-231	this work
MSIII	369	91	214	32	-246	this work
H_2TPC	364	63	184	58	-242	232
H_2TPP	383	78	205	50	-255	233
H_2TCP	377	79	205	46	-251	228
H_2TPPS	391	75	205	56	-261	160

As can be seen in table 6.7, the D values for all the short chain basket handle porphyrins are lower (4-19%) than the values obtained for the parent H_2TPP. The magnitude of the decrease varies with the structure of the isomer. D for MSIII is comparable to the value observed for H_2TPC[216] while for MSII and PSI the values differ substantially.

The E-values for MSII and MSIII are slightly larger than the value found for the parent compound H_2TPP, while for the PSI isomer a slight decrease is observed. The spin polarization pattern of all the isomers is same (eaeaea) as that observed for H_2TPP.[217]

6.4.2 DISCUSSION

(a) Emission Studies

The quantum yield data in the table 6.6 reflect the strong fluorescence quenching in the basket handle porphyrins which vary as PSI < MSIII < MSII. This cannot be solely due to the ortho substituent effect on the H_2TPP since the ortho methyl substituent on the phenyl ring of H_2TPP decreases the quantum yield only by about 7% which is far less than the observed 60-90% reduction for different isomers.[218] It is interesting to note that the decrease in the quantum yields are comparable to those observed for ortho substituted halogens on H_2TPP which show the heavy atom effect. Alternately, this has to be attributed to the distortion of the porphyrin skeleton due to the short strapping group. Many covalently linked porphyrins containing a wide variety of linking groups (having both electron donating and electron withdrawing properties) exhibit strong fluorescent quenching and the quantum yield of these compounds are a function of distance between the porphyrin ring and the capping group.[219-221]

An intramolecular electron transfer has been proposed as quenching mechanism in most of the cases which has been recently verified by EPR[222] and picosecond transient absorption and fluorescence studies.[223]

The natural radiative life time (τ^o) increases for PSI and MSIII relative to the reference compound H_2TPP. τ^o estimated for H_2TPP (123 ns) in the present study using Strickler-Berg equation is in good agreement (129 ns) with those reported by Gouterman and workers using the same equation.[70] Also, the rates of fluorescent decay (K_f) and intersystem crossing (K_{isc}) decreases and increases relative to H_2TPP respectively. Thus the decrease in the quantum yield of PSI and MSIII is attributed to the combined effect of increased natural radiative life time and the enhanced rate of intersystem crossing from $S_1 \leadsto T_1$. For the MSII isomer there is a slight decrease in the τ^o relative to H_2TPP but the magnitude of K_{isc} increase is same as found for PSI and MSIII. This suggests that the rate of radiationless decay from $S_1 \leadsto S_0$ is slightly enhanced in this isomer.[83] However, the presence of a charge-transfer state between S_1(π , π^*) and S_0 is highly unlikely.

Introduction of Zn^{2+} ion into the free base MSII decrease the quantum yield by 35% relative to free bas MSII with a small change in τ^o . However for ZnMSIII, an anonymously high quantum yield has been observed and infact this is about 16% higher than the free base MSIII. Generally, introduction of Zn^{2+} ion to a porphyrin ring results in a decrease in quantum yield and the observation for ZnMSII is consistent with this.[83] The reason for

high quantum yield of Zn MSIII is not clear at this time. Since the closed shell porphyrins are known to phosphoresce at low temperature, it is interesting to see whether high phosphorescence yield complement the relatively low fluorescence yields. Another note worthy result in the Zn^{2+} derivatives of MSII and MSIII is the observation of a weak emission band at 450 nm (ZnMSIII) and 447nm (ZnMSII) upon excitation in soret region. The rough estimates of quantum yield is of the order of 0.0001 in both the cases. This has been tentatively assigned to the $S_2 \longrightarrow S_0$ emission. S_2 emission has been observed in many Zn porphyrins[224] including the ZnTPP which show an emission maxima for $S_2 \longrightarrow S_0$ emission at 440 nm.

(b) Excited State Potentials

The details of the calculating potentials are described in chapter 2. The singlet excited state potentials were estimated under the assumption that the excited states are not very much distorted relative to the ground state. This method has been used earlier for porphyrin systems.[225,226] A comparison of these potentials displayed in fig. 6.7 revealed the following. (a) Free base derivatives are better oxidants and reductants in the excited state than their Zn derivatives. (b) Among the free base derivatives; PSI is the better electron donor in the excited state. Thus, it appears that the distortion of the porphyrin skeleton leads to better electron donating ability with the excited state reduction potential getting 225, 126 and 140mV less positive for PSI, MSII and MSIII respectively relative to planar H_2TPP. Even in the ground state these distorted porphyrins are easier to oxidize relative to planar H_2TPP. This

is in keeping with the recent theoretical prediction on nonplanar porphyrins.[178] Since the energy of the first excited states in these distorted porphyrins are infact lower than that of H_2TPP, an oxidative quenching is expected rather than an energy transfer for the bimolecular reaction involving the porphyrin and the quencher.[73]

(c) Triplet ESR:

A comparison (Table 6.7) of D values of H_2TCP (in which four crown ether rings are substituted at the meso position) and H_2TPPS (in which four sulfonato groups are attached to the para position of the meso phenyl ring) with H_2TPP show negligible differences(table 6.7). This shows that substituents at the meso phenyl ring do not alter the delocalization in the porphyrin triplets significantly. In H_2TPC, the reduction of the one of the pyrrole rings perturbs the electron spin delocalization to a slightly greater extent and this is reflected in a small decrease in D value relative to H_2TPP ($\triangle D = 19 \times 10^{-4}$ cm^{-1}). The change in D value observed on going from H_2TPP to MSIII is comparable to this ($\triangle D = 14 \times 10^{-4}$ cm^{-1}). However, for MSII ($\triangle D = 36 \times 10^{-4}$ cm^{-1}) and PSI ($\triangle D = 66 \times 10^{-4}$ cm^{-1}) the decrease in D values is two to three times larger in magnitude indicating a more significant disruption of electron spin delocalization.

The changes in the triplet spin density distribution are reflected in changes in the ZFS parameters D and E which characterize the dipolar spin Hamiltonian[227]. The parameter D is a measure of the distance between the two unpaired electrons. E is a measure of the inplane anisotropy of spin distribution.[227]

An inspection of the table 6.7 shows that in general, there is a decrease in D values of all basket handle porphyrin relative to that of the parent H_2TPP suggesting an increase in the average separation between the unpaired electrons.

The observed reduction in D value can have a number of origins. Our earlier ESR studies of the photoexcited triplet ESR of H_2TPPS,[160] H_2TCP[228] and studies of photoexcited triplets of natural chlorophylls[213,215] have shown considerable reductions (~20%) in D values relative to their monomeric parent analagoue. In these cases, the reduction in D values have been explained invoking a dimeric structure and mechanisms such as; (a) localized triplets (under very weak coupling conditions i.e., J < D where J is exchange coupling), (b) Triplet exciton (J is of the order of D) and (c) radical pair mechanism (J >> D) have been used to account for the reduction in ZFS parameters.[160,213,216] Apparently, the reduction in D observed in the present study cannot be explained in terms of dimeric structure.

The observed reduction in D probably is due to the fact that the porphyrin ring is not a rigid structure so that its geometry can be modified by intermolecular interactions. In TPP systems, as pointed out by Van der Waals et al.[227], a lowering of D value is expected on (i) delocalization of the π-electrons into the phenyl groups and (ii) when the porphyrin ring becomes noncoplanar. ^{1}H NMR studies of these porphyrins have indicated that the meso-phenyl ring is under considerable strain at least in the PSI isomer, because of the tension imposed by the bridging chain. This might reduce the dihedral angle between the phenyl and porphyrin planes thus allowing increased spin delocalization into the phenyl rings. The large red shifts of both the Soret

and Q-bands in the optical spectrum relative to H_2TPP supports this observation. Thus it is likely that atleast in the PSI isomer, spin delocalization into the phenyl ring is increased which would account inpart for the observed reduction in D value data from optical spectra, and electrochemical studies of these systems provide strong evidence that the porphyrin plane is significantly distorted in these basket handle porphyrins and the most pronounced effects are observed for PSI. It is noted that X-ray structure of a free base capped porphyrin (which has bridging group similar to the one in the molecules considered here) shows that the porphyrin skeleton is markedly nonplanar with buckling of the porphyrin plane.[217] Thus, the reduction in D values observed in the present study is attributed to the structural change induced by the introduction of short phenylenedimethylene-dioxy chain across the porphyrin periphery.

A reduction in D value was also observed when the pyrrole rings in TPP were substituted by strong electron withdrawing CN^- groups.[223] For example substitution of two CN^- groups on the opposite pyrrole rings reduces D value by 20% while introduction of four CN^- groups symmetrically on four pyrrole rings in ZnTPP reduces D by about 33%. Furthermore, the substitution on the pyrrole ring causes significant changes in the electronic structure of the porphyrin ring by altering the energies of π-molecular orbitals.[230,231] The observation that the magnitude of D decrease for PSI isomer in the present study is comparable to that observed for substitution of two CN^- groups on pyrrole ring of TPP suggests a significant rearrangement of energies of π-molecular orbitals in this isomer relative to that of H_2TPP. This is also consistent with electrochemical studies. However, a

quantitative understanding of this is possible only when a theoretical frame work for calculating D and E from molecular π - electron wave functions are available. The E parameters change only slightly in these isomers relative to H_2TPP indicating that the inplane symmetry of the spin distribution is not appreciably disturbed by the introduction of the bridging group. The intersystem crossing (isc) process generating the triplets and the triplet decay process is known to be spin selective[227]. For porphyrins, in dilute frozen solution at 100K, the relative magnitudes of the triplet lifetime and electron spin relaxation time (T_1) are such that, even under steady state illumination, thermal equilibrium is not established. With light modulation coupled with synchronous detection using a Lock-in-amplifier the spin polarization effect is enhanced strongly. This accounts for the observation of absorption (a) as well as emission (e) signals in the ESR spectra. The spin polarization pattern observed in the spectra of all three isomers, eaeaea corresponds to that found in the parent H_2TPP. Even H_2TPC show a similar polarization pattern.[232] The pattern shows that the middle (Y) zero field spin level is the most active (following the convention, the order of the energy levels is chosen, $T_x>T_y>T_z$) in the triplet state $T_1 \rightsquigarrow S_0$ inter system crossing in the basket handle porphyrins relative to the other two states (X and Z).

6.5 CONCLUSIONS:

The short phenylenedimethylenedioxy bridging chain enforces considerable distortion in the porphyrin skeleton of basket handle porphyrins as evidenced by their spectroscopic and

electrochemical behaviour. This inturn reflects significant changes in the energies of π-molecular orbitals of the porphyrin ring. The studies of substituent effects on H_2TPP have clearly demonstrated that the substituent on the pyrrole ring influence the electronic structure of the porphyrin ring more significantly than the substituent on the phenyl ring. It should be pointed out here that the magnitude and direction of the redox potential shifts observed in the present study are comparable to those observed for pyrrole substituted H_2TPP suggesting significant changes in the electronic structure of the porphyrin ring in these basket handle porphyrins.[208b] However, the limited studies does not allow any direct correlation between the electronic structure and the degree of distortion in the porphyrin skeleton. Also it has been shown that the excited state properties of porphyrins can be significantly altered in the nonplanar conformation relative to its planar conformation. However, a detailed understanding of the nature of the photophysical processes in this class of molecules requires further accumulation of quantitative experimental data. It is hoped that a better understanding is possible by synthesizing and studying variety of short chain basket handle porphyrins by changing the nature of the bridging group as well as the chain length.

CHAPTER 7

SUMMARY

The present study has characterized the electronic interactions between the tetrapyrrole pigments and the conventional electron acceptor/donors and between two phthalocyanine units oriented in a face to face geometry using metalloporphyrins and metallophthalocyanines as the model compounds. The choice of these model compounds are appropriate because of their similarity in structure with natural hemes. Also, it has been shown how the photophysical and electrochemical properties can be modified by making the porphyrin skeleton nonplanar. The structural characterization of the model compounds includes many spectroscopic techniques i.e., optical absorption, emission, ^{1}H and ^{19}F NMR, ESR and photoexcited triplet ESR.

The first part of the work has shown that the π-π interaction between donor and acceptor are metal dependent for example Cu^{2+} and Zn^{2+} porphyrins form only charge- transfer complexes while Co^{2+} porphyrins undergo oxidation after the initial charger-transfer complex formation. Gouterman et al.[234] have carried out extensive theoretical calculations on the electronic structure of porphyrins and their metal derivatives. It has been shown that the highest occupied molecular orbitals [HOMO] of the free base porphyrin, a_{1u} and a_{2u}, are essentially degenerate. Further, the two HOMO's are characterized by the magnitude of the coefficient of p_z orbital. The orbital a_{1u} has large coefficient of p_z on C_α and C_β atoms while a_{2u} has the

large coefficient of p_z on nitrogen and meso-carbon atoms. Photoelectron spectral studies[235] of the porphyrin and its metal derivatives revealed reasonable agreement with the predicted ionization energies of the HOMO's. The experimentally observed π-orbital ionization energies are grouped into 7 sets. The lowest energy peaks around 6.4 to 6.8 eV are assigned to the electron ionization from a_{1u} and a_{2u} orbitals. The third ionization around 7.8 eV is shown to be dependent on the nature of the metal ion. These ionization energies of the donor porphyrins are useful in the prediction of charge transfer transition energy, $h\nu_{CT}$ and also the symmetry of the donor orbital involved in the π-overlap with the acceptor. There exist various emperical equations relating $h\nu_{CT}$ to the ionization energy of the donor, electron affinity of the acceptor and the coefficients to take into account the energies of the charge-transfer excited states. Here we employed the following empirical equation[236] to calculate $h\nu_{CT}$ of the charge-transfer complexes formed by BFO with Cu^{2+} and Zn^{2+} porphyrins.

$$h\nu_{CT} = aI^D + b \qquad\qquad 7.1$$

where I^D is the ionization energy of the donor. a and b are constants for a given acceptor. The values of a and b taken for BFO are 0.89 and -4.25 eV respectively [since BFO is structurally similar to trinitrobenzene (TNB), the a and b values reported for TNB is used][236]. The values of $h\nu_{CT}$ were then computed for different ionization energies of the porphyrin (table 7.1). It is seen from the table that the position of the expected charge-transfer band depends upon the ionization potential value used. The use of first ionization potential

Table 7.1: Calculated spectral data of the charge-transfer complexes

Porphyrin	IP(eV) I	IP(eV) II	IP(eV) III	CT band* (nm) BFO	$h\nu_{CT}cm^{-1}$* BFO	CT band# (nm) BFO	$h\nu_{CT}cm^{-1}$# BFO
CuTPP	6.49	6.66	7.77	465	21,499	808	12,362
ZnTPP	6.42	6.62	7.76	467	21,427	843	11,858

* CT band calculated using I ionization potential of metalloporphryin.

\# CT band calculated using III ionization potential of metalloporphyrin.

123

value of the metalloporphyrins predicts the charge-transfer band at 808 nm and 843 nm for Cu^{2+} porphyrin and Zn^{2+} porphyrin respectively, while the use of III ionization potential values which are metal dependent predicts the charge-transfer band at 467 and 465 nm for Cu^{2+} and Zn^{2+} porphyrins respectively. This is consistent with the prediction of Gouterman et al.[234] in an earlier work, that the charge transfer transition for the TNB complexes lie around 500 nm, probably hidden in the intense absorptions of porphyrins in this region. This is also consistent with metal dependence of association constant of TNB complexes reported earlier.[120]

The aerobic and anaerobic oxidation of cobalt(II) protoporphyrins[29-33] in presence of molecular oxygen and various amine ligands is known to proceed readily. Spectrophotometric measurements show that the final product is hexa co-ordinated $[L_2Co(III)P]^+$ complex. The rate of $[L_2Co(III)P]^+$ formation increases with increasing entering ligand concentration and decreases when the oxygen content is lowered. When O_2 is completely removed no $[L_2Co(III)P]^+$ is formed. The reaction is very strongly proton catalysed. Furthermore, the rates are dependent on basicity and π-bonding characteristics of the ligands. However in the present study it has been shown that in the presence of electron acceptor Co(II) porphyrins undergo oxidation to Co(III) porphyrins. Even in the absence of molecular oxygen it has been shown that the oxidation is taking place, though not completely. The mechanism of oxidation is not clear at this time except to state that the presence of molecular oxygen promotes the equilibrium to the right hand side. The observation for Co(II) tetraphenylchlorin that the ring oxidation

is prior to the metal oxidation is consistent with the oxidation potentials. The last part of this section describes the interaction of electron donors with water soluble metalloporphyrins and it is interesting to note that the complexes formed are of $\pi-\pi$ type with extensive stacking inspite the presence of strong donor sites in the nucleic acid bases.

The second part of this thesis deals with the interaction between the two π- systems. It has been shown that there is a strong coupling between the chromophores with perturbation in the electronic structure. This perturbation is seen in the spectral shifts upon going from monomer to dimer. It has been found that the dimerization can be promoted by presence of cations and also by specific solvent compositions. Apparently the role of cation is to complex with the crown ether moieties attached to the phthalocyanine rings. This affinity of cations for crown ethers brings the two phthalocyanine units in a face to face orientation promoting the electronic interactions between the two π- systems. The interaction between two π- systems is also reflected in the EPR spectrum of Ag^{2+} and VO^{2+} derivatives of tetracrowned phthalocyanines. Thus, these are ideal spectroscopic probes to study interaction between the two metal centers. The observed metal-metal distances are in agreement with the literature data for similar systems. The fact that the observed optical spectral shifts can be satisfactorily accounted interms of exciton coupling theory indicate that the dipole-dipole interaction between the transition moments associated with the optical transitions in the dimer constituents are dominant.

The last part of the thesis describes the effect of nonplanar conformation of the porphyrin skeleton on the spectroscopic properties. In view of the recent realization of importance of nonplanar conformations of porphyrin system to its function, such studies are important. However, the understanding of importance of nonplanar conformation of macrocyclic systems is still at its infancy and more spectroscopic probes are needed to aid the evaluation of the importance of these structures in the function of many natural systems. In this regard many workers have started synthesizing and characterizing a variety of nonplanar porphyrin systems and the present work has added some input to an understanding of the spectroscopic properties. It has been clearly shown that the spectroscopic properties of the porphyrin skeleton can be significantly altered in a distorted conformation. Introduction of short bridging chains has proved successful in inducing distortion. However, more systematic investigvation by varying the 'chain lengths and the nature of the chain would throw more light on an understanding of spectroscopic properties.

The research work reported in this thesis describes the results obtained in three different directions i.e. simple charge transfer complexation as well as characterization of charge separated species, the dimer hypothesis and the electronic coupling between two ring systems. Also a comparision of spectroscopic and electrochemical properties of planar and distorted porphyrins have yielded valuable information. Further studies such as oxygenation of Iron derivatives of this porphyrins and reaction of these porphyrins with small molecules such as CO, NO, would add more to an understanding of the

spectral properties. It is hoped that in future such measurements would be takenup in this laboratory.

REFERENCES

1. (a) R.S. Mulliken; J. Am. Chem. Soc., **74**, 811, 1952.
   (b) R.S. Mulliken; J. Phys. Chem., **56**, 801, 1952.

2. M.J.S. Dewar and A.R. Lepley; J. Am. Chem. Soc., **83**, 4560, 1961.

3. M.J.S. Dewar and H. Rogers; J. Am. Chem. Soc., **84**, 395, 1965.

4. J.N. Murrel; J. Am. Chem. Soc., **81**, 5037, 1959.

5. J.N. Murrel; Quart. Revs. (Lon)., **15**, 191, 1961.

6. R.L. Flurry Jr.; J. Phys. Chem., **69**, 1927, 1965.

7. K. Fukai; A. Imamura; T. Yanezawa and C. Nagata; Bull. Chem. Soc. Japan, **34**, 1076, 1961 and **35**, 33, 1962.

8. J. Manassen and A. Barllan; J. Catal., **17**, 86, 1970.

9. H.A.O. Hill; A. Roder and R.J.P. Williams; Struct. Bond., **8**, 123, 1970.

10. R.E. Dickerson; Advan. Biochem., **72**, 815, 1972.

11. J.H. Fuhrop; M. Baccouche; H. Grabon and H. Aryaunanian; J. Mol. Catal., **7**, 245, 1980.

12. E. Antonini and M. Brunori; "Hemoglobin and Myoglobin in reaction with Ligands", North Holland Publishers, Amsterdam, 1971.

13. E.H. Abbott; and P.A. Piafson; J. Am. Chem. Soc., **96**, 7378, 1974.

14. D.F. Bradley and M. Calvin; Proc. Natl. Acad. Sci., U.S.A., **41**, 563, 1955.

15. R.C. Nelson; J. Chem. Phys., **27**, 864, 1957.

16. J.R. Norris; H. Scheer; M. Drugan and T.J. Katz; Proc. Natl. Acad. Sci. USA., **71**, 4897, 1974.

17. G.R. Seely, in "The chlorophylls", Eds. L.P. Vernon; G.R. Seely; Academic Press, New York, 1966.

18. W.R. Boon; Chem. Ind. (Lon); 782, 1965.

19. M.A. Slifkin; "Charge transfer complexes in Biomolecules", Academic Press, London, 1971.

20. J.G. Heathcote and M.A. Slifkin; Biochem. Biophys. Acta., **158**, 167, 1968.

21. A. Veillard and B. Pullman; _J. Theor. Biol._, 8, 307, 1965.

22. (a) G.Tollin and G. Green; _Biochim. Biophys. Acta._, 66, 308, 1964. (b) G. Tollin and G. Green; _Biochim. Biophys. Acta._, 60, 524, 1962.

23. (a) J.J. Katz and L.J. Boucher; _J. Am. Chem. Soc._, 89, 1703, 1967. (b) J.J. Katz, in "Inorganic Biochemistry", Ed. G.L. Eichorn, Elesevier, Amsterdam, 1973.

24. R. Livingston; L. Thompson and M.V. Rama Rao; _J. Am. Chem. Soc._, 74, 1073, 1952.

25. J.R. Larry and Q. Vanwinkle; _J. Phys. Chem._, 73, 570, 1969.

26. M.N. Hughes; "The Inorganic Chemistry of Biological processes; Second edition, 1984, pp. 147.

27. C. Swistak and K.M. Kadish; _Inorg. Chem._, 26, 405, 1987.

28. S.L. Kelly and K.M. Kadish; _Inorg. Chem._, 21, 3631, 1982.

29. Z. Dokuzovic; Xh. Ahmeti; D. Pavlovic; I. Murati and S. Asperger; _Inorg. Chem._, 21, 1576, 1982.

30. D. Pavlovic; S. Asperger; Z. Dokuzovic; B. Jurisic; Xh. Ahmeti; M. Sertic and I. Murati; _J. Chem. Soc. Dalton Trans._, 1095, 1985.

31. D. Pavlovic; S. Asperger and B. Domi; _J. Chem. Soc. Dalton Trans._, 2535, 1986

32. D. Pavlovic; S. Asperger; Xh. Ahmeti; B.C. Cizonek; B. Jurisic and Z. Veksli; _Inorg. Chem._, 27, 1515, 1988.

33. D.M. Wagnerova and K. Lang; _Inorg. Chim. Acta._, 162, 1, 1989.

34. D.V. Stynes; H.C. Stynes; J.A. Ibers and B.R. James; _J. Am. Chem. Soc._, 95, 1142 and 1796, 1973.

35. (a) "Primary processes of photosynthesis"; Barber, J., Ed.,; Elsevier; Amsterdam, 1977. (b) "Bioenergetics of Photosynthesis"; Govindjee, E., Ed.; Academic Press; New York, 1975. (c) J.J. Katz; J.R. Norris; L.L. Shipman; M.C. Thurhauer and M.R. Wasielewski, _Ann. Rev. Biophys. Bioenerg._, 7, 393, 1978. (d) K. Sauer; _Ann. Rev. Phys. Chem._, 30, 155, 1979. (e) B.D. Kauff, and R. Malkin; _Curr. Top. Bioenerg._, 7, 137, 1978. (f) "Photosynetheis in Relation to Model-Systems"; Barber, E., Ed.; Elsevier; Amsterdam, 1979. (g) "Photosynthesis Vols. I and II; Govindjee, Ed.,; Academic Press, New York, 1979. (h) R.E. Blanken ship; _Acc. Chem. Res._, 14, 163, 1981.

36. (a) J.P. Collman; J.I. Braumann; J.R. Dovsee; E. Halbert; E. Bunnenburg; R.E. Linder; G.N. LaMar; J.D. Gaudio; G. Lang and K. Spartalian; J. Am. Chem. Soc., 102, 4182, 1980. (b) T.G. Traylor; C.K. Chang; J. Giebel; A. Berzilis,; T. Miheey; and J. Cannon; J. Am. Chem. Soc., 102, 4182, 1980. (c) F.S. Moliwaro; R.G. Little and J.A. Ibers; J. Am. Chem. Soc., 99, 5628, 1977. (d) M. Momenteau; B. Loock; E. Bisagani and M. Rongee; Can. J. Chem., 1804, 1979. (e) J. Kong and P.A. Loach; J. Heterocycle. Chem., 1737, 1980. (f) T. Katagi; T. Yamamura; T. Saito and Y. Sasak; Chem. Lett., 417, 1982. (g) J.P. Collmann; In "Metal ion activation of dioxygen", Spiro, T.G., Ed.; Academic Press: New York, 1982, pp. 1.

37. (a) J. Fajer and M.S. Davis; In "The Porphyrins" Ed. by D. Dolphin; Academic Press, New York, Vol. IV, 1979, p. 197. (b) L.A. Anderson and J.H. Dawson; Struct. Bond. Springer-Verlag., 74, 1, 1991.

38. (a) D. Dolphin; A. Forman; D.C. Borg and J. Fajer; Proc. Natl. Acad. Sci. USA, 68, 614, 1971. (b) D. Dolphin and R.H. Felton; Acc. Chem. Res., 7, 26, 1974.

39. (a) J.T. Groves and T.J. McMurry; Rev. Port. Quim., 27, 102, 1985. (b) B. Boso; G. Lang; T.J. McMurry; and J.T. Groves; J. Chem. Phys., 79, 1122, 1983.

40. (a) D.H. Chin; G.N. La Mar and A.L. Balch; J. Am. Chem. Soc., 102, 4344, 1980. (b) D.H. Chin; A.L. Balch and G.N. La Mar; J. Am. Chem. Soc., 102, 1446, 1980.

41. (a) M. Schappacher; G. Chottard and R. Weiss; J. Chem. Soc. Chem. Commun., 93, 1986. (b) A. Gold; K. Jayaraj; P. Doppett; R.Weiss; G. Chottard; E. Bill; X. Ding and A.X. Trantwein; J. Am. Chem. Soc., 110, 5756, 1988.

42. M.A. Ator and P.R.O. de Montellano; J. Biol. Chem., 262, 1542, 1987.

43. (a) V. Balzani; F. Bolletta; M.T. Gandolfi and M. Maestri; Topics Curr. Chem., 1, 75, 1978. (b) N. Sutin; J. Photochem., 10, 19, 1979. (c) N.J. Turro; In "Modern Molecular Photochemistry"; W.A. Benjaman, Menlo park, California, 1978.

44. (a) N. Sutin; Ann. Rev. Nucl. Sci., 12, 285, 1962. (b) J.J. Jortner; J. Am. Chem. Soc., 102, 6676, 1980.

45. (a) R.A. Marcus; Faraday. Disc. Chem. Soc., 29, 21, 1960; Ann. Rev. Phys. Chem., 15, 155, 1964; J. Chem. Phys., 43, 679, 1965; Electro-Chim. Acta., 13, 995, 1968; In "Tunneling in Biological Systems" (B. Chance; D.C. Devault; H. Frauenfelder; M.A. Marcus; J.R. Schrieffer; N. Sutin; Ed.) Academic Press: New York, pp. 109, 1979. (b) N.S. Hush; Electrochim. Acta., 13, 1005, 1968. (c) N. Sutin; In "Inorganic Photochemistry", Eichorn, G. Ed.; Elsevier;

Amsterdam; pp. 611, 1973. (d) G.M. Brown and N. Sutin; J. Am. Chem. Soc., 101, 883, 1979. (e) Faraday. Disc. Chem. Soc., 1981.

46. (a) V. Krishnan; Proc. Ind. Natl. Acad. Sci., 83, 767, 1984. (b) G.R. Seely; J. Phys. Chem., 73, 125, 1969. (c) D. Holten; M.W. Windsor; W.W. Parson, and M. Gouterman; Phtochem. Photobiol., 28, 951, 1978.

47. A. Harriman; J. Chem. Soc. Faraday Trans. II, 77, 1281, 1981.

48. W.R. Scheidt and Y.J. Lee; Struct. Bond., Vol. 64, P. 1, 1987.

49. (a) E. Fujita and J. Fajer; J. Am. Chem. Soc., 105, 6743, 1983. (b) Y.J. Lee; W.R. Scheidt and G. Lang; J. Am. Chem. Soc., 104, 6791, 1982.

50. C. Kratky; R. Waditschatka; C. Angst; J.E. Johansen; J.C. Plaquerent; J. Schreiber and A.Eschenmoser; Helv. Chim. Acta., 68, 1312, 1985.

51. A.M. Stolzenberg and M.T. Stershic; Inorg. Chem., 27, 1614, 1988.

52. A.M. Stolzenberg and L.J. Schussel; Inorg. Chem., 30, 3205, 1991.

53. A.M. Stolzenberg and M.T. Stershic; J. Am. Chem. Soc., 110, 6391, 1988.

54. A.M. Stolzenberg and M.T. Stershic; Inorg. chem., 26, 3082, 1987.

55. A.M. Stolzenberg and M.T. Stershic; J. Am. Chem. Soc., 110, 5397, 1988.

56. A.M. Stolzenberg; P.A. Glazer and B.M. Foxman; Inorg. Chem., 25, 983, 1986.

57. R.C. Ladner; E.J. Heidner and M.F. Perutz; J. Mol. Biol., 114, 385, 1977.

58. J.F. Deatherage; R.S. Loe; C.M. Anderson and K. Moffat; J. Mol. Biol., 104, 687, 1976.

59. (a) J. Deisenhofer; O. Epp; K. Miki; R. Huber and H. Michel; Nature, 318, 618, 1985. (b) J. Deisenhofer; O. Epp; K. Miki; R. Huber and H. Michel; J. Mol. Biol., 180, 385, 1984. (c) W. Zinth; E.W. Knapp; S.F. Fischer; W. Kaiser; J. Deisenhofer and W. Michel; Chem. Phys. Lett., 119, 1, 1985.

60. B. Jaun and A. Pfaltz; J. Chem. Soc. Chem. Commun., 1327, 1986.

61. (a) L.R. Furenlid; M.W. Renner; K.M. Smith and J. Fajer; J. Am. Chem. Soc., **112**, 1634, 1990. (b) L.R. Furenlid; M.W. Renner and J. Fajer; J. Am. Chem. Soc., **112**, 8987, 1990.

62. T.P. Wijesekera; J.B. Paine III; D. Dolphin; F.W.B. Einstein and T. Jones; J. Am. Chem. Soc., **105**, 6747, 1983.

63. U. Simonis; F.A. Walker; P.L. Lee; B.J. Hanquet; D.J. Meyerhoff and W.R. Scheidt; J. Am. Chem. Soc., **109**, 2659, 1987.

64. (a) Vogel's Text Book of practical organic chemistry; ELBS and Longman, Fourth Edition, 1978, Chapter 2. (b) A. Weissberger; E.S. proskaner; J.A. Riddick; E.F. Toppos Jr.; "Organic solvents in Techniques of Organic Chemistry", Third Edition, Inc. N.Y. Vol. 7, 1970.

65. A.G. Green; F.M. Rowe; J. Chem. Soc., **101**, 2452, 1912.

66. A.G. Green; F.M. Rowe; J. Chem. Soc., **103**, 2023, 1913.

67. (a) A.S. Bailey; J.R. Case; Proc. Chem. Soc., 176, 1957.
(b) A.S. Bailey; J.R. Case; Tetrahedron, **3**, 113, 1958.

68. Organic Synthesis, Vol. 34, p. 100.

69. R.L. Hill; M. Gouterman; A. Ulman. Inorg. Chem., **21**, 1450, 1982.

70. P.G. Seybold, M. Gouterman, J. Mol. Spectrosc., **31**, 1, 1982.

71. J.B. Birks; D.J. Dyson. Proc. Roy. Soc. (London), **A275**, 135, 1963.

72. S.J. Strickler; R.A. Berg. J. Chem. Phys., **37**, 814, 1962.

73. V. Balzani; F.Bolletta; M.T. Ganadolfi; M. Maestri; Topics in current chemistry. **75**, 1, 1978.

74. W.D. Hewson and L.P. Hager, In "Porphyrins"; Dolphin, D., Ed.; Academic Press; New York, 1979, Vol. 7, 295.

75. D. Dolphin and R.H. Felton, Acc. Chem. Res., **7**, 26, 1974.

76. J. Fajer and H.S. Davies, In "Porphyrins"; Dolphin, D., Ed.; Academic Press; New York, 1979, Vol. 4, 197.

77. H.S. Davies, A. Forman and J. Fajer, Proc. Natl. Acad. Sci. USA, **76**, 4170, 1979.

78. A.R. McIntosh, A. Siemiarczuk, J.R. Bolton, M.J. Stillman, Te-Fe.Ho and A.C. Weedon, J. Am. Chem. Soc., **105**, 7215, 1983.

79. J.R. Darvent, P. Douglas, A. Harriman, G. Porter and M.-C. Richoux, Coord. Chem. Rev., **44**, 83, 1982.

99. E. Samuels; R. Shuttleworth and T.S. Stevens, J. Chem. Soc. (c), 145, 1968.

100. H.W. Whitlock Jr.; R. Hanauer; M.Y. Oester and B.K. Bower, J. Am. Chem. Soc., 91, 7485, 1969.

101. F.A. Walker; D. Beroiz and K.M. Kadish, J. Am. Chem. Soc., 98, 3484, 1976.

102. (a) D.W. Thomas and A.E. Martell, Arch. Biochem. Biophys., 76, 286, 1958. (b) D.W. Thomas and A.E. Martell, J. Am. Chem. Soc., 81, 5111, 1959.

103. A. Mahmood; H.L. Liu; J.G. Jones; J.O. Edwards, and D.A. Sweigart, Inorg. Chem., 27, 2149, 1988.

104. C.D. Barry, H.A.O. Hill; B.E. Mann; P.J. Sadler and R.J.P. Williams, J. Am. Chem. Soc., 95, 4545, 1973.

105. T.K. Chandrashekar and V. Krishnan, Can. J. Chem., 62, 475, 1984.

106. D.V. Stynes; H.C. Stynes; B.R. James and J.A. Ibers, J. Am. Chem. Soc., 94, 1320, 1972.

107. (a) B.S. Tovrog; D.J. Kitko and R.S. Drago, J. Am. Chem. Soc., 98, 5144, 1976. (b) R. Breos; G. Tauzher; G. Costa and M. Green, J. Chem. Soc. Dalton. Trans., 2329, 1975.

108. R.S. Drago; T. Beugelsdijk; J. A. Breese and J.P. Cannady, J. Am. Chem. Soc., 100, 5374, 1978.

109. A. Tabard; P. Cocolios; G. Lagrange; R. Gerardiu; J. Hubsch; C. Lecomte, J. Zarembowitch and R. Guilard, Inorg. Chem., 27, 110, 1988.

110. E. Fujita; C.K. Chang and J. Faser, J. Am. Chem. Soc., 107, 7665, 1985.

111. J.M. Assour and W.K. Khan, J. Am. Chem. Soc., 87, 207, 1965.

112. C.J. Brown, J. Chem. Soc.(A), 2488, 1968.

113. J.S. Griffiths, Discus. Farday. Soc., 26, 81, 1958.

114. B.R. McGarvey, J. Phys. Chem., 60, 71, 1956.

115. W.C. Lin and P.W. Lau, J. Am. Chem. Soc., 98, 1447, 1976.

116. L.M. Engelhardt and M. Green, J. Chem. Soc., Dalton Trans., 724, 1972.

117. (a) W.C. Lin, Inorg. Chem., 15, 1114, 1976. (b) K. Alston and C.B. Storm, Biochem., 18, 4292, 1979.

118. J.M. Assour, J. Chem. Phys., 43, 2477, 1965.

119. (a) G.N. LaMar and F.A. Walker, In "The Porphyrins" Dolphin, D. Ed., Acad. Press, N.Y., 1979, Vol. 4, 61. (b) G.N. LaMar and F.A. Walker, J. Am. Chem. Soc., 95, 1790, 1973.

120. T.K. Chandrashekar and V. Krishnan, Inorg. Chem., 20, 2782, 1981.

121. Y. Yamashita; T. Suzuki; G. Saito and T. Mukai, J. Chem. Soc. Chem. Commun., 1489, 1986.

122. (a) Lustig and E.A. Hansen, J. Chem. Soc.(D), 661, 1970. (b) D.D. Callander; L. Coe; M.F.S. Matough; E.F. Mooney; A.J. Uff and P.H. Winson, Chem. Commun., 820, 1966.

123. H.A.O. Hill; A.J. Macfarlane and R.J.P. Williams, J. Chem. Soc. (A), 1704, 1969.

124. F.A. Walker, J. Mag. Reso., 15, 201, 1974.

125. F.A. Walker, J. Am. Chem. Soc., 95, 1150 and 1154, 1973.

126. J.D. Satterlee; G.N. LaMar and J.S. Frye, J. Am. Chem. Soc., 98, 7275, 1976.

127. G.N. LaMar and F.A. Walker, J. Am. Chem. Soc., 94, 8607, 1972.

128. (a) H.C. Stynes and J.A. Ibers, J. Am. Chem. Soc., 94, 5125, 1972. (b) D.V. Stynes; H.C. Stynes; B.R. James and J.A. Ibers, J. Am. Chem. Soc., 95, 1976, 1973. (c) D.V. Stynes; H.C. Stynes; J.A. Ibers and B.R. James, J. Am. Chem. Soc., 95, 1142, 1973.

129. A.H. Corwin; D.G. Whitten; E.W. Baker and Kleinspehn, J. Am. Chem. Soc., 85, 3621, 1963.

130. H.C. Stynes and J.A. Ibers, J. Am. Chem. Soc., 94, 1559, 1972.

131. F.A. Walker, J. Am. Chem. Soc., 92, 4235, 1970.

132. B.M. Hoffman and D.H. Petering, Proc. Natl. Acad. Sci., 67, 637, 1970.

133. R.F. Pasternack; E.J. Gibbs; A. Gaudemer; A. Antebi; S. Bassner; L. De Poy; D.H. Turner; A. Williams; F. Laplace; M.H. Lansard; C. Merienne, and M. Perree-Fauvet, J. Am. Chem. Soc., 107, 8179, 1985.

134. (a) R.F. Posternack; E.G. Spiro and M. Teach, J. Inorg. Nucl. Chem., 36, 599, 1974. (b) K. Kalyanasundaram; Inorg. Chem., 23, 2453, 1984.

135. K. Kano; T. Miyake; K. Uomoto; T. Sato; T. Ogawa and S. Hashimoto, Chem. Lett., 1867, 1983.

136. C.J. Nash; *J. Phys. Chem.*, **64**, 950, 1960.

137. H.E. Bent and C.L. French, *J. Am. Chem. Soc.*, **63**, 568, 1941.

138. R.F. Pasternack; B.S. Gillies and J.R. Stahlbush, *J. Am. Chem. Soc.*, **100**, 2613, 1978.

139. A.N. Thomson and M. Krishnamurthy, *Inorg. Chim. Acta.*, **34**, 145, 1979.

140. I. Constantinidis and J.D. Satterlee, *J. Am. Chem. Soc.*, **110**, 927, 1988.

141. (a) R.F. Pasternack; *Inorg. Chem.*, **15**, 643, 1976.
(b) R.F. Pasternack and N. Sutin, *Inorg. Chem.*, **13**, 1956, 1974.

142. R.F. Pasternack; H. Lee; P. Malek and C.Spencer, *J. Inorg. Nucl. Chem.*, **39**, 1865, 1977.

143. (a) D.J.E. Ingram; J.E. Bennel; P. George, and J.M. Goldstein, *J. Am. Chem. Soc.*, **78**, 3545, 1956. (b) P.W. Lau and W.C. Lin, *J. Inorg. Nucl. Chem.*, **37**, 2389, 1975. (c) A. Abkowitz; I. Chen and J.H. Sharp, *J. Chem. Phys.*, **48**, 4561, 1968. (d) I. Chen; A. Abkowitz and J.H. Sharp, *J. Chem. Phys.*, **50**, 2237, 1969. (e) J. Bhonday and B.F. Kim, *J. Mag. Reso.*, **26**, 341, 1977.

144. (a) J. Subramanian; J.H. Fuhrhop; A. Salek and A. Gossauer, *J. Mag. Reso.*, **15**, 9, 1974. (b) J.M. Assour; *J. Chem. Phys.*, **43**, 2477, 1965. (c) M. Momenteau; J. Mispelter; B. Loock and J.M. Lhoste, *Can. J. Chem.*, **56**, 2598, 1978. (d) W.C. Lin, in "The porphyrins" Ed., D. Dolphin; *Acad. Press*, N.Y., Vol. 4, 1979, p. 355.

145. (a) D. Kievelson, and R. Neiman, *J. Chem. Phys.*, **35**, 149, 1961. (b) D. Kievelson and S.K. Lee, *J. Chem. Phys.*, **41**, 1896, 1964.

146. (a) H. Hokoi and M. Iwaizumi, *Bull. Chem. Soc.*, Japan, **53**, 1489, 1980. (b) M. Iwaizumi; Y. Masamoto; H.I. Ohba and M. Hirayama, *Inorg. Chim. Acta*, **82**, 47, 1984. (c) H. Yokoi and M. Iwaizumi, *Bull. Chem. Soc.*, Japan, **53**, 633, 1980.

147. T.k. Chandrashekar and V. Krishnan, *J. Inorg. Nucl. Chem.*, **43**, 3287, 1981.

148. J.P. Allen; G. Feher; T.O. Yates; D.C. Rees; J. Deisenhofer; H. Michel and R. Huber. *Proc. Natl. Acad. Sci.*, U.S.A. **83**, 8589, 1986.

149. (a) J.J. Katz; J.R. Norris; L.L. Shipman; M.C. Thurnauer; M.R. Wasilewski; *Ann. Rev. Biophys. Bio-energy*. **7**, 393, 1978. (b) J.R. Norris; H. Scheer; M.E. Druyan; J.J. Katz; *Proc. Natl. Acad. Sci. U.S.A.* **71**, 4897, 1974. (c) G. Foher;

A.J. Hoff; R.A. Isaacson; L.C. Ackerson; Ann. N.Y. Acad. Sci., **244**, 239, 1975. (d) K.D. Phillipson; V.L. Sato; K. Sauer, Biochemistry, **11**, 4591, 1972.

150. (a) D. Dolphin; A. Hiom; J.B. Paine III; Heterocycl., **16**, 417, 1981. (b) M.R. Wasielewski; Mol. Biol. Biochem. and Biophys., **35**, 234, 1982. (c) S.G. Boxer; Biochem. Biophys. Acta. **723**, 65, 1983.

151. (a) R.G. Little; J. Heterocyclic Chem., **15**, 203, 1978. (b) B.C. Bookser and T.C. Bruice, J. Am. Chem. Soc., **113**, 4208, 1991.

152. T.K. Chandrashekar; H. Van Willigen and M.H. Ebersole, J. Phys. Chem., **88**, 4326, 1984.

153. N. Kobayashi and A.B.P. Lever; J. Am. Chem. Soc., **109**, 7433, 1987.

154. (a) V. Thanabal and V. Krishnan, J. Am. Chem. Soc., **104**, 3644, 1982. (b) V. Thanabal and V. Krishnan, Inorg. Chem., 21, 3606, 1982.

155. V. Ahsen; E. Yilmazer; M. Ertas and O. Bekaroglu, J. Chem. Soc. Dalton Trans., 401, 1988.

156. Ot. E. Sielken; M.M. Van Tilberg; M.F.M. Roks; R. Handriks; W.Drenth and R.J.M. Nolte; J. Am. Chem. Soc., **109**, 4261, 1987.

157. (a) N. Kobayashi and Y. Nishiyama, J. Chem. Soc. Chem. Commun.,1462, 1986. (b) R. Hendriks; Ot. E. Sielcken; W. Drenth and R.J.M. Nolte, J. Chem. Soc. Chem. Commun., 1464, 1986.

158. A.B.P. Lever; Adv. Inorg. Chem. Radiochem., 7, 27, 1965.

159. (a) M. Ravikant; D. Reddy and T.K. Chandrashekar, J. Chem. Soc. Dalton Trans., 2103, 1991. (b) T.K. Chandrashekar; H. Van Willigen and M.H. Ebersole, J. Phys. Chem., **89**, 3453, 1985.

160. (a) T.K. Chandrashekar and H. Van Willigen, Chem. Phys. Lett., **106**, 237, 1984. (b) T.K. Chandrashekar, and H.V. Willigen; J. Am. Chem. Soc., 105, 6323, 1983.

161. C.J. Pederson, J. Am. Chem. Soc., **89**, 7017, 1967.

162. (a) M. Kasha, H.R. Rawls and M. El-Bayoumi, Pure Appl. Chem., **11**, 371, 1965. (b) M. Gouterman, D. Holten and E. Lieberman, Chem. Phys., 25, 139, 1977. (c) C.A. Hunter, J.K.M. Sanders and A.J. Stone, Chem. Phys., **133**, 395, 1989.

163. L.D. Rollmann and R.T. Iwamoto, J. Am. Chem. Soc., **90**, 1455, 1965.

164. (a) K.M. Kadish and M.M. Morrison, J. Am. Chem. Soc., 98, 3326, 1976. (b) K.M. Kadish and M.M. Morrison, Bio Inorg. Chem., 7, 107, 1977.

165. J. Subramanian; In "The porphyrins and Metalloporphyrins", Smith, K.M., Ed.; Elsevier; Amsterdam, 1975, Chapter 13.

166. N.D. Chasteen and R.L. Bolford, Inorg. Chem., 9, 169, 1970.

167. A. MacCragh; C.B. Storm and W.S. Koshi, J. Am. Chem. Soc., 87, 1470, 1965.

168. P.D.W. Boyd; T.D. Smith, J. Chem. Soc., Dalton Trans., 839, 1972.

169. A.D. Toy; T.D. Smith; J.R. Pilbrow, Aust. J. Chem., 27, 1, 1974.

170. E. Setten, Acta Crystallogr., Sect. B, B25, 1480, 1969.

171. J.C. Forrest and C.K. Prout, J. Chem. Soc. A., 1312, 1967.

172. S.G. Carr; T.D. Smith; J.R. Pilbrow, J. Chem. Soc., Faraday Trans. 2., 497, 1974.

173. P.D.W. Boyd; T.D. Smith; J.H. Price; and J.R. Pilbrow, J. Chem. Phys., 56, 1253, 1972.

174. Subramanian, J., Private communication.

175. J.A. Shelnutt; C.J. Medforth; M.D. Berber; K.M. Barkigia and K.M. Smith, J. Am. Chem. Soc., 113, 4077, 1991.

176. M.K. Geno and J. Halpern, J. Am. Chem. Soc., 109, 1238, 1987.

177. (a) L.R. Furenlid; M.W. Renner; K.M. Smith and J. Fajer; J. Am. Chem. Soc., 112, 1634, 1990. (b) L.R. Furenlid; M.W. Renner and J. Fajer; J. Am. Chem. Soc., 112, 8987, 1990.

178. K.M. Berkigia; L. Chantranupong, K.M. Smith and J. Fajer; J. Am. Chem. Soc., 110, 7566, 1988.

179. T. Takano, J. Mol. Biol., 110, 537, 1977.

180. Protein Data Bank, Brookhaven National Laboratories, Upton, NY.

181. A. Pfaltz; B. Jaun; A. Fassler; A. Eschenmoser, R. Jaenchem; H.H. Gilles; G. Diekert and R.K. Thauer, Helv. Chim. Acta., 65, 828, 1982.

182. J.A. Shelnutt; K. Alston, J.-Y. Ho; N.-T. Yu; T. Yamamoto and J.M. Rifkind, Biochemistry, 25, 620, 1986.

183. J.A. Shelnutt; K. Alston; E.W. Findsen; M.R. Ondrias and J.M. Rifkind, In porphyrins: Excited states and Dynamics; M. Gouterman; P.M. Rentzepis and K.D. Straub; Eds: ACS symp. Series 321; American Chemical Society: Washington, DC, 1986; Chapter 16.

184. E.W. Findsen; K. Alston; J.A. Shelnutt, and M.R. Ondrias, J. Am. Chem. Soc., **108**, 4009, 1986.

185. J. A. Shelnutt; E.W. Findsen; M.R. Ondrias and K. Alston; In metal complexes in Fossil fuels; Filby, R.H., Branthaver, J.F., Eds.; ACS Symp. Series 344; American Chemical Society; Washington, DC, 1987; Chapter 24.

186. R.G. Alden; B.A. Crawford; R. Doolen; M.R. Ondrias and J. A. Shelnutt, J. Am. Chem. Soc., **111**, 2070, 1989.

187. T.D. Brennan; W.R. Scheidt and J.A. Shelnutt, J. Am. Chem. Soc., **110**, 3919, 1988.

188. R.G. Alden; M.R. Ondrias and J.A. Shelnutt, J. Am. Chem. Soc., **112**, 691, 1990.

189. B. Morgan and D. Dolphin, Struct. Bond., **64**, 115, 1987.

190. C.K. Chang, J. Am. Chem. Soc., **99**, 2819, 1977.

191. J.P. Collman, Acc. Chem. Res., **10**, 265, 1977.

192. A.R. Battersby and A.D. Hamilton, J. Chem. Soc., Chem. Commun., **117**, 1980.

193. J.E. Baldwin, M.J. Crossley, T. Klose, E.A. O'Rear and M.K. Peters, Tetrahedron, **38**, 27, 1982.

194. M. Mometeau, J. Mispelter, B. Loock and E. Bisagni, J. Chem. Soc. Perkin Trans. I, 189, 1983.

195. J. Weiser and H.A. Staab, Angew. Chem. Int. Ed. Eng., **23**, 623, 1984.

196. J. Weiser and H.A. Staab, Tetrahedron Lett., **26**, 6059, 1985.

197. A. Ulman and J. Manassen, J. Am. Chem. Soc., **97**, 6540, 1975.

198. M.M. ner and A.D. Alder, J. Am. Chem. Soc., **97**, 5107, 1975.

199. F.A. Walker, D. Beroiz and K.M. Kadish, J. Am. Chem. Soc., **98**, 3484, 1976.

200. M. Nappa and J.S. Valentine, J. Am. Chem. Soc., **100**, 5075, 1978.

201. D. Reddy, N.S. Reddy, T.K. Chandrashekar and H.V. Willigen, J. Chem. Soc. Dalton Trans, 2097, 1991.

202. X. Q. Lin, B.B. Cocolios and K.M. Kadish, *Inorg. Chem.*, **25**, 3242, 1986.

203. X. H. Mu and K.M. Kadish, *Inorg. Chem.*, **28**, 3743, 1989.

204. J. Mispelter; M. Momenteau and J.M. Lhoste, *J. Chem. Phys.*, **72**, 1003, 1980.

205. K.N. Ganesh and J.K.M. Sanders, *J. Chem. Soc. Perkin Trans. I*; 1611, 1982.

206. K.N. Ganesh; J.K.M. Sanders and J.C. Waterton; *J. Chem. Soc. Perkin Trans. I*, 1617, 1982.

207. (a) P.J. Spellane, M. Gouterman, A. Antipas, S. Kim and Y.C. Liu, *Inorg. Chem.*, **19**, 386, 1980.

208. (a) D.J. Quimby and F.R. Longo, *J. Am. Chem. Soc.*, **97**, 5111, 1985. (b) R.A. Binstead, M.J. Crossley and N.S. Hush, *Inorg. Chem.*, **30**, 1259, 1991.

209. (a) A. Stone and E.B. Fleischer, *J. Am. Chem. Soc.*, **90**, 2735, 1968. (b) J.B. Kim, J.J. Leonard and F.R. Longo, *J. Am. Chem. Soc.*, **94**, 3986, 1972.

210. J.Y. Becker, D. Dolphin, J.B. Paine and T. Wijesekera, *J. Electroanal. Chem.*, **164**, 335, 1984.

211. (a) D. Lexa, M. Momenteau, P. Rentien, G. Rytz, J.M. Saveant and F. Xu, *J. Am. Chem. Soc.*, **106**, 4755, 1984. (b) M. Momenteau, *Pure & Appl. Chem.*, **58**, 1493, 1986. (c) D. Lexa, P. Maillard, M. Momenteau and J.M. Saveant, *J. Am. Chem. Soc.*, **106**, 6321, 1984.

212. K.M. Kadish, in the "Progress in Inorg. Chem., Ed. Lippard, **34**, p. 437, 1986.

213. H. Levanon; J.R. Norris, *Chem. Rev.*, **78**, 185, 1978.

214. Z.P. Gribova; L.P. Kayushin, *Russ. Chem. Rev.*, **41**, 154, 1972.

215. R.C. Prince; J.S. Leigh, Jr.; P.L. Dutton, *Biochem. Biophysica. Acta*, **440**, 622, 1976.

216. H.V. Willigen; T.K. Chandrashekar; U. Das; Ebersole, M.H. *ACS Sympo. Ser.*, **321**, 140, 1986.

217. G.B. Jameson; J.A. Ibers, *J. Am. Chem. Soc.*, **102**, 2823, 1980.

218. D.J. Quimby; F.R. Longo *J. Am. Chem. Soc.*, **97**, 5111, 1975.

219. A. Harriman; R.J. Hosie, *J. Photo. Chem.*, **15**, 163, 1981.

220. J. Weiser; H.A. Staab, *Tetrahedron Lett.*, **26**, 6059, 1985.

221. M.R. Wasielewski; M.P. Niemczyk, _ACS Sympo. Ser._ **321**, 154, 1986.

222. A.R. McIntosh; A. Siemiarczuk; J.R. Bolton; M.J. Stillman; Te-Fu Ho; A.C. Weedon, _J. Am. Chem. Soc.,_ **105**, 7215, 1983.

223. T.L. Netzel; M.A. Bergkamp; C-K. Chang; J. Dalton, _J. Photo. Chem.,_ **17**, 451, 1981.

224. (a) Y. Kurabayashi; K. Kikuchi; H. Kokubun; Y, Kaizu; H. Kobayashi, _J. Phys. Chem.,_ **88**, 1308, 1984. (b) S. Tabita; Y. Kajii; I. Tauaka, _ACS Symp. Ser.,_ **321**, 219, 1986.

225. K. Kalyanasundaram; M.N. Spallart, _J. Phys. Chem._ **86**, 5163, 1982.

226. (a) K. Sauer, _Acc. Chem. Res.,_ **13**, 249, 1980. (b) M. Calvin, _Acc. Chem. Res.,_ **11**, 869, 1978.

227. J.H. Van der Waals; W.G. Van Drop; T.J. Schaafsma, in "The porphyrins", D. Dolphin Ed., Academic press, New York, 1979, Vol. IV, p. 257.

228. T.K. Chandrashekar; H.V. Willigen; M.J. Ebersole, _J. Phys. Chem.,_ **88**, 3453, 1985.

229. H.V. Willigen; T.K. Chandrashekar, _J. Chem. Phys.,_ **78**, 7093, 1983.

230. R.A. Binstead; M.J. Crossley; N.S. Hush, _Inorg. Chem.,_ **30**, 1259, 1991.

231. P. Bhyrappa; V. Krishnan, _Inorg. Chem.,_ **30**, 239, 1991.

232. E. Nissani; A. Scherz; H. Levanon, _Photochem. Photobiol.,_ **25**, 93, 1977.

233. H. Levanon; A. Wolberg, _Chem. Phys. Lett.,_ **24**, 96, 1974.

234. (a) M.C. Zerner and M. Gouterman, _Theor. Chem. Acta.,_ **4**, 44, 1966. (b) M. Gouterman, _J. Mol. Spect.,_ **6**, 138, 1961.

235. (a) S.C. Khandelwal and J.L. Robber, _Chem. Phys. Lett.,_ **34**, 355, 1975. (b) S. Kitagawa; I. Morishima; T. Yonezawa and N. Sato, _Inorg. Chem.,_ **18**, 1345, 1979.

236. R. Foster, _Nature (London),_ **183**, 1253, 1959.

LIST OF PUBLICATIONS

(1) Optical, NMR and ESR evidence for the oxidation of cobalt porphyrins in the presence of an electron acceptor.

Inorg. Chim. Acta., **166**, 147, 1989.

(2) Interaction of water soluble metallo porphyrins with nucleic acid bases.

Indian J. Chem., **A29**, 312, 1990.

(3) Oxidation of Co(II) tetrapyrroles in the presence of an electron acceptor.

J. Chem. Soc. Dalton Trans., 2097, 1991.

(4) Short chain basket handle porphyrins: Synthesis and characterisation.

J. Chem. Soc. Dalton Trans., 1992 (in press).

(5) Excited state properties of short chain basket handle porphyrins.

Communicated (1992).

(6)* Spectroscopic studies on monomers and dimers of thia-porphyrins.

Proc. Indian Acad. Sci. (Chem. Sci.), **102**, 307, 1990.

(7)* Dimerization effects on spectroscopic properties of water soluble porphyrins in aqueous and micellar media.

J. Chem. Soc. Dalton Trans., 2103, 1991.

(8)* Cyclotriphosphazene linked tetraphenyl porphyrins.

Heterocycles, **32**, 703, 1991.

* This work is not included in the thesis.